Macrocyclization and Fatty Acid Modification during the Synthesis of Nonribosomal Peptides

---

Makrozyklisierung und Fettsäuremodifikation während der Synthese nichtribosomaler Peptide

Dissertation
zur Erlangung des Doktorgrades
der Naturwissenschaften
(Dr. rer. nat.)

dem
Fachbereich Chemie
der Philipps-Universität Marburg
vorgelegt von

Florian Kopp

aus Gießen

Marburg/Lahn 2008

Vom Fachbereich Chemie

der Philipps-Universität Marburg als Dissertation

am 15.02.2008 angenommen.

Erstgutachter : Prof. Dr. M. A. Marahiel

Zweitgutachter : Prof. Dr. A. Geyer

Tag der Disputation: 17.03.2008

Dedicated to Katharina

Summary

Nonribosomal peptides (NRPs) constitute a large and diverse class of pharmacologically important natural products that find useful therapeutic application as immunosuppressants, antibiotics, or anticancer agents. The biological activity of many of these compounds relies on the macrocyclic structure of their peptide backbone and the incorporation of a wide assortment of building blocks including proteinogenic and nonproteinogenic amino acids as well as modified fatty acid moieties. Particularly, these structural features are key determinants of nonribosomal lipopeptide antibiotics that are in the focus of this thesis.

To provide rapid access to these structurally demanding compounds, a chemoenzymatic approach towards the synthesis of the lipopeptide antibiotics daptomycin and A54145 was developed, based on the combined utilization of powerful solid-phase peptide synthesis and the recombinant daptomycin and A54145 thioesterase (TE) domains. *In vitro* studies with these so-called peptide cyclases revealed their ability to catalyze the macrocyclization of linear peptidyl-thiophenol substrates with relaxed specificity for the cyclization nucleophile and electrophile. Ten lipopeptide variants were synthesized in order to explore the relatively sparse known acidic lipopeptide structure-activity relationship. Remarkably, this small library included a lipopeptide hybrid with a minimal inhibition concentration close to that of chemoenzymatic derived daptomycin as well as a bioactive macrolactam variant of A54145. Thus, single amino acid residues within the daptomycin and A54145 peptide sequences could be identified that are crucial for their antimicrobial potency.

Additionally, a unique and hitherto unknown type of imine macrocyclization as found for the cyanobacterial nostocyclopeptide (ncp) was investigated during the course of these studies. Experiments with ncp-CoA substrate mimics showed that a reductase (R) domain located at the C-terminal end of the ncp nonribosomal peptide synthetase (NRPS) is responsible for the reductive release of a reactive peptide aldehyde. Subsequently, imine macrocyclization occurs enzyme-independent under physiological pH conditions as proven with synthetic analogs of the ncp peptide aldehyde. An alanine scan experiment elucidated structural elements within the linear heptapeptide precursor that are essential for imine macrocyclization. Further, the biochemical characterization of ncp R also revealed its broad tolerance towards the C- and N-terminal amino acids of ncp substrate mimics.

In the third part of this work, the tailoring enzymes HxcO and HcmO from the calcium-dependent antibiotic (CDA) *trans*-2,3-epoxyhexanoic acid biosynthetic pathway were chosen as a model system to investigate fatty acid modification during nonribosomal lipopeptide synthesis. While HxcO was characterized as a novel type of enzyme with dual function as an FAD-dependent fatty acid oxidase paired with intrinsic epoxidase activity, HcmO could be identified as a second epoxidase acting on 2,3-unsaturated fatty acids. Experiments with acyl-CoAs, acyl-CoAs loaded onto an acyl carrier protein (ACP), and chemoenzymatically synthesized CDA variants revealed that both enzymes only accept ACP-bound substrates. To compare these ACP-bound HxcO and HcmO reaction products with synthetic standards a novel experimental approach had to be developed. Based on the thermodynamic activation inherent to thioester derivatives, the enzymatic products were cleaved from the ACP under mild conditions utilizing an amide ligation reaction and directly transformed into derivatives of smaller size suitable for HPLC-MS analysis. By the application of this versatile method the *trans*-2,3-epoxyhexanoic acid products of HxcO and HcmO were ascertained to have opposite absolute configuration, namely (2*R*,3*S*) and (2*S*,3*R*), respectively. In general, the established experimental approach holds great potential for the detailed analysis of all biochemical systems involving carrier protein-bound intermediates. These include integrated enzymes from NRPS and polyketide synthase (PKS) assembly lines or *in trans* acting tailoring enzymes.

Zusammenfassung

Nichtribosomale Peptide (NRPs) bilden eine große und vielseitige Klasse von pharmakologisch bedeutsamen Naturstoffen, die als Immunosupressiva, Antibiotika oder Antikrebs-Wirkstoffe nützliche therapeutische Anwendung finden. Die biologische Aktivität vieler dieser Verbindungen beruht auf der makrozyklischen Struktur ihres Peptidrückgrats und der Inkorporierung eines großen Sortiments an Bausteinen, das proteinogene und nicht-proteinogene Aminosäuren sowie modifizierte Fettsäurereste umfasst. Diese strukturellen Merkmale sind Schlüsseleigenschaften nichtribosomaler Lipopeptidantibiotika, die im Fokus dieser Arbeit stehen.

Um einen Zugang zu den strukturell anspruchsvollen Lipopeptiden Daptomycin und A54145 zu schaffen, wurde ein chemoenzymatischer Ansatz entwickelt, der auf dem kombinierten Einsatz von leistungsstarker Peptid-Festphasensynthese und rekombinanten Thioesterase-Domänen basiert. *In vitro* Studien mit diesen so genannten Peptidzyklasen zeigten deren Fähigkeit, lineare Peptidyl-Thiophenol-Substrate mit entspannter Substratspezifität zu zyklisieren. Zehn Lipopeptidanaloga wurden hergestellt, um die relativ unbekannte Struktur-Aktivitäts-Beziehung der aziden Lipopeptide zu erforschen. Bemerkenswerterweise enthielt diese kleine Bibliothek einen Lipopeptidhybrid mit einer minimalen Inhibitionskonzentration ähnlich der von chemoenzymatisch hergestelltem Daptomycin, sowie eine bioaktive A54145-Makrolactamvariante. Somit konnten einzelne Aminosäurereste in der Daptomycin- und A54145-Peptidsequenz identifiziert werden, die essentiell für deren antimikrobielle Eigenschaften sind.

Des Weiteren wurde im Rahmen dieser Arbeit eine bisher unbekannte Form der Iminmakrozyklisierung, wie sie für das cyanobakterielle Nostocyclopeptid (ncp) auftritt, untersucht. Experimente mit ncp-CoA-Substratmimikry zeigten, dass eine außergewöhnliche Reduktase (R)-Domäne, die sich am C-terminalen Ende der ncp nicht-ribosomalen Peptidsynthetase (NRPS) befindet, für die reduktive Freisetzung eines reaktiven Peptidaldehyds verantwortlich ist. Anschließend verläuft die Iminmakrozyklisierung enzymunabhängig unter physiologischen pH Bedingungen, was durch synthetische ncp-Aldehyde belegt werden konnte. Ein Alanin-Scan-Experiment identifizierte einzelne strukturelle Elemente im linearen Heptapeptidvorläufer, die entscheidend für den intramolekularen Zyklisierungsprozess sind.

Im dritten Teil dieser Arbeit wurden die CDA Tailoring Enzyme HxcO und HcmO des *trans*-2,3-Epoxyhexansäure Biosynthesewegs als Modellsystem gewählt, um die Fettsäuremodifikation in der Synthese nichtribosomaler Lipopeptide zu untersuchen. Während HxcO als ein neuer Enzymtyp mit dualer Funktion als FAD-abhängige Fettsäure-Oxidase mit intrinsischer Epoxidaseaktivität charakterisiert wurde, konnte HcmO als eine zweite Epoxidase identifiziert werden, die an 2,3-ungesättigten Fettsäuren arbeitet. Experimente mit Acyl-CoAs, Acy-CoA beladenem Acyl Carrier Protein (ACP) sowie chemoenzymatisch hergestellten CDA-Varianten ergaben, dass beide Enzyme nur ACP-gebundene Substrate akzeptieren. Um diese ACP-gebundenen Reaktionsprodukte mit synthetischen Standards vergleichen zu können, musste ein neuer experimenteller Ansatz entwickelt werden. Aufgrund der thermodynamischen Aktivierung von Thioesterderivaten, wurden die Enzymprodukte über eine Amidligationsreaktion unter milden Bedingungen vom ACP abgespalten und direkt in kleinere Derivate überführt, die für die HPLC-MS-Analyse geeignet sind. Es wurde ermittelt, dass die *trans*-2,3-Epoxyhexansäure-Produkte von HxcO und HcmO entgegensetzte absolute Konfiguration, nämlich (2*R*,3*S*) bzw. (2*S*,3*R*), besitzen. Der etablierte experimentelle Ansatz birgt ein hohes Potenzial für die Analyse aller biochemischen Systeme, die an Carrier Protein-gebundenen Intermediaten arbeiten, wie z.B. integrierte Enzyme aus NRPSs und Polyketidsynthasen (PKSs) oder andere *in trans* agierende Tailoring Enzyme.

The majority of the work presented here has been published:

Kopp F, Linne U, Oberthür M & Marahiel MA (2008): Harnessing the chemical activation inherent to carrier protein-bound thioesters for the characterization of lipopeptide fatty acid tailoring enzymes. *J. Am. Chem. Soc.*, online.

Kopp F & Marahiel MA (2007): Where chemistry meets biology: the chemoenzymatic synthesis of nonribosomal peptides and polyketides. *Curr. Opin. Biotechnol.* **18**: 513-520.

Kopp F & Marahiel MA (2007): Macrocyclization strategies in polyketide and nonribosomal peptide biosynthesis. *Nat. Prod. Rep.* **24**: 735-749.

Kopp F, Mahlert C, Grünewald J & Marahiel MA (2006): Peptide macrocyclization: the reductase of the nostocyclopeptide synthetase triggers the self-assembly of a macrocyclic imine. *J. Am. Chem. Soc.* **128**: 16478-16479.

Kopp F, Grünewald J, Mahlert C & Marahiel MA (2006): Chemoenzymatic design of acidic lipopeptide hybrids: new insights into the structure-activity relationship of daptomycin and A54145. *Biochemistry* **45**: 10474-10481.

Further publications of the author:

Enck S, **Kopp F**, Marahiel MA & Geyer A: Entropy loss of a peptide chain in macrocyclization. *Manuscript in preparation.*

Mahlert C, **Kopp F**, Linne U, Thirlway J, Micklefield J & Marahiel MA (2007): Stereospecific enzymatic transformation of alpha-ketoglutarate to (2S,3R)-3-methyl glutamate during acidic lipopeptide biosynthesis. *J. Am. Chem. Soc.* **129**: 12011-12018.

Strieker M, **Kopp F**, Mahlert C, Essen LO & Marahiel MA (2007): Mechanistic and structural basis of stereospecific C_β-hydroxylation in calcium-dependent antibiotic, a daptomycin-type lipopeptide. *ACS Chem. Biol.* **2**: 187-196.

Grünewald J, Mahlert C, **Kopp F** & Marahiel MA (2005): Chemoenzymatic pathways towards novel peptide antibiotics. *Curr. Med. Chem.* **5**: 227-243.

Grünewald J, **Kopp F**, Mahlert C, Linne U, Sieber SA & Marahiel MA (2005): Fluorescence resonance energy transfer as a probe of peptide cyclization catalyzed by nonribosomal thioesterase domains. *Chem. Biol*. **12**: 873-881.

Table of contents

Inhaltsverzeichnis

1 Abbreviations

aa	amino acid
Ac	acetyl
AcOH	acetic acid
ACP	acyl carrier protein
A domain	adenylation domain
Aloc	allyloxycarbonyl
Amp	ampicillin
AMP	adenosine-5'-monophosphate
ADP	adenosine-5'-diphosphate
AT	acyltransferase
ATP	adenosine-5'-triphosphate
Boc	tert-butyloxycarbonyl
bp	base pairs
BSA	bovine serum albumin
calcd.	calculated
CDA	calcium-dependent antibiotic
C domain	condensation domain
CoA	coenzyme A
CP	carrier protein
Cy domain	heterocyclization domain
Da	Dalton
DCC	dicyclohexylcarbodiimide
DCM	dichloromethane
Dec	decanoyl
DHB	dihydroxybenzoyl
DMSO	dimethyl sulfoxide
DIPEA	diisopropylethylamine
DMF	N,N-dimethylformamide
DH	dehydratase
dNTP	2'-desoxynucleosid-5'-triphosphate
E domain	epimerization domain
EDCI	1-(3-dimethylaminopropyl)-3-ethylcarbodiimide
EDTA	ethylene-diamino-tetraacetic acid
ESI-MS	electron spray ionization – mass spectrometry
eq.	equivalent
ER	enoylreductase
FA	fatty acid
FAAL	fatty acyl-AMP ligase
FAD	flavin adenine dinucleotide
FAS	fatty acid synthase
Fen	fengycin
FMN	flavin mononucleotide
Fmoc	9-fluorenylmethyloxycarbonyl
FPLC	fast performance liquid chromatography
FT-MS	Fourier-transform mass spectrometry
h	hours
HBTU	2-(1H-benzotriazole-1-yl)-1,1,3,3-tetramethyluronium hexafluorophosphate
Hepes	2-N'-[N-(2-hydroxylethyl)-piperazinyl]-ethansulfonic acid

Hex	hexanoyl
HOBt	1-hydroxybenzotriazole
HPLC	high performance liquid chromatography
IPTG	isopropyl-β-D-thiogalactoside
Kan	kanamycin
KR	ketoreductase
KS	ketosynthase
Kyn	kynurenine
LB medium	Luria-Bertani medium
LC/MS	liquid chromatography/mass spectrometry
LG	leaving group
MALDI-TOF	matrix assisted laser desorption ionization-time of flight
MCS	multiple cloning site
ME	methylation
MIC	minimal inhibitory concentration
Min	minutes
MS	mass spectrometry
MW	molecular weight
n.d.	not detected
NADH	nicotinamide adenine dinucleotide
NADPH	nicotinamide adenine dinucleotide phosphate
Ncp	nostocyclopeptide
NMR	nuclear magnetic resonance
NRP	nonribosomal peptide
NRPS	nonribosomal peptide synthetase
NTA	nitrilotriacetate
OD	optical density
PAGE	polyacrylamide gel electrophoresis
PCP	peptidyl carrier protein or thiolation domain
PCR	polymerase chain reaction
PEGA	poly(ethylene glycol)acrylamide copolymer
PK	polyketide
PKS	polyketide synthase
PheGly	phenylglycine
PLP	pyridoxal phosphate
ppan	4'-phosphopantetheine
PP_i	inorganic pyrophosphate
PPTase	4'-phosphopantetheine transferase
PyBOP	benzotriazole-1-yl-oxy-tris-pyrrolidino-phosphonium hexafluorophosphate
R domain	reductase domain
rpm	rounds per minute
RT	room temperature
SAM	S-adenosylmethionine
SDS	sodium dodecylsulfate
Sfp	4'-phosphopantetheine transferase involved in surfactin production
SNAC	N-acetylcysteamine
SPPS	solid-phase peptide synthesis
SPh	thiophenol
Srf	surfactin
tBu	tert-butyl

TCEP	tris(carboxyethyl)phosphine
TE domain	thioesterase domain
TFA	trifluoroacetic acid
TFE	trifluoroethanol
THF	tetrahydrofuran
TIPS	triisopropylsilane
t_R	retention time
Trt	trityl
v/v	volume per volume
w/v	weight per volume

Table 1.1: Proteinogenic amino acids: abbreviations and molecular weights.

Amino acid	3-Letter code	1-Letter code	MW[g/mol]
alanine	Ala	A	89
arginine	Arg	R	174
asparagine	Asn	N	132
aspartate	Asp	D	133
cysteine	Cys	C	121
glutamine	Gln	Q	146
glutamate	Glu	E	147
glycine	Gly	G	75
histidine	His	H	155
isoleucine	Ile	I	131
leucine	Leu	L	131
lysine	Lys	K	146
methionine	Met	M	149
phenylalanine	Phe	F	165
proline	Pro	P	115
serine	Ser	S	105
threonine	Thr	T	119
tryptophan	Trp	W	204
tyrosine	Tyr	Y	181
valine	Val	V	117

2 Introduction

Nonribosomal peptides (NRPs) and polyketides (PKs) have been the source for a multitude of therapeutic agents used in different medical fields including infectious diseases (daptomycin), cancer (epothilone) or immunosupression (cyclosporine) [1-3]. These molecules are biosynthesized by the consecutive condensation of amino acids or acyl-CoAs, which is achieved by large multi-domain enzymes, termed nonribosomal peptide synthetases (NRPSs) and polyketide synthases (PKSs) that follow a parallel biosynthetic mechanism.

Remarkably, the complex chemical scaffolds of these valuable compounds mostly have restricted conformations for selective recognition by their specific molecular receptors. The required molecular constraints are typically introduced by thioesterase (TE) domains at the C-terminal end of the biosynthetic assembly lines that catalyze the formation of intramolecular covalent linkages between distant parts of the molecule. In addition to being cyclic, nonribosomal peptides often have a second outstanding structural feature necessary for proper biological activity: the presence of highly diverse monomer building blocks. Besides the 20 canonical amino acids, various pathway-specific enzymes are responsible for the production of the unusual monomer units that include modified amino acids as well as functionalized fatty acid moieties.

This introduction chapter aims to give a brief outline of NRPS and PKS biosynthetic principles with a focus on macrocyclization and precursor biosynthesis. Special attention will be given to the class of acidic lipopeptide antibiotics, which are addressed separately in the last paragraph.

2.1 Versatility of macrocyclization strategies in complex natural products

Many diverse natural products, including polyketides, nonribosomal peptides and other biologically active peptides and proteins have restricted conformations for their selective recognition by biological targets. A common strategy employed by nature to achieve this aim is the introduction of an intramolecular covalent linkage between distant parts of the molecule. Thereby the immense number of possible conformations of linear molecules is dramatically reduced, and the proper orientation of the bioactive molecule, required for the specific interaction with the receptor protein, becomes entropically favored [4]. Additionally, macrocyclization leads to an increased physicochemical stability of the

corresponding compound and confers protection against enzymatic degradation by peptidases [5].

2.1.1 Macrocyclic nonribosomal peptides

Among the multitude of nonribosomal peptides different types of macrocyclization strategies can be found that principally vary in two major respects - the nature of the chemical bond and the type of cyclic structure formed.

The peptide antibiotic tyrocidine (Figure 2.1) for example, is cyclized "head-to-tail" via an amide bond linkage between the N-terminal D-Phe$_1$ and the C-terminal Leu$_{10}$ of the linear decapeptide chain [6, 7]. In addition to this type of closed structure, branched-cyclic peptidolactams and -lactones exist, as illustrated by bacitracin and the last-resort antibiotic daptomycin [8-10]. In the case of the dodecapeptide bacitracin, amide bond formation occurs between the C-terminal Asn$_{12}$ residue and an amino nucleophile arising from the ε-amino group of Lys$_6$. A similar lariat structure is displayed by daptomycin, but the side chain nucleophile is the hydroxyl group of Thr$_4$ instead of an amine, resulting in an intramolecular ester bond with the C-terminal kynurenine (Kyn).

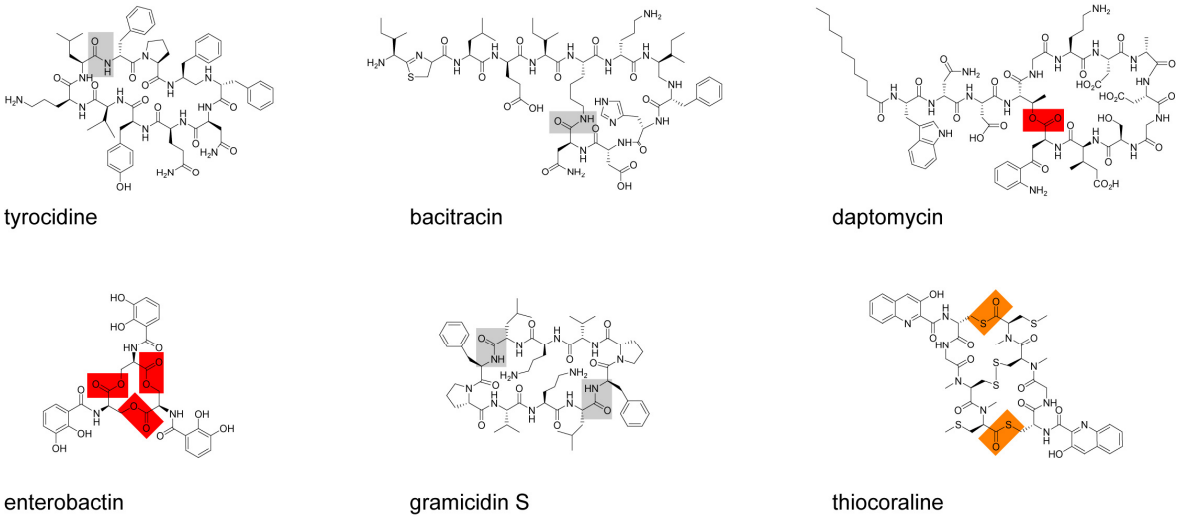

Figure 2.1: Macrocyclic nonribosomal peptides. Amide bonds are indicated in grey, esters in red and thioesters in orange.

A variation of this type of macrocyclization is present in the cyclooligomerized nonribosomal peptides, including the trilactone enterobactin (Figure 2.1) [11]. This iron-chelating siderophore, produced by *Escherichia coli*, is built up by the trimerization of 2,3-dihydroxybenzoyl-seryl dipeptide units to generate a 12-membered macrocyclic ring. Analogously, the decapeptide antibiotic gramicidin S consists of two identical pentapeptides that are linked to each other head-to-tail by the formation of two amide

bonds [12]. Among those cyclooligomerized compounds, an unusual thioester variant is displayed by the antitumor agent thiocoraline [13]. This two-fold symmetric octapeptide with DNA intercalating properties is cyclized via two thioester bonds between the SH group of the D-Cys_1 side chain and the C-terminal Cys_4 of each monomer. Interestingly, a second molecular constraint is introduced to this molecule by an additional disulfide bridge that actually divides the thiodepsipeptide into a bicyclic compound.

Another modification concerning the nature of the macrocycle forming chemical bond occurs for the nostocyclopeptide (Figure 2.2), a cytotoxin produced by the terrestrial cyanobacterium *Nostoc* sp. ATCC53789 [14]. Instead of the well-known formation of an amide, ester or thioester bond, a stable imino bond covalently links both ends of the linear heptapeptide chain in this case. One of the most exceptional natural products in this class of compounds is the potent telomerase inhibitor telomestatin (Figure 2.2) [15]. This highly constrained molecule is built up by eight heterocycles - five oxazoles, two methyloxazoles and one thiazoline derived from serines, threonines and cysteines respectively - that are directly linked to each other. Remarkably, by amino acid side chain heterocyclization a second level of molecular constraint is introduced into this astonishing macrocyclic molecule.

nostocyclopeptide A2 telomestatin

Figure 2.2: The nostocyclopeptide A2 contains an intramolecular imino bond indicated in orange. In telomestatin macrocyclization is achieved via the formation of eight heterocycles indicated in grey.

2.1.2 Macrocyclic polyketides and polyketide/nonribosomal peptide hybrids

As for nonribosomal peptides, similar macrocyclization strategies are employed by nature during the synthesis of polyketides. In PKS assembly lines, the nucleophiles for intramolecular macrocyclization commonly arise from hydroxyl groups, leading to the formation of lactones. Such scaffolds can be found for the 12-membered 10-deoxymethynolide or the 14-membered 6-deoxyerythronolide B, the aglycones of the macrolide antibiotics methymycin and erythromycin (Figure 2.3) [16-19]. Macrocyclic

lactams are displayed by the ansa-bridged antibiotics rifamycin and geldanamycin (Figure 2.3) [20, 21].

As the parallel logic of type I PKS and NRPS assembly line machinery suggests, there are natural products that are polyketide/nonribosomal peptide hybrids [22]. Based on similar molecular architecture, nature has mixed NRPS and PKS modules into hybrid assembly lines that produce such valuable compounds as the immunosuppressant FK506 or the antitumor agent epothilone (Figure 2.3) [23-25].

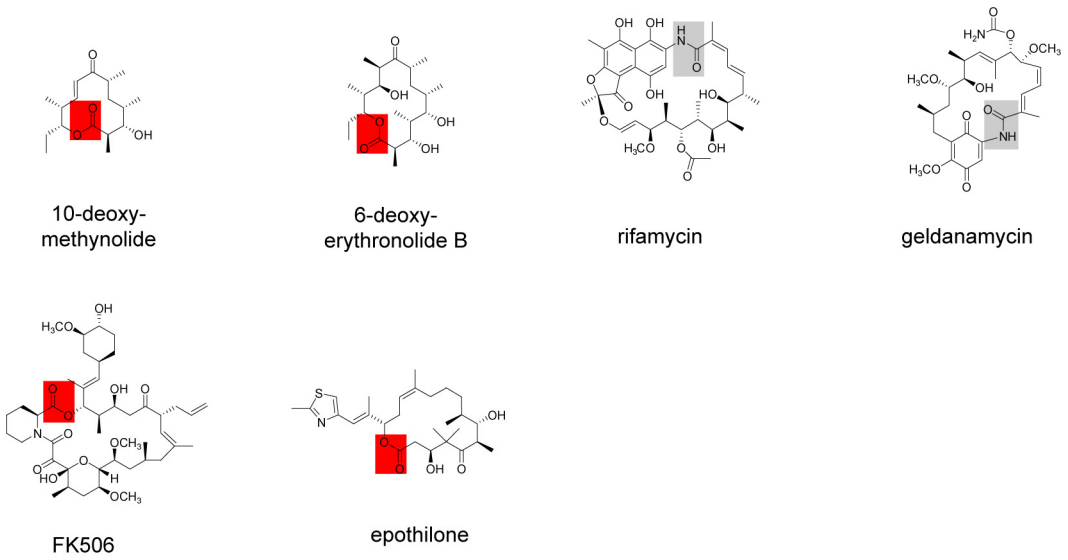

Figure 2.3: Macrocyclic polyketides and NRPS/PKS hybrid molecules. Amide bonds are indicated in grey, esters in red.

2.1.3 Macrocyclic ribosomal peptides

The existence of other naturally occurring macrocyclic peptides with ribosomal origin impressively underlines the fact that biological activity often relies on conformationally constrained structures. Lantibiotics, as the model compound nisin for example (Figure 2.4), are ribosomally synthesized antimicrobial agents that show cyclic structural elements [26, 27]. Specifically, extensive post-translational modification, including the enzyme assisted formation of five characteristic thioether rings, is required for the proper functionality of this 34-residue peptide. After the dehydration of serine and threonine to 2,3-dehydroalanine and 2,3-dehydrobutyrine residues, respectively, a single zinc-dependent enzyme catalyzes five distinct cyclization reactions to generate the typical lanthionine and methyllanthionine thioether bridges [28].

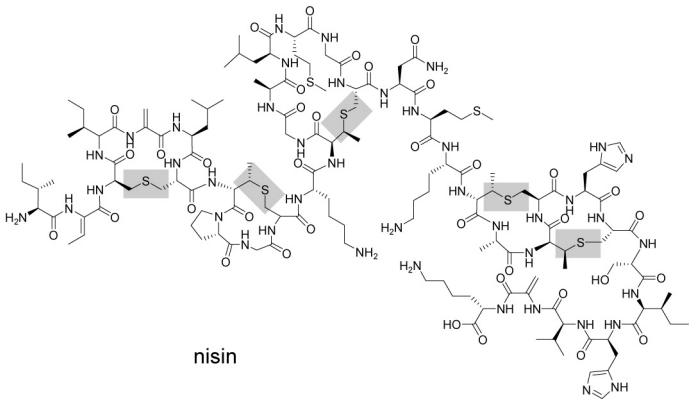

Figure 2.4: The lantibiotic nisin contains five macrocyclic rings formed by lanthionine thioether bridges as indicated.

2.2 NRPS assembly line logic: synthesis of the peptide backbone

The unique structures of many hundreds of nonribosomal peptides share a common mode of synthesis that is achieved by modularly organized enzymes termed NRPSs. These multienzyme complexes simultaneously specify the sequence of the peptide products and catalyze all necessary chemical reactions for the activation and subsequent condensation of the amino acid building blocks [29-31]. In principle, NRPSs are comprised of an array of distinct modular sections, each of which is responsible for the incorporation of one defined monomer into the final peptide product. Consequently, in linear NRPSs, the number of these so-called modules exactly matches the number of amino acids found in the backbone of the corresponding peptide (Figure 2.5) [32].

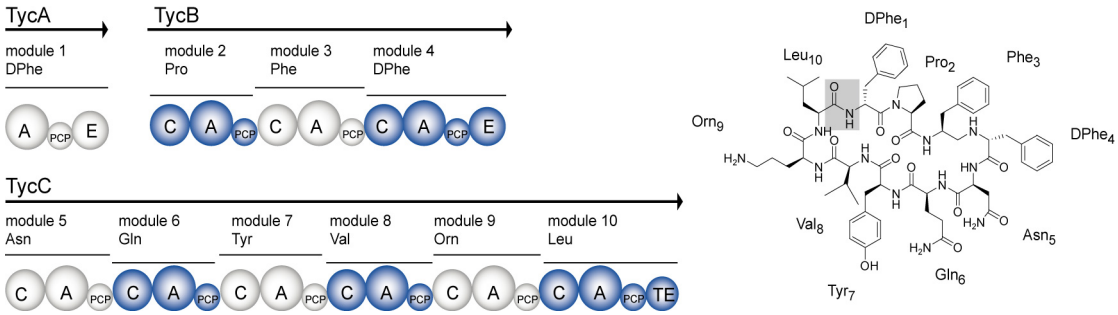

Figure 2.5: Molecular organization of the tyrocidine biosynthetic complex. The tyrocidine synthetase consists of three subunits, TycA, TycB, and TycC. The identity and order of modules, indicated in blue and grey shades, direct the incorporation of the amino acid building blocks into the peptide backbone of tyrocidine. The modules can be further dissected into independent catalytic domains (C, A, PCP, E, and TE) that catalyze the single synthetic steps during peptide assembly.

Modules can be further subdivided into catalytically active domains, each responsible for a specific synthetic step during peptide production. At least three essential domains are

needed to carry out the elongation of a growing peptide chain for one amino acid residue (Figure 2.6).

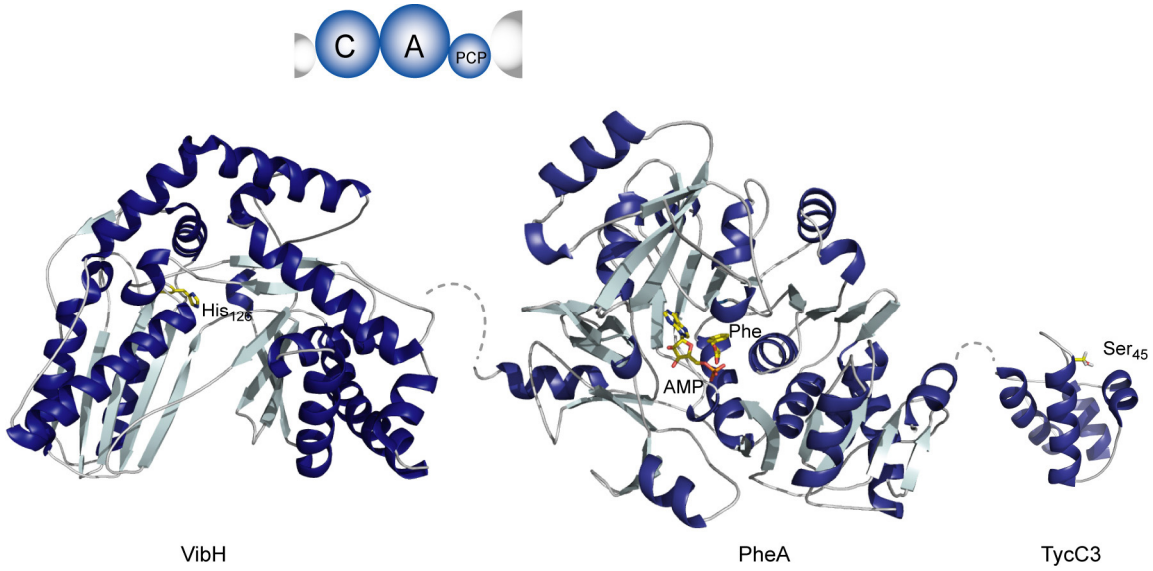

Figure 2.6: 3-D structures of NRPS core domains. The minimum set for the elongation of a growing peptide chain by one amino acid residue consists of a condensation domain (C), an adenylation domain (A), and a peptidyl carrier protein (PCP). Structures of the stand-alone C domain (VibH) from the vibriobactin synthetase, the A domain (PheA) from the first module of the gramicidin S synthetase, and the PCP (TycC3) from the tyrocidine biosynthetic complex are shown. Indicated in yellow are the catalytically active His residue of the C domain, the A domain bound amino acid substrate with AMP, and the phosphopantetheinylation site of the PCP.

The first step in nonribosomal synthesis is the selection of a specific amino acid from the pool of available substrates by an adenylation domain (A domain; ~500 amino acids), followed by the generation of an aminoacyl-AMP mixed anhydride (Figure 2.7) [33]. This reactive intermediate is further transferred onto the thiol moiety of a 4'-phosphopantetheine (ppan) prosthetic group that is attached to a peptidyl carrier protein (PCP; ~100 amino acids) [34]. The PCP, also referred to as a thiolation domain, is responsible for the transport of the resulting energy-rich thioester-bound substrates and all elongation intermediates between the catalytic active domains. In the next step of nonribosomal peptide synthesis, peptide bond formation is mediated by so-called condensation domains (C domains; ~450 amino acids). The C domain catalyzes the nucleophilic attack of the downstream PCP-bound acceptor amino acid with its α-amino group onto the activated thioester of the upstream PCP-bound donor amino acid or peptide (Figure 2.7) [35, 36]. The resulting peptidyl-intermediate is thereby translocated down the NRPS assembly line for subsequent condensation and modification steps.

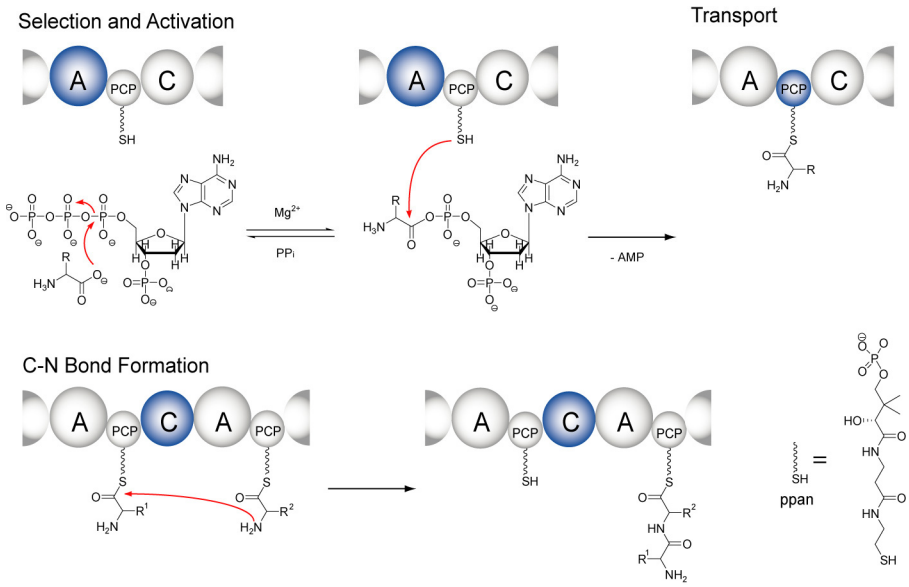

Figure 2.7: Chemical reactions catalyzed by NRPS core domains. Peptide assembly starts with the selection of a specific amino acid building block and formation of an aminoacyl-AMP by an A domain. The activated amino acid is subsequently transferred onto the free thiol of the PCP-bound cofactor phosphopantetheine (ppan). Amide bond formation occurs by the action of a C domain that mediates the nucleophilic attack of the downstream amino acid on the upstream electrophilic aminoacyl- or peptidyl-thioester. The growing peptidyl-intermediate is thereby translocated down the NRPS assembly line. Domains in action are highlighted in blue.

2.3 Peptide release mechanisms

2.3.1 The thioesterase domain

When the full-length peptide chain has reached the ultimate PCP, it has to be cleaved off from the covalent tethering in order to release the mature product and to regenerate the multienzyme complex for the next catalytic cycle. Most commonly, this disconnection from the NRPS is carried out by a C-terminal thioesterase domain (TE domain; ~280 amino acids) that serves as a chain termination catalyst [37, 38]. In the last biosynthetic step, the linear peptide chain is transferred to a catalytically active serine residue of the TE domain and the so called acyl-O-TE intermediate is formed. Depending on the nature of the NRPS template, there are two possibilities for further reaction: sometimes hydrolysis leads to the formation of linear peptide acids as observed during the biosynthesis of the vancomycin-type antibiotics. More commonly for compounds of medicinal interest, the reaction with intramolecular nucleophiles results in cyclic structures as represented by the macrolactone daptomycin (Figure 2.8).

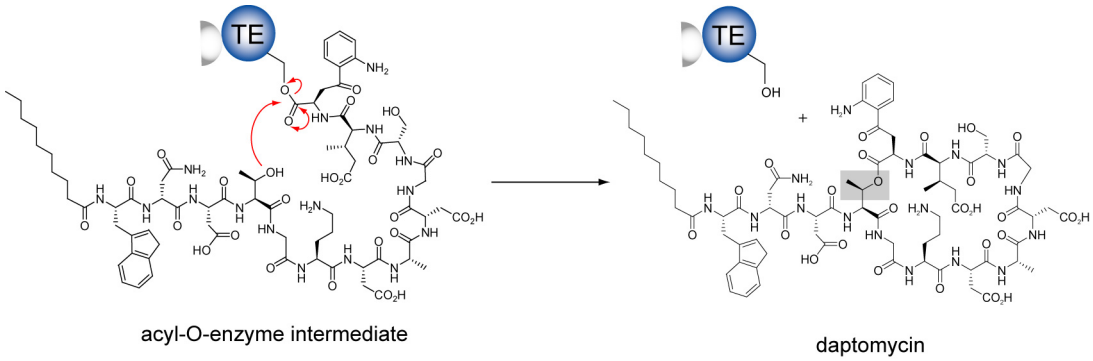

Figure 2.8: Enzymatic peptide cyclization during daptomycin biosynthesis. A thioesterase (TE) domain catalyzes the formation of the characteristic 10-membered macrolactone ring. The acyl-O-TE intermediate is cleaved by the attack of a threonine side chain nucleophile onto the activated C-terminus and the cyclized product is released from the modular assembly line.

Significant progress towards the understanding of the principles underlying TE-mediated peptide cyclization has been made by solving the crystal structures of the excised TE domains from the surfactin (Srf) and fengycin (Fen) NRPSs [39, 40]. TE domains belong to the α/β-hydrolase superfamily that includes diverse enzymes such as lipases, proteases and esterases. Thus, TE domains possess a conserved catalytic triad of Asp, His and Ser which forms the active site.

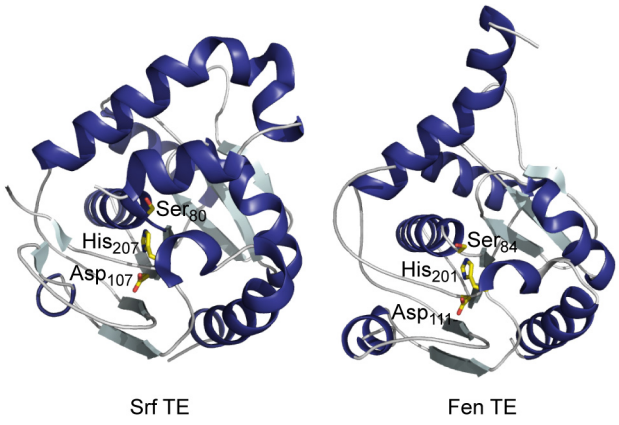

Figure 2.9: Crystal structures of the thioesterase domains from the surfactin synthetase (Srf TE) and the fengycin synthetase (Fen TE). The conserved catalytic triad (Asp-His-Ser) is indicated in yellow.

The overall structure of Srf and Fen TE has been described as a globular α/β-sandwich, corresponding to the characteristic α/β-hydrolase fold that lacks the commonly found amino terminal β-strand. Like other bacterial lipases, these two proteins contain a characteristic insertion between core β-strands, also referred to as the lid region. Sequence alignments showed that this lid region can significantly differ between single TE domains. For Srf TE, this structurally flexible part of the protein is extended over three α-helices and can adopt two distinct conformations. In the "open" state of the enzyme the lid is folded back, allowing access to the active site cavity, whereas in the closed state the active site is

covered almost completely by this part of the enzyme. Hence, an important role for this part of the Srf TE in substrate binding and catalysis has been deduced. In contrast to this, the lid region of Fen TE is the shortest observed for NRPS TE domains. This results in an open structure of the Fen TE active site with a freely accessible catalytic triad. In this case, the lid region seems to have a more indirect influence on substrate recognition and may simply serve as a "sieve" for sterically demanding substrates. Taken together, the general role of the lid region can not be finally defined at this point, and further crystallographic studies might be necessary to clarify its function in stereo- and regioselective peptide cyclization.

Additionally, the crystal structures enabled the identification of enzyme-substrate interaction sites and underlined the importance of substrate preorganization for the regioselective intramolecular cyclization reaction. Srf TE, for example, has bowl shaped active site geometry, forming a distinct cavity large enough to host the surfactin heptapeptide substrate. Within this predominantly hydrophobic environment, two positively charged amino acids Lys_{111} and Arg_{120} were experimentally confirmed to be crucial in substrate binding via the coordination of the negatively charged residues Glu_1 and Asp_5 of the surfactin peptide sequence [41]. Similarly, Fen TE exhibited binding sites for the C-terminal amino acid Ile_{11} of the fengycin decapeptide and a model of the fengycin substrate binding was deduced, suggesting that the substrate specificity of NRPS TE domains is mostly dependent on both, the electrophilic and the nucleophilic amino acid residues of the peptidyl substrate [40].

2.3.2 TE-independent chain termination

Alternative TE-independent routes of chain termination are mediated by other assembly line domains, which can replace the canonical TE domain in several NRPS systems [42]. The NRPSs of myxochelin or linear gramicidin, for example, contain a relatively rare C-terminal reductase domain (R domain; ~350 amino acids). In these cases the associated compounds are linear alcohols or amines, arising from further enzymatic modification of the initially formed peptide aldehydes [43, 44]. Additionally, it has been shown during the course of this study that R domains can also trigger the formation of macrocyclic imines such as the nostocyclopeptide A2 (Figure 2.2) [14, 45].

In addition to NAD(P)H-dependent R domains, C domains can also be implicated in peptide release. The formation of the head-to-tail linkage between the amino group of D-Ala_1 and the carbonyl group of L-Ala_{11} of the immunosuppressant cyclosporine, for example, is predicted to be performed by a C-terminal C domain [46]. Usually, C domains

catalyze the nucleophilic attack of an α-amino group of a downstream PCP-bound amino acid on the upstream thioester-linked peptide or amino acid. The C domain of the cyclosporine synthetase is proposed instead to function in an analogous manner, but the nucleophile is an intramolecular amino group, rather than the next amino acid building block.

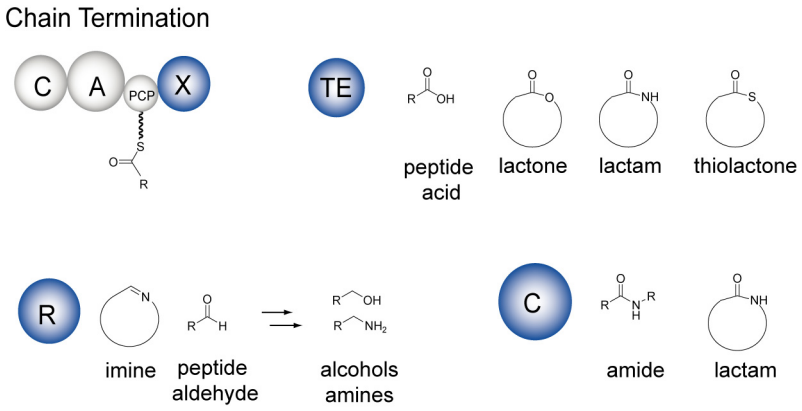

Figure 2.10: Chain termination strategies found in NRPSs. The C-terminal module in NRPS assembly lines ends with a thioesterase (TE), a reductase (R), or a condensation (C) domain. In some cases, TE domains release the mature peptide chain by hydrolysis; predominantly cyclization via intramolecular nucleophiles occurs. R domains are involved in the formation of peptide aldehydes, which spontaneously form a macrocyclic imine or are further enzymatically modified to alcohols or primary amines. Sometimes the TE domain function can be replaced by a C domain.

2.4 Chemoenzymatic strategies towards cyclic peptides

With the genomic sequences of several antibiotic-producing microbes available, there have been sophisticated efforts to reengineer secondary metabolite biosynthetic pathways *in vivo* for the production of novel structural variants [3, 47, 48]. This has led to a robust platform for the generation of structural diversity, as recently illustrated for acidic lipopeptide antibiotics by Cubist pharmaceuticals [49-51]. However, a major challenge of these labour intensive genetic engineering approaches remains the size of new compound libraries, due to the time consuming construction of genetically manipulated organisms. On the other hand, classical chemical methodology can provide access to altered natural products, but usually involves multistep organic synthesis and can also suffer from low yields caused by inefficient acyl chain macrocyclization methods [52]. Confronted with these hurdles, the past seven years have seen a rapid increase in the development of alternative chemoenzymatic synthesis approaches towards bioactive macrocyclic nonribosomal peptides and polyketides [37, 38, 53, 54].

The chemoenzymatic synthesis of macrocyclic nonribosomal peptides combines powerful chemical methods for the generation of the linear precursor molecules by solid-phase peptide synthesis (SPPS) with stereo- and regioselective enzymatic macrocyclization. To activate the artificial substrates, they are C-terminally coupled with the short cofactor mimic N-acetylcysteamine (SNAC) that imitates the natural situation where the mature acyl chain is bound to the biosynthetic machinery via the cofactor 4'-phosphopantetheine (Figure 2.11). Upon incubation with the recombinant TE, the reactive SNAC-thioesters are nucleophilically attacked by the catalytic triads' serine residue and regioselective macrocyclization occurs. In some cases, for example during the chemoenzymatic synthesis of fengycin and mycosubtilin, the use of different substrate activation strategies, such as the thiophenol leaving group, commonly used in native chemical ligation, revealed superior yields, due to improved reaction kinetics [55, 56].

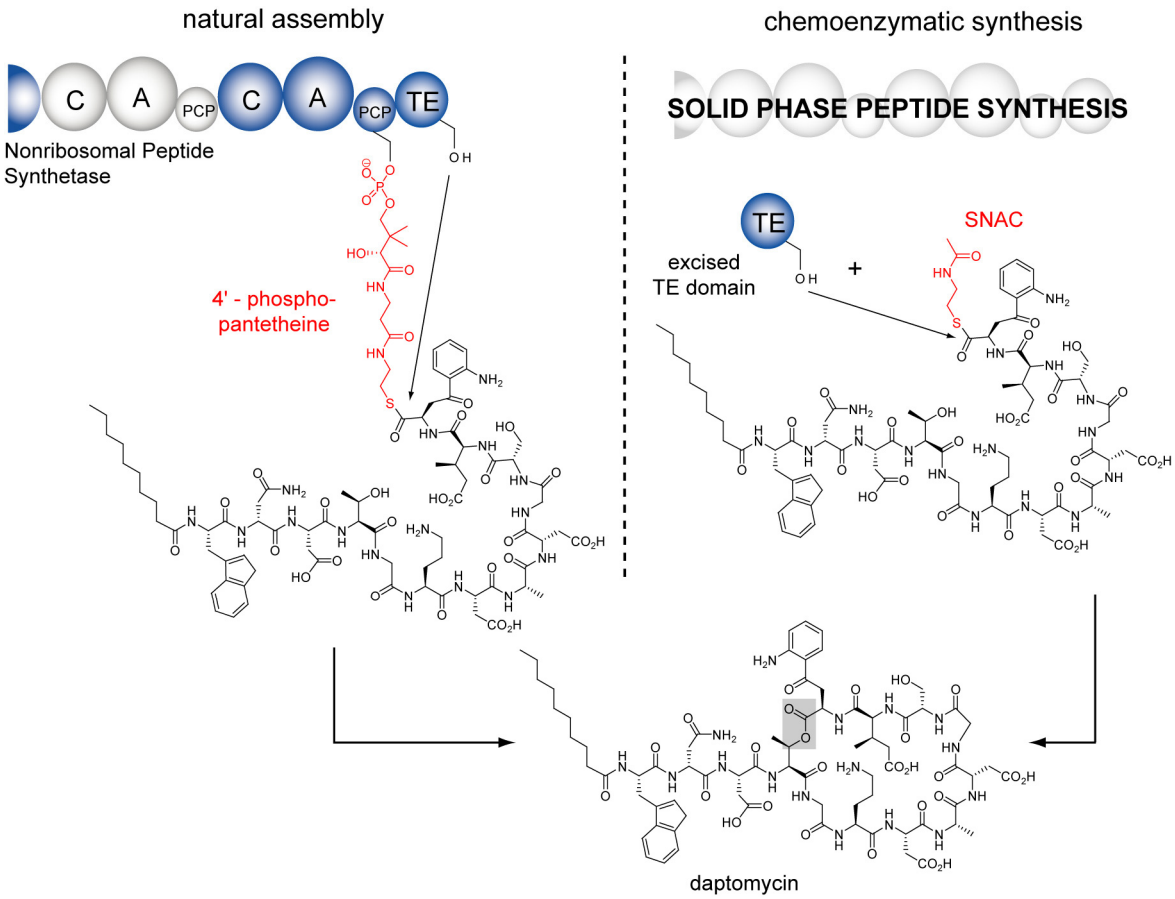

Figure 2.11: Natural vs. chemoenzymatic peptide cyclization. During nonribosomal peptide biosynthesis, as shown for daptomycin, the mature linear peptide chain is bound to a peptidyl carrier protein (PCP) of the NRPS via the cofactor 4'-phosphopantetheine. The reactive thioester is subsequently attacked by the catalytically active serine residue and macrocyclization occurs. For the chemoenzymatic synthesis of macrocyclic peptides artificial substrates are provided by chemical means, for example powerful solid-phase peptide synthesis (SPPS), and C-terminally activated with the cofactor mimic N-acetylcysteamine (SNAC). After incubation with the recombinant TE domain, stereo- and regioselective macrocyclization is efficiently catalyzed.

Initial contributions from the Walsh group impressively demonstrated that TE domains excised from biosynthetic assembly lines can act as versatile tools for the *in vitro* macrocyclization of chemically derived peptide substrates [7, 57-60]. Especially powerful SPPS enabled detailed studies on the substrate tolerance of several NRPS TE domains and provided rapid access to a multitude of synthetically demanding compounds with clinical relevance including for example the antibiotic tyrocidine [7, 57-60], type B streptogramins [61, 62], or potential anticancer agents of the cryptophycin class [63, 64].

2.5 Enzymatic tailoring of NRP scaffolds

2.5.1 The diverse building blocks of nonribosomal peptides

A diagnostic feature of nonribosomal peptides is the presence of a wide variety of amino acid monomers that are not found in proteins and peptides with ribosomal origin. In addition to the rather uniform set of 20 canonical L-amino acids, NRPs include D-configured, α,β-unsaturated, and β-amino acids, or even fatty acid building blocks. This leads to a high density of functional groups and to a significant structural diversity, which is often closely connected to the biological activity of these complex compounds. While some of the utilized monomers are primary metabolites, many of them require dedicated free-standing enzymes that are clustered with the NRPS assembly line genes for coordinate regulation of precursor synthesis [65].

The lipopeptide antibiotics from the daptomycin-class, such as CDA, contain several nonproteinogenic amino acids including a conserved β-methylglutamate residue at the penultimate position of their peptide backbone (Figure 2.12). Together with *in vivo* data obtained by the Micklefield laboratory, the biochemical characterization of the recombinant methyltransferase GlmT from the CDA system showed that the corresponding β-keto acid is methylated with an electrophilic methyl group from S-adenosylmethionine (SAM) followed by transamination to yield the unique β-methylglutamate [66, 67]. Another intriguing monomer unit of CDA is a β-hydroxylated asparagine residue, which can even be further modified to β-phosphohydroxyasparagine in certain CDA variants (Figure 2.12). During biosynthesis, a non-heme FeII α-ketoglutarate-dependent oxygenase AsnO converts asparagine into β-hydroxyasparagine. This unusual amino acid is also part of the closely related lipopeptide A54145 [68, 69].

In addition to this, there are many secondary metabolites that contain halogenated amino acids, such as the indolocarbazole natural product rebeccamycin or the enediyne antitumor

compound C-1027. The unusual 7-chlorotryptophan residue of rebeccamycin, for example, arises from the chlorination of the electron rich tryptophan side chain by a flavin-dependent halogenase RebH (see also Discussion section). The chlorinated amino acid present in C-1027 is a 3-Cl-4,5-$(OH)_2$-β-phenylalanine residue. Recently, this outstanding chlorinated β-amino acid was shown to be generated out of tryptophan by extensive enzymatic tailoring [70].

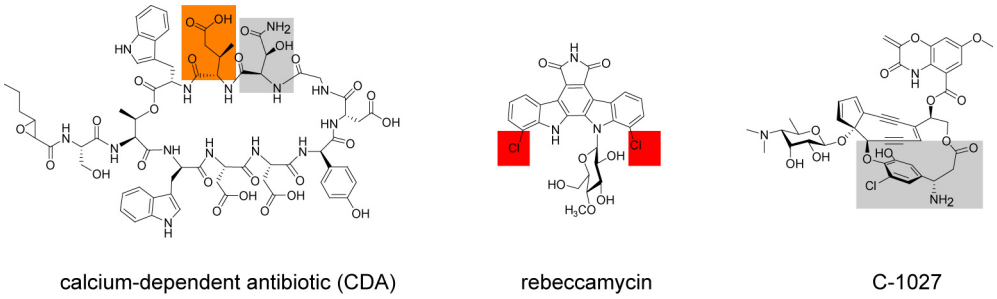

Figure 2.12: Structurally diverse amino acid building blocks found in nonribosomal peptides and related natural products.

The generation of the elaborated monomer building blocks of many nonribosomal peptides is achieved by enzymes acting on free amino acid substrates. Sometimes, in contrast, nature employs different strategies and precursor tailoring occurs on carrier protein-bound amino acids that are isolated from the cellular pool of substances.

2.5.2 Tailoring on assembly lines in cis and in trans

Besides the A domain, the PCP and the C domain, which together form the minimal set for the synthesis of a linear peptide, the modification of the monomer building blocks can be achieved by optional domains that are integrated parts of the NRPS assembly line machinery. These *in cis* acting tailoring enzymes include epimerization domains (E domain; ~450 amino acids) for the generation of frequently found D-configured amino acids (Figure 2.5) or N-methyl transferase domains (Me domain; ~420 amino acids) to control the methylation state of the peptide products. For example, seven out of the eleven residues in cyclosporine are N-methylated. Another remarkable alteration of backbone connectivity in NRP scaffolds occurs when cysteine, serine, or threonine side chains are intramolecularly cyclized and dehydrated to the thiazoline and oxazoline rings, respectively, by cyclization domains (Cy domain; ~450 amino acids) [71, 72]. In the biosynthesis of the previously mentioned telomestatin further enzymatic oxidation presumably leads to the finally observed oxazoles and thiazoles (Figure 2.2).

Additionally, tailoring enzymes working *in trans* as isolated proteins on assembly lines are known in literature and have been biochemically characterized. During the biosynthesis of the vancomycin-type glycopeptides, there are three heme iron monooxygenases, OxyA, -B, -C, that act to cross-link the heptapeptidyl-*S*-PCP, generating two aryl ether linkages between Tyr_2 and $PheGly_4$ and Tyr_6 and a direct C-C cross-link between $PheGly_5$ and $PheGly_7$ [73, 74]. Oxidative cross-linking significantly contributes to the rigidification of vancomycin or balhimycin – both molecules share the same aglycon – necessary to bind its biological target, the bacterial peptidoglycan D-Ala-D-Ala termini, with high affinity. Analogously, biosynthesis of coronamic acid (1-amino-1-carboxy-2-ethylcyclopropane), which is a building block of the pseudomonal phytotoxin coronatine, involves intermediates that are covalently bound to carrier proteins. The cyclopropyl ring is formed out of a γ-Cl-L-*allo*-Ile moiety, which is in turn produced by the chlorination of a L-*allo*-Ile-*S*-carrier protein substrate by a mononuclear non-heme iron halogenase [75, 76].

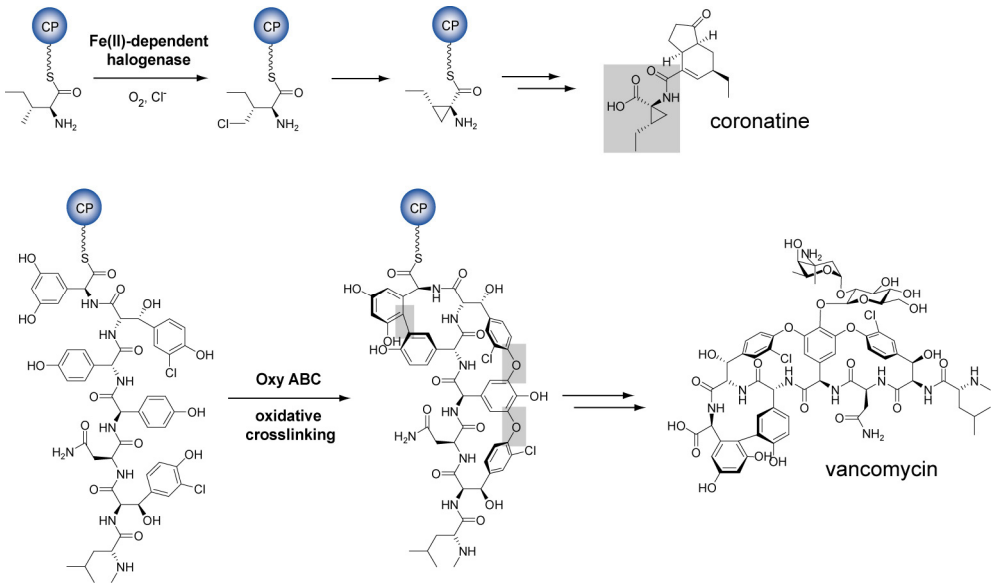

Figure 2.13: Enzymatic tailoring *in trans* to NRPS assembly lines occurs during coronatine and vancomycin biosynthesis. The unusual coronamic acid moiety of coronatine and the oxidative cross bridges of vancomycin are highlighted.

2.5.3 Post-assembly line tailoring

In this context it is worth noting that many NRPs can be enzymatically tailored in the state of the readily assembled molecule, which has been cleaved off from the molecular assembly line [65]. In the above discussed examples of vancomycin or the enediyne antitumor compound C-1027, the mature aglycon scaffolds are further decorated by the attachment of carbohydrates (Figure 2.12 and 2.13) [77, 78]. The incorporation of sugar

molecules can modulate the water-solubility of natural products since sugars contain hydroxyl groups or increase the affinity to biological macromolecules by serving as interaction partners for hydrogen bonding [79].

2.6 Biosynthetic analogies with other multimodular enzymes

2.6.1 Basic principles of polyketide assembly

Since PKSs and NRPSs follow a parallel synthetic logic, utilizing similar thioester chemistry and enzymatic macrocyclization strategies, it is very useful to compare both closely related types of assembly line-organized multienzyme complexes [1, 3, 80]. In contrast to the vast variety of monomer building blocks employed in nonribosomal peptide biosynthesis, structurally diverse PKs arise from the consecutive condensation of only a few simple acyl-CoA substrates. Acetyl-CoA, malonyl-CoA, and methylmalonyl-CoA, available from the microbial producer's primary metabolism, represent the monomer units for the acyl chain assembly and complexity is introduced by an iterative sequence involving ketone reduction, dehydration, and enone reduction.

Comparable to the function of an A domain, the acyltransferase domain (AT domain; ~450 amino acids) selects a distinct acyl-CoA substrate to be incorporated and transfers it to an acyl carrier protein (ACP; ~100 amino acids), where it is bound as a thioester to a ppan arm (Figure 2.14). C–C bond formation between two acyl-thioesters is catalyzed by the ketosynthase domain (KS domain; ~400 amino acids), analogous to the role of a C domain in nonribosomal peptide biosynthesis. The KS domain transiently binds the upstream acyl substrate, which is nucleophilically attacked by the downstream thioester enolate intermediate resulting from previous decarboxylation.

Together, the KS-AT-ACP catalytic domains represent the catalytic core set required for each chain elongation step. In addition to this obligatory repeating unit, ketoreductase (KR), dehydratase (DH), and enoylreductase (ER) domains can be embedded in the multienzyme for further diversification of the condensation product. In full analogy to nonribosomal peptide biosynthesis, the most downstream domain within PKS assembly lines is usually a dedicated thioesterase (TE) domain that performs the regio- and stereospecific formation of a macrolactone between a hydroxyl group on the polyketide chain and the enzyme-bound oxoester.

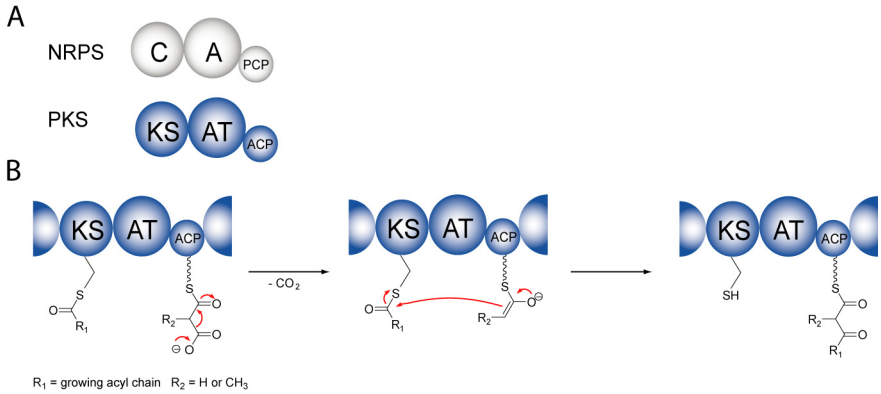

Figure 2.14: A: Template-directed polyketide and nonribosomal peptide assembly follows a parallel biosynthetic logic. The core set of domains required for polyketide synthesis consists of a ketosynthase (KS), an acyltransferase (AT) and an acyl carrier protein (ACP). The KS domain catalyzes C–C bond formation, the AT domain selects and activates a distinct monomer, and the ACP carries the thioester intermediates bound to the cofactor phosphopantetheine (ppan). B: A Claisen condensation leads to C-C bond formation during polyketide biosynthesis. Decarboxylation of the downstream ACP-bound (methyl)malonyl unit leads to the generation of a nucleophilic ester enolate that subsequently attacks the upstream KS-bound acyl chain.

The close relationship between both, NRPS and PKS biosynthetic logic, is reflected by the existence of NRPS/PKS hybrids. In those mixed biosynthetic machineries, catalytic domains from both types of systems act together in assembly line fashion or as distinct enzymes, and produce mixed NRP/PK hybrids such as epothilone or FK 506 (Figure 2.3) [22].

2.6.2 Fatty acid synthesis in primary metabolism

Another even closer relationship exists between PKSs and fatty acid synthases (FASs) that are involved in primary metabolism as reviewed by Lu and White [81, 82]. FASs function very much like PKSs, starting with malonyl-CoAs as carbon monomers that are built from acetyl-CoA and CO_2 by biotin carboxylase [83, 84]. Through the action of malonyl-CoA-ACP transacylase (MAT) [85], malonyl-CoA is loaded onto an ACP to isolate the growing lipid chain from the cellular milieu (Figure 2.15). Next, a ketoacyl-ACP synthase III (KSIII) elongates the carbon chain via decarboxylative addition of malonyl-CoA on acetyl-CoA to give acetoacetyl-ACP, the starter unit for fatty acid synthesis [86]. The β-carbon of the ACP-bound intermediate undergoes subsequent reduction by a KR and dehydration by a DH before an ER fully reduces the Cβ-carbon to methylene. Further elongation of the resulting acyl-ACP proceeds in subsequent rounds of synthesis by other KSs, each of which catalyzes the condensation with an additional malonyl-ACP to extend the lipid chain by two carbon atoms. This process can be multiply repeated until the growing fatty acid chain has reached its specific length [87, 88].

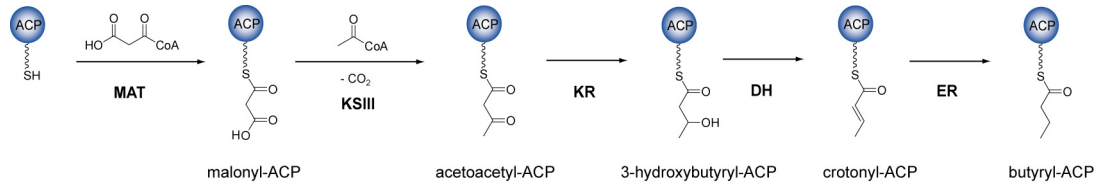

Figure 2.15: Reactions catalyzed by fatty acid synthases (FASs). Instead of forming a modular assembly line, the catalytic domains of type II FASs are independent proteins that interact with the ACP-bound substrate *in trans*.

According to their architectural configuration FASs and PKSs can be classified: FASs and PKSs from type I are similar to NRPSs multimodular proteins with molecular weights up to several hundred kilo Daltons containing the catalytic domains required for product extension. Type II FASs and PKSs function in full analogy to type I systems, but instead of forming a multi-domain assembly line each catalytic domain is a separate polypeptide chain that interacts with the ACP *in trans* [80]. In general, type I FASs accomplish fatty acid synthesis in the cytosol of eukaryotes [89-91], whereas type II FASs systems are found in prokaryotes and plants [92, 93].

2.7 Lipopeptide antibiotics

Among the multitude of medicinally relevant nonribosomal peptides, lipopeptide antibiotics such as daptomycin and the calcium-dependent antibiotic (CDA) are of considerable interest. The last-resort antibiotic daptomycin, for example, is highly active against multi-drug resistant pathogens including those resistant to vancomycin and represents the first member of a new structural class of natural antimicrobial agents to be approved for clinical use in over 30 years [94-97].

A structural key feature of such lipopeptide antibiotics is the eponymous long chain fatty acid, which is invariably attached to the macrocyclic peptide core. Straight and branched chain fatty acids that can significantly differ in the degree of saturation and the oxidation state are frequently found and contribute to the high structural diversity of this class of compounds (Figure 2.16). In particular, the lipid portion has a high impact on the biological properties of these molecules, since antimicrobial behavior and toxicity are dramatically affected by the nature of the incorporated fatty acid group [95, 98]. However, today we still lack a detailed understanding of the biochemical mechanisms underlying fatty acid incorporation in nonribosomal lipopeptides and the dedicated tailoring steps for the generation of modified fatty acid building blocks.

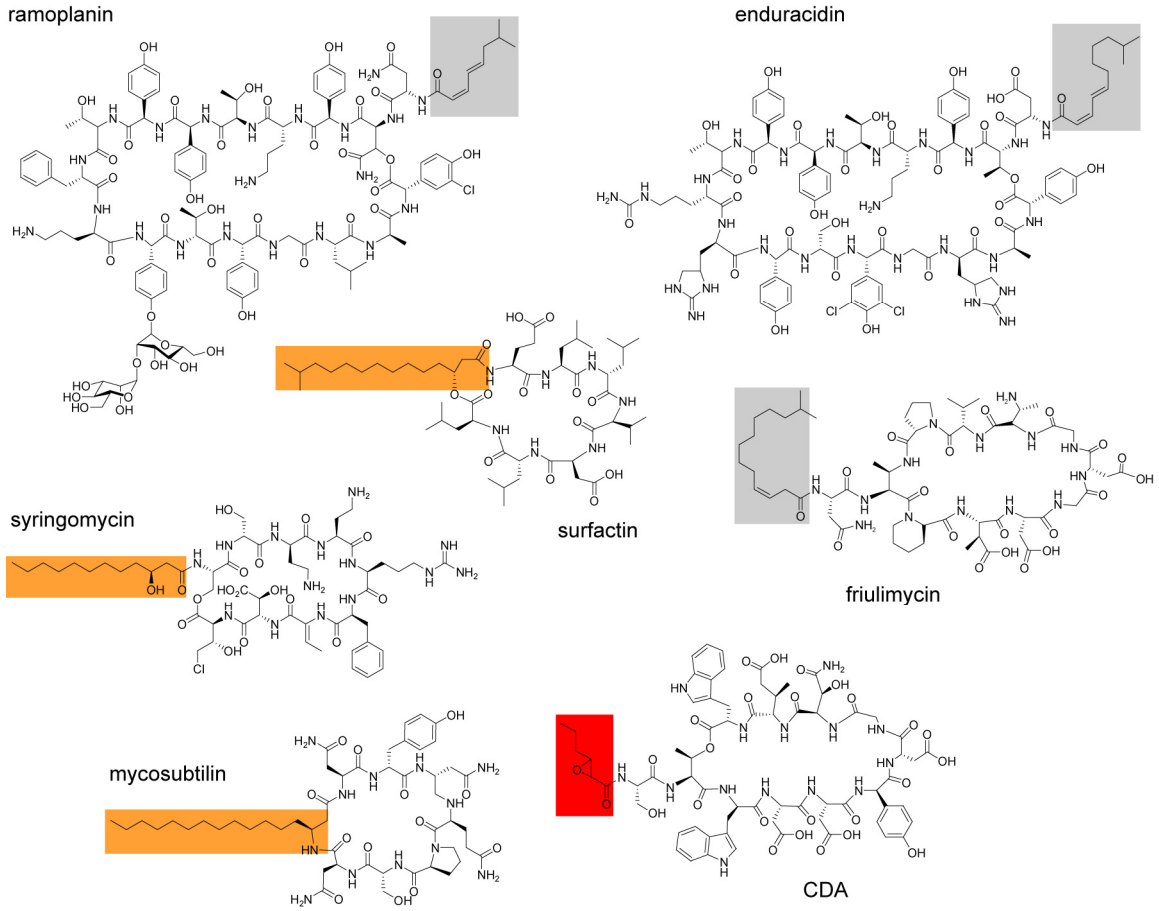

Figure 2.16: Chemical structures of nonribosomal lipopeptides containing modified fatty acid building blocks. Unsaturated fatty acids (grey) and Cβ-modified fatty acids (orange) are predominantly found. The calcium-dependent antibiotic CDA contains a *trans*-2,3-epoxidized hexanoyl moiety (red) with unknown absolute configuration.

2.7.1 Lipidation of nonribosomal peptides

Recently, important contributions from the Walsh laboratory elucidated the activation and tailoring processes involved in the formation of the β-amino fatty acid moiety of the octalipopeptide mycosubtilin (Figure 2.16) [99-101]. This potent antifungal is produced by *Bacillus subtilis* and synthesized by an NRPS/PKS hybrid system consisting of four proteins: FenF, MycA, MycB, and MycC. The first enzymatic subunit MycA is comprised by NRPS and PKS domains and additionally shows elements of FASs [102]. *In vitro* studies with the excised AL-ACP_1 from MycA characterized the AL domain to function as a fatty acyl-AMP ligase (FAAL), that in analogy to an A domain found in NRPSs activates the fatty acid substrate as an acyl-adenylate and further transfers it to the adjacent ACP [100, 103]. FenF is a free-standing acyltransferase (AT) enzyme that has been shown to load malonyl-CoA onto the second ACP of MycA *in trans*, before condensation via a

KS domain gives a β-ketoacyl thioester that is reductively aminated by the AMT domain (Figure 2.17) [99].

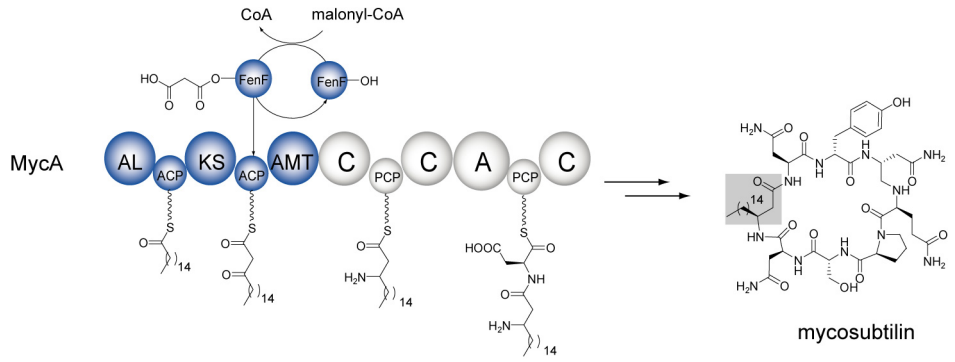

Figure 2.17: Fatty acid activation and modification during mycosubtilin biosynthesis. PKS elements of MycA are indicated in blue.

The NRPSs of the lipopeptide antibiotics from the daptomycin-class do not contain integrated PKS elements. Instead, different biosynthetic pathways for fatty acid activation and modification can be deduced from their biosynthetic gene clusters [9, 104, 105]. In the daptomycin biosynthetic system, the stand-alone proteins DptE and DptF are a putative fatty acyl-AMP ligase and an ACP, respectively, responsible for activation of the fatty acid building blocks [9, 95]. In analogy to the above discussed AL domain of MycA, DptE is likely to recruit fatty acids provided by primary metabolism and to activate them as acyl-adenylates, which are subsequently transferred to the carrier protein DptF. A fused equivalent of DptE and DptF is present in the A54145 NRPS system, where LptEF was proposed to carry out the same biosynthetic function during lipoinitiation. After fatty acid activation and attachment to the respective ACP, the activated intermediates are possibly transferred to the amino acid that is bound to the first module of the daptomycin or A54145 peptide synthetase (Figure 2.18).

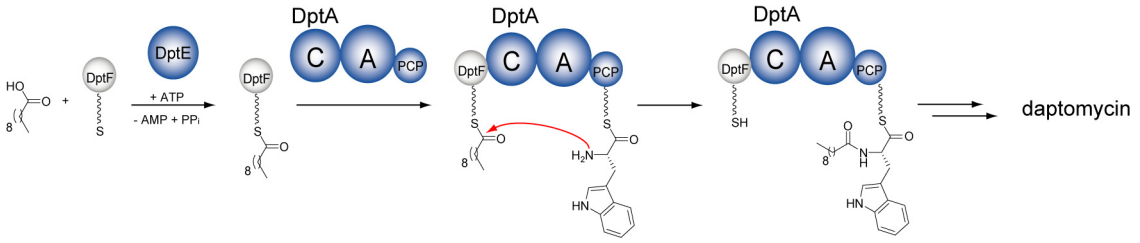

Figure 2.18: Proposed model for fatty acid activation and transfer during daptomycin biosynthesis. DptE is a putative fatty acyl-AMP ligase that activates decanoic acid as decanoyl-adenylate under the consumption of ATP. DptF is a free-standing ACP possibly loaded *in trans* by DptE. Finally, the thioester-bound decanoyl moiety is transferred to tryptophan that is tethered to the first module of DptA.

2.7.2 Fatty acid tailoring during CDA biosynthesis

As with the generation of the exceptional amino acid monomers found in NRPs, enzymatic modification leads to the diversification of the fatty acid building blocks found in lipopeptide antibiotics. Recently, the cloning and sequencing of the CDA biosynthetic gene cluster suggested that enzymatic tailoring mediated by stand-alone enzymes working *in trans* to the assembly line machinery could be responsible for fatty acid modification. A putative *fatty acid biosynthesis (fab)* operon adjacent to the genes encoding for the NRPS, comprised of five open reading frames, was predicted to be involved in the synthesis and modification of the unique *trans*-2,3-epoxyhexanoyl moiety of CDA (Figure 2.19) [104].

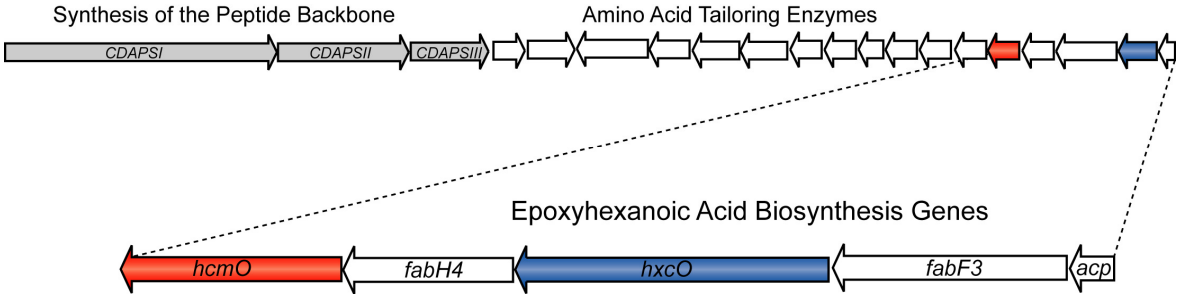

Figure 2.19: The *fab* operon implicated in the biosynthesis of the 2,3-epoxyhexanoic acid of CDA.

While SCO3249 encodes for a protein with similarity to an ACP from FASs and PKSs, the gene product of *fabH4* was predicted to be a KSIII that catalyzes the first condensation reaction of acetyl and malonyl units, resulting in acetoacetyl-ACP. FabF3 is likely to be responsible for the second condensation reaction to give β-ketohexanoyl-ACP. Since genes encoding for additional FAS enzymes, like acetyl and malonyl transacylases, KRs, DHs, as well as an ERs are absent from the cluster, presumably enzymes from primary metabolism contribute to the synthesis of the fatty acid moiety precursor. HxcO was suggested to encode for a fatty acid modifying enzyme that functions in analogy to acyl-CoA oxidases, which utilize FAD in the desaturation of acyl-CoAs to enoyl-CoAs during fatty acid degradation. Further it was anticipated that HcmO subsequently epoxidizes the hexenoyl-CoA product generated by HxcO. In order to elucidate the function of the two enzymes HxcO and HcmO in CDA biosynthesis, fatty acid tailoring was reconstituted *in vitro* during the course of this study.

2.7.3 Acidic lipopeptide mode of action

A large number of papers and reviews have appeared in recent literature on the mode of action of daptomycin, the far most prominent representative of the lipopeptide class of compounds [95, 106]. The general consensus at present is that the biological target of daptomycin is the bacterial cell membrane, to which it binds in a calcium-dependent manner. Initially, the lipid tail of the peptide is supposed to partly insert into the cytoplasma-membrane, followed by calcium-dependent integration of the daptomycin molecules into the membrane and the formation of aggregates. Finally, cell death occurs via membrane perforation leading to an efflux of potassium from the bacterial cell, which causes dysfunction of macromolecular synthesis (Figure 2.20) [107].

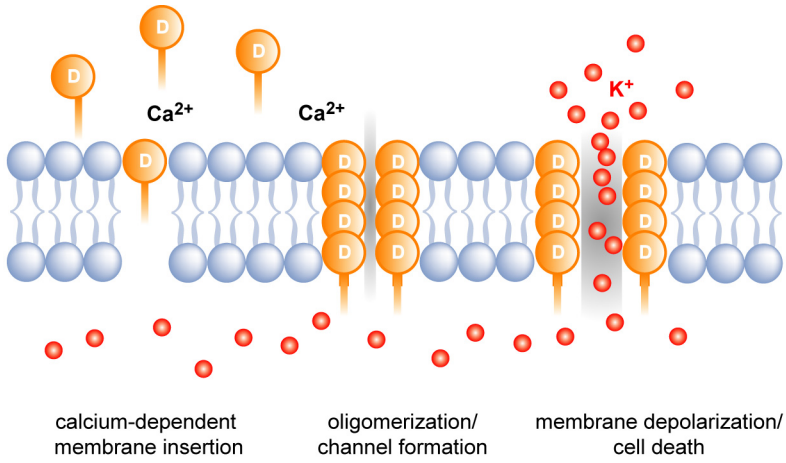

Figure 2.20: Daptomycin's mode of action works via the cell membrane.

To understand the molecular mechanism of how daptomycin goes on to perturb bacterial membranes in more detail, its three-dimensional structure has been determined by NMR spectroscopy in three separate studies [108-110]. Two of these investigated daptomycin solutions in the presence of calcium (holo-daptomycin) [108, 109], while a third focused on calcium-free solutions (apo-daptomycin) [110]. Whereas the 3-D structure derived by Ball et al. indicates no significant conformational change upon calcium binding, Jung and coworkers postulated distinct structural transitions caused by Ca^{2+}-ions (Figure 2.21). Binding of Ca^{2+}-ions was proposed to draw the core decapeptide closer together, with Asp_3 and Asp_7 probably coordinating the divalent cation. In addition to reducing the net charge of the overall cationic daptomycin from −3 at neutral pH to −1 and constraining the conformational freedom of the peptide core, calcium binding was further suggested to increase the solvent exposed surface of the daptomycin molecule. Redistribution of

charged side chains towards the top of the peptide ring and the clustering of the lipid chain with the hydrophobic Trp_1 and Kyn_{13} at the bottom or the ring structure is supposed to overall lead to an increased amphipathicity that facilitates interaction with the phospholipid membrane and the oligomerization of the lipopeptide.

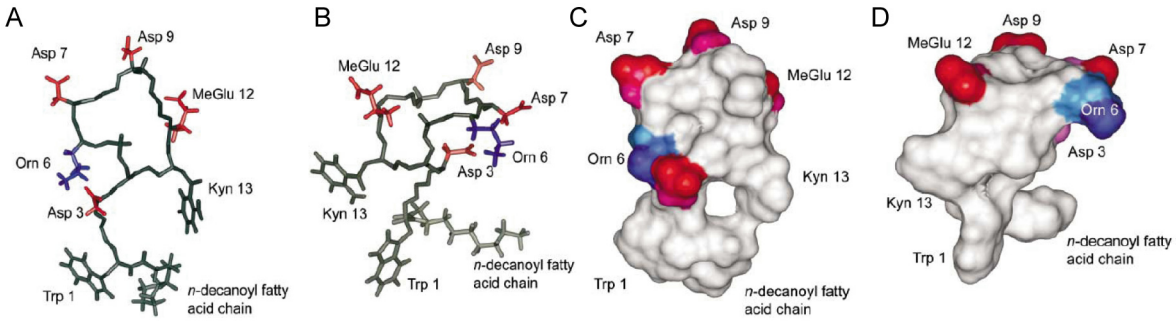

Figure 2.21: Structures of daptomycin in the absence (A,C) and presence (B,D) of Ca^{2+}-ions. Backbone (A,B) and surface (C,D) representations of the apo- and holo-structure are shown. Negative charges are indicated in red, positive charges in blue and uncharged residues and regions are indicated in grey. This figure is adopted from Ball et al. [108].

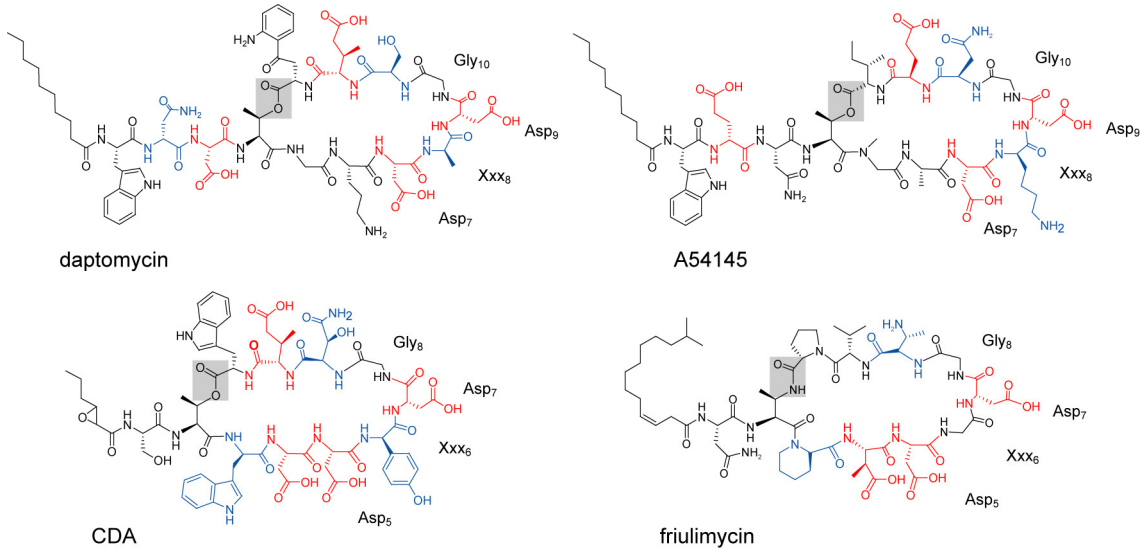

Figure 2.22: Structures of the acidic lipopeptide family. The peptide backbones of these compounds contain several aspartate and glutamate residues colored in red, leading to the overall acidic nature. At least two D-configured amino acids, colored in blue, can be found for each member. Macrocyclization occurs via the formation of lactones and lactams as highlighted in grey.

Since other acidic lipopeptide antibiotics such as CDA, A54145, friulimycins, and amphomycins share several characteristic structural features with daptomycin, they are likely to function via a similar mode of action based on the calcium-dependent interaction with the bacterial cytoplasma membrane. To illustrate the close relationship between these compounds, it should be noted that, besides the conserved decapeptidelactone or -lactam ring, all members of the acidic lipopeptide family contain two conserved aspartic acid

residues at ring positions 7 and 9, followed by glycine at position 10, using the daptomycin numbering convention (Figure 2.22). Moreover, D-configured and achiral amino acids commonly occupy positions 5 and 8 of the acidic peptide core, while position 11 is strictly reserved for D-configured amino acids, suggesting a general importance of these conserved structural motifs for antibacterial activity.

2.8 Tasks of this study

One aim of this study was to investigate the synthetic potential of the excised peptide cyclases from the daptomycin and A54145 gene clusters. In addition to the question, whether these two enzymes are suited for the chemoenzymatic generation of daptomycin and A54145 analogs, their substrate specificity should be explored with synthetic peptidyl-thiophenol substrates. Based on this information, lipopeptide variants could be synthesized and tested for antimicrobial activity.

In the context of macrocyclic lipopeptide antibiotics, which are commonly lactones and lactams, an unusual type of peptide cyclization, as found for the nostocyclopeptide (ncp), via an intramolecular imino bond was of interest. Thus, one aim of this thesis was the biochemical characterization of an exceptional reductase domain located at the C-terminal end of the ncp NRPS. In detail, assays with the recombinant enzyme, chemically produced substrate mimics, and linear peptide aldehydes were envisioned.

The third task of this thesis was to explore the enzymatic tailoring reactions catalyzed by HxcO and HcmO during the formation of the unusual *trans*-2,3-epoxyhexanoic moiety residue of CDA. Experiments to test three possible biosynthetic routes were planned with acyl-CoA substrates, acyl substrates loaded on an ACP, and chemoenzymatically derived CDA variants. An additional goal of these investigations was to examine the substrate specificity of HxcO and HcmO for different fatty acids.

3 Materials

3.1 Chemicals, enzymes, and general materials

Chemicals that are not listed were purchased as standard compounds from other manufacturers in p.a. quality.

Table 3.1: Chemicals, enzymes, and general material.

Manufacturer (location)	**Product**
Agilent Technologies (Böblingen)	2,5-dihydroxybenzoate matrix
Amersham Biosciences (Braunschweig)	various restriction endonucleases, ampicillin, IPTG, kanamycin, yeast extract, Coomassie brilliant blue G and R250, agar Nr.1, HiTrap™-desalting columns
Bachem (Weil am Rhein)	N_α-Fmoc-protected amino acids, N_α-Boc-protected amino acids
Böhringer Mannheim (Mannheim)	Expand™ Long Template PCR Kit, lysozyme
Eurogentech (Seraing, Belgium)	agarose, electroporation cuvettes
Fermentas (St. Leon-Rot)	PageRuler™ Protein Ladder
Fluka (Neu-Ulm)	SDS, TEMED, DMF
Finnzymes (Heidelberg)	Phusion DNA Polymerase
Invitrogen (Karlsruhe)	pBAD Directional TOPO® Expression Kit, Champion TM pET SUMO Protein Expression System
Macherey and Nagel (Düren)	C_{18}-Nucleodur HPLC column, C_{18}-Nucleosil-HPLC column
Merck (Darmstadt)	silica gel 60 F254 plates
Millipore (Bedford, USA)	Amicon® Ultra-4 Centrifugal Filter Devices
MPBiomedicals (Solon, USA)	coenzyme A
New England Biolabs (Schwalbach)	desoxyribonucleotides (dATP, dTTP, dGTP, dCTP), prestained protein molmarker, various restriction endonucleases, 1kb-DNA-ladder
Novabiochem (Darmstadt)	N_α-Fmoc-protected amino acids, 2-chlorotritylchloride resin, HBTU, HOBt, PyBOP
Oxoid (Wesel)	agar Nr.1, tryptone, oxoid nutrient broth (ONA)

Qiagen (Hilden)	QIAquick-spin PCR purification kit, Ni^{2+}-NTA-agarose, QIAexpress vector kit ATG, QIAEXII extraction kit
Qiagen-Operon (Köln)	oligodeoxynucleotides
Roth (Karlsruhe)	ethidiumbromide, β-mercaptoethanol, acrylamide for SDS-PAGE, piperidine
Schleicher & Schüll (Kassel)	Whatmann-3MM paper
Serva (Heidelberg)	Visking dialysis tubes, APS
Sigma (Deisenhofen)	EDTA, N-acetylcysteamine, thiophenol, nucleotide pyrophosphatase
Stratagene (Heidelberg)	PfuTurbo DNA polymerase

3.2 Equipment

Table 3.2: Equipment

Device	**Manufacturer**
Autoclave	Tuttnauer 5075 ELV
Bidestilled water supply	Seral Seralpur Pro90CN
Centrifugation	Heraeus Biofuge pico Sorvall RC 26 plus, rotors SS34 und SLA3000 Sorvall RC 5B Plus
Clean-Bench	Antair BSK
DNA-gel documentation	Cybertech CS1, thermoprinter Mitsubishi Video Copy processor
Electrophoresis	Mini-PROTEAN®, Bio-Rad Laboratories GmbH
Electroporation-pulse control	Bio-Rad Gene Pulser II
Emulsifier (cell disruption)	Avestin (EmulsiFlex-C5)
ESI-MS	Agilent Technologies (1100 MSD, Series A)
FTICR (Finnigan LTQ-FT)	Thermo Scientific
FPLC-system	Pharmacia FPLC-biotechnology FPLC-System 250: gradient-programmer GP-250 Pump P-500 Uvicord optical device UV-1 (λ = 280 nm)

	Uvicord control element UV-1 2-channel printer REC-102 Injection valve V-7 3-way-valve PSV-100 Fraction collector FRAC-100
FPLC-columns	Amersham Biosciences HiTrap® desalting columns Amersham Biosciences HiLoad Superdex gelfiltration
French Press	SLM Aminco; French-Pressure Cell-Version 5.1; 20k Rapid-fill cell (40 mL)
HPLC-system	Agilent series 1100 HPLC-system with DAD-detection, vacuum degasser, quaternary pump, auto sampler and HP-chemstation software
HPLC-columns	Macherey & Nagel Nucleosil 250/3, pore diameter 120 Å, particle size 3 µm Nucleodur 250/3, pore diameter 100 Å, particle size 3 µm Nucleodur 250/21, pore diameter 100 Å, particle size 3 µm
Incubator	Köttermann 2736
Lyophilizer	Christ
NMR	Bruker Avance AC-300
MALDI-TOF	Per Septive Biosystems Voyager-DE RP BioSpectrometry, Bruker FLEX III
MS-MS sequencing	Applied Biosystems, API Qstar Pulsar I
Peptide synthesizer	Advanced ChemTech APEX 396 synthesizer
Photometer	Pharmacia Biotech Ultraspec 3100 *pro*
Shaker	New Brunswick Scientific Series 25 Incubator Shaker, New Brunswick Scientific Innova 4300 Incubator, Heidolph Instruments GmbH
Speed-Vac	Savant Speed Vac Concentrator, Uniequip Univapo 150
Vortexer	Scientific Industries Vortex Genie 2
Thermocycler	eppendorf mastercycler personal
Water bath	Infors Aquatron Shaker

3.3 Vector systems

3.3.1 The pET28a(+) vector

The pET28a(+) vector system (Novagen) was used for the production of recombinant proteins (Figure 3.1). The vector allows Ni^{2+}-NTA chromatography purification by fusing a His_6-tag to the C- or N-terminus of the overproduced protein. The transcription of the cloned genes is dependent on the T7 RNA polymerase and IPTG-induced.

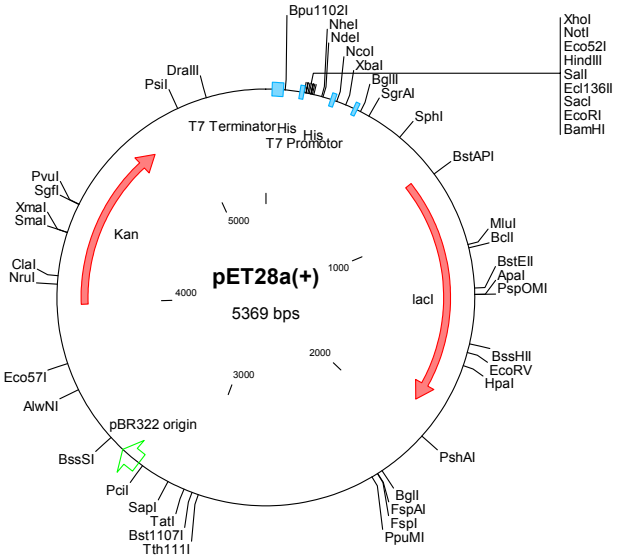

Figure 3.1: Physical map of pET28a(+).

3.3.2 The pQTEV vector

The pQTEV vector is a derivatized pQE60 vector (Qiagen) that allows purification of recombinant proteins by Ni^{2+}-NTA chromatography, by fusing a His_7-tag to the N-terminal end of the produced protein (Figure 3.2). After purification, the His_7-tag can be removed from the recombinant protein via a recognition site of the tobacco etch virus (TEV) protease. The pQTEV vector carries two *lac*-operators in the promotor region and can therefore be precisely induced with IPTG for protein expression. The tandem *lac*-operators may also represent a disadvantage since excisive recombination is frequently observed at this site.

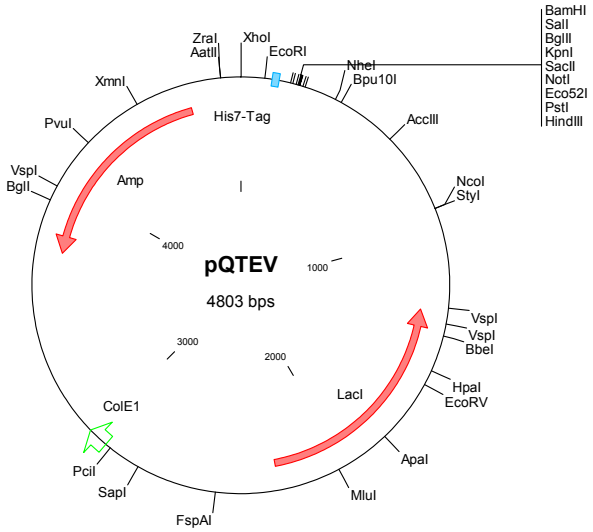

Figure 3.2: Physical map of the pQTEV vector.

3.4 Primer

Primers used for vector construction are listed in Table 3.3.

Table 3.3: Primers used in this study (restriction sites are underlined).

Primer name	Primer sequence (5'-3')	Restriction site	Expression vector	Target gene
FK01	AAAAAAGGTACCGGCGCGCACC CCAGTCGC	KpnI	pQTEV	*dap PCP-TE*
FK02	AAAAAAAAGCTTTCAGGTGCCG GCGCCCAGCC	HindIII		
FK03	AAAAAAGGTACCCGGCGTACGA CCCGTTCGAGAC	KpnI	pQTEV	*dap TE*
FK02	AAAAAAAAGCTTTCAGGTGCCG GCGCCCAGCC	HindIII		
FK19	AAAAAGGATCCGGCCGTCCGCC GCGCGAC	BamHI	pQTEV	*A54 PCP-TE*
FK17	AAAAAAGCGGCCGCTCATACCT CTCGTTTCTTCGTGGTGGCTCC	NotI		
FK15	AAAAAAGGATCCGGCGCCGAAC GCCGCGCC	BamHI	pQTEV	*A54 TE*
FK17	AAAAAAGCGGCCGCTCATACCT CTCGTTTCTTCGTGGTGGCTCC	NotI		
FK19	AAAAAAGGATCCATGGACACGA AAGCCTGCACAGCACCC	BamHI	pQTEV	*ncp R*
FK20	AAAAAAGCGGCCGCTTAGCGTC GGGGGGCGAGTCGCC	NotI		

FK40	AAAAAAGGATCCATGAGTACGG ACCCCAAGTCGGTTG	BamHI	pQTEV	*ACP (SCO3249)*
FK41	AAAAAAAAGCTTTCACGCCGCT TCCAGACCCG	HindIII		
FK42	AAAAAAGAATTCACGCAACGCG AAGAAGAGCTGGCC	EcoRI	pET28a(+)	*hxcO*
FK43	AAAAAACTCGAGCGGGCGTACT CCGGCCTGCA	XhoI		
FK44	AAAAAAGAATTCCCGAAGCTGC GGATCGCAGTCG	EcoRI	pET28a(+)	*hcmO*
FK45	AAAAAACTCGCTCGAGCGGCGG CGGCAGCGGTG	XhoI		

3.5 Microorganisms

3.5.1 E. coli TOP 10

E. coli TOP 10 (Invitrogen) was used for cloning and sequencing purposes. The genotype is as follows: F-*mcr*A. (*mrr-hsd*RMS-*mcr*BC) 80*lacZ*.M15.*lac*X74 *deo*R *rec*A1 *ara*D139. (*ara-leu*)7697 *gal*U *gal*K *rps*L (StrR) *end*A1 *nup*G.

3.5.2 E. coli BL21(DE3)

The *E. coli* strain BL21(DE3) (Novagen) with the genotype F- *ompT*[*Ion*]$r_b^-m_b^-$ was used as a bacterial host for the expression of plasmid DNA. It is characterized by a deficiency of the Lon and OmpT protease (protein of the outer membrane). The strain further contains the IPTG-inducible T7 RNA polymerase gene, which is inserted in the chromosome after *lacZ* and the promoter *lac*uV5 on a λ-prophage. This is essential for the IPTG induction of genes under T7-promotor control.

3.5.3 Streptomyces

S. fradiae (NRRL 18158) and *S. coelicolor* A3(2) (DSM 40783) were cultivated for the subsequent preparation of genomic DNA.

3.6 Media

The following media were used for the cultivation of microorganisms. Culture plate medium was prepared by adding 1.2% (w/v) of agar no.1 to the respective medium, which was heated at 121 °C and 1.5 bar for 30 min. Antibiotics for selection were added after cooling down to 55 °C in the following standard concentrations: 100 μg/mL ampicillin, 50 μg/mL kanamycin.

3.6.1 LB Medium

E. coli strains were grown in LB media.

LB Medium (adjusted to pH 7.0):

Bactotrypton	16 g/L
Yeast-extract	10g/L
NaCl	5 g/L

3.6.2 Medium 65

Streptomyces species were grown in medium 65.

Medium 65:

glucose	4 g/L
yeast-extract	4 g/L
malt-extract	10 g/L
$CaCO_3$	2 g/L

4 Methods

4.1 Molecular biology techniques

4.1.1 Streptomyces cultivation and DNA preparation

Streptomyces species were grown in liquid culture under agitation (250 rpm) at 28 °C for 5-7 days. The isolation of chromosomal DNA was carried out as described previously [111].

4.1.2 Construction of overexpression plasmids

Amplification of all gene fragments was performed by polymerase chain reaction (PCR) with Phusion DNA Polymerase (Finnzymes) according to the manufacturer's protocol for GC-rich DNA templates. Purification of PCR products was performed by the "QIAquick-spin PCR purification kit" following the manufacturer's manual (Qiagen). All constructs were analyzed by restriction digests and DNA-sequencing (carried out by GATC-Biotech, Konstanz).

Construction of pQTEV[dap PCP-TE] – The *dap PCP-TE* gene fragment was amplified from genomic DNA of *S. roseosporus* by PCR using the primer pairs listed in the Materials section (Table 3.3). The resulting amplicons were digested with the enzymes indicated in Table 3.3 and cloned into appropriate restriction sites of a pQTEV vector. The resulting overexpression plasmids were checked by DNA sequencing and transformed into *E. coli* BL21(DE3) for protein production.

Construction of pQTEV[dap TE] – The *dap TE* gene fragment was amplified from genomic DNA of *S. roseosporus* by PCR using the primer pairs listed in the Materials section (Table 3.3). The resulting amplicons were digested with the enzymes indicated in Table 3.3 and cloned into appropriate restriction sites of a pQTEV vector. The resulting overexpression plasmids were checked by DNA sequencing and transformed into *E. coli* BL21(DE3) for protein production.

Construction of pQTEV[A54 PCP-TE] – The *A54 PCP-TE* gene fragment was amplified from genomic DNA of *S. fradiae* by PCR using the primer pairs listed in the Materials section (Table 3.3). The resulting amplicons were digested with the enzymes indicated in Table 3.3 and cloned into appropriate restriction sites of a pQTEV vector. The resulting

overexpression plasmids were checked by DNA sequencing and transformed into *E. coli* BL21(DE3) for protein production.

Construction of pQTEV[A54 TE] – The *A54 TE* gene fragment was amplified from genomic DNA of *S. fradiae* by PCR using the primer pairs listed in the Materials section (Table 3.3). The resulting amplicons were digested with the enzymes indicated in Table 3.3 and cloned into appropriate restriction sites of a pQTEV vector. The resulting overexpression plasmids were checked by DNA sequencing and transformed into *E. coli* BL21(DE3) for protein production.

Construction of pQTEV[ncp PCP-R] – The *ncp PCP-R* gene fragment flanked by BamHI and NotI was synthesized by solid-phase oligonucleotide synthesis (EZBiolab). After enzymatic digest, the synthesized DNA fragment was cloned into appropriate restriction sites of a pQTEV vector. The resulting overexpression plasmids were checked by DNA sequencing and transformed into *E. coli* BL21(DE3) for protein production.

Construction of pQTEV[ncp R] – *ncp R* was amplified from *pQTEV[ncp PCP-R]* by PCR using the primer pairs listed in the Materials section (Table 3.3). The resulting amplicons were digested with the enzymes indicated in Table 3.3 and cloned into appropriate restriction sites of a pQTEV vector. The resulting overexpression plasmids were checked by DNA sequencing and transformed into *E. coli* BL21(DE3) for protein production.

Construction of pQTEV[acp] – The *acp* gene fragment from the CDA *fab* operon was amplified from genomic DNA of *S. coelicolor* A3(2) by PCR using the primer pairs listed in the Materials section (Table 3.3). The resulting amplicons were digested with the enzymes indicated in Table 3.3 and cloned into appropriate restriction sites of a pQTEV vector. The resulting overexpression plasmids were checked by DNA sequencing and transformed into *E. coli* BL21(DE3) for protein production.

Construction of pET28a(+)[hxcO] – The *hxcO* gene fragment from the CDA *fab* operon was amplified from genomic DNA of *S. coelicolor* A3(2) by PCR using the primer pairs listed in the Materials section (Table3.3). The resulting amplicons were digested with the enzymes indicated in Table 3.3 and cloned into appropriate restriction sites of a pET28a(+)

vector. The resulting overexpression plasmids were checked by DNA sequencing and transformed into *E. coli* BL21(DE3) for protein production.

Construction of pET28a(+)[hcmO] – The *hcmO* gene fragment from the CDA *fab* operon was amplified from genomic DNA of *S. coelicolor* A3(2) by PCR using the primer pairs listed in the Materials section (Table 3.3). The resulting amplicons were digested with the enzymes indicated in Table 3.3 and cloned into appropriate restriction sites of a pET28a(+) vector. The resulting overexpression plasmids were checked by DNA sequencing and transformed into *E. coli* BL21(DE3) for protein production.

4.2 Protein methods

Standard methods frequently used in protein analysis, such as SDS-PAGE and Coomassie staining have been described elsewhere [112, 113].

4.2.1 Gene expression

4.2.1.1 Expression with the pQTEV vector system

0.5 L of cultures in 2 L Erlenmeyer flasks were inoculated with 5 mL of an overnight culture and grown to an optical density of 0.5 at 37 °C. The temperature was lowered to 30 °C and cultures were induced by the addition of IPTG to a final concentration of 1 mM. The cultures were incubated for another 3 to 4 h, then harvested by centrifugation (7000 rpm, 4 °C, 30 min). The pellet resulting from 5 L expression culture was resuspended in 50 mL Hepes A buffer (50 mM Hepes, 300 mM NaCl, pH 8.0). The cell suspension was stored at -20 °C.

4.2.1.2 Expression with the pET28a(+) Vector System

0.5 L of cultures in 2 L Erlenmeyer flasks were inoculated with 5 mL of an overnight culture and grown to an optical density of 0.5 at 37 °C. The cultures were cooled to 16 °C and protein production was induced by the addition of IPTG to a final concentration of 0.1 mM. The cultures were incubated for another 14-16 h, then harvested by centrifugation (7000 rpm, 4 °C, 30 min). The pellet resulting from 5 L expression culture was resuspended in 50 mL Hepes A buffer (50 mM Hepes, 300 mM NaCl, pH 8.0). The cell suspension was stored at –20 °C.

4.2.2 Protein purification

For purification of the His-tagged proteins, cell suspensions were thawed and disrupted by the use of an EmulsiFlex®-C5 High Pressure Homogenizer (Avestin). After centrifugation (17000 rpm, 4 °C, 30 min) the supernatant was carefully removed and applied to Ni^{2+}-NTA chromatography on an FPLC® system (Amersham Pharmacia Biotech). Briefly, the protein raw extract was run over a column filled with 500 µL Ni^{2+}-NTA superflow resin (Qiagen) with a flow rate of 0.5 mL/min. The bound proteins were washed with Hepes A buffer containing 2% Hepes B buffer (50 mM Hepes, pH 8.0, 300 mM NaCl, 250 mM imidazole) for 5 min and eluted by applying a linear gradient of 2-50% buffer B over 30 min with a flow rate of 0.7 mL/min.

Fractions containing the recombinant proteins were monitored by SDS-PAGE, pooled, and dialyzed against the respective assay buffer using Hi-Trap™ desalting columns (Amersham Biosciences). In the case of the FAD-dependent enzymes HxcO and HcmO the flavin cofactor was added in a 5-fold molar excess to increase protein stability. The recombinant proteins could be stored at −80 °C for 3 months without significant loss of activity.

4.2.3 Determination of protein concentrations

Generally, the concentrations of the purified proteins were determined spectrophotometrically using the calculated extinction coefficient at 280 nm, which was determined by the program "Protean" (DNAStar).

Table 4.1: Theoretical extinction coefficients (λ=280 nm)

Recombinant protein	Theoretical extinction coefficient [mg/mL]
Dap PCP-TE	1.14
Dap TE	0.92
A54 PCP-TE	1.11
A54 TE	0.89
Ncp PCP-R	0.88
Ncp R	0.80
ACP	4.48
HxcO	1.10
HcmO	0.73

Due to the FAD cofactor of HxcO and HcmO, the Bradford assay was used for concentration determination in these cases [114]. During the Bradford assay, the blue dye Coomassie G 250 binds to proteins and shifts their absorption maximum from 465 nm (blue) to 595 nm (orange) in an acidic solution. Based on the absorption intensity at 595 nm the amount of a protein in solution can be quantified.

4.3 Biochemical methods

4.3.1 Enzymatic cyclization assay

Enzymatic macrocyclization reactions were carried out in a total volume of 50 μL, containing 25 mM Hepes, 50 mM NaCl, and 5% DMSO (v/v) at pH 7.0. The mixture containing 250 µM peptidyl-thiophenol substrate and 5 μM enzyme was incubated at 25 °C for 2.5 h. All assays were analyzed by LC-MS on a C18 Nucleodur column (Macherey and Nagel, 250/3, pore diameter of 100 Å, particle size of 3 μm) with the following gradient: 15-60% acetonitrile, 0.1% TFA in water, 0.1% TFA over 40 min at 0.3 mL/min and 45 °C. Identities of the products were verified by ESI-MS.

Connection regiochemistry of cyclic products was determined by MS-MS analysis on an API Qstar Pulsar i Q-q-TOF mass spectrometer (Applied Biosystems). Concentrations of various peptidyl-thioesters were calculated using experimentally determined extinction coefficients at a wavelength of 220 nm. The extinction coefficient of peptidyl-thiophenol substrates was assumed to be identical to that of cyclized and hydrolyzed products.

For kinetic studies, the substrate concentration was varied from 50 μM to 1 mM, and reactions were quenched by the addition of 35 μL of a 4% TFA/H_2O solution. Kinetic characterization of the cyclization reactions was performed by determining initial rates at 5-10 substrate concentrations using two time points at each concentration within the linear region of the enzyme verified by time courses.

4.3.2 Preparation of cyclic peptides for bioassays

For the semipreparative scale preparation of cyclic acidic lipopeptides, the reactions were carried out in a total volume of 3-6 mL with 5 μM purified TE domain, 250 μM peptidyl-SPh substrate, 25 mM Hepes, 50 mM NaCl, and 5% DMSO (v/v) at pH 7.0 and 25 °C. The reaction was monitored by analytical HPLC and thin-layer chromatography (TLC) on silica gel 60 F_{254} plates (Merck) and visualized under UV (365 nm). After 3-5 h, the reaction mixture was directly run over a 250/21 Nucleodur 100-5 C18 reverse phase

column (Macherey and Nagel) by applying a linear gradient from 35 to 55% acetonitrile, 0.1% TFA in water, 0.1% TFA over 30 min at a flow rate of 20 mL/min and 25 °C. The purity of the obtained products was analyzed by analytical HPLC (>95% purity).

4.3.3 Antimicrobial activity assays

To determine the antimicrobial activity of the synthesized lipopeptides, the chemoenzymatically cyclized compounds were assayed against *Bacillus subtilis* PY79. Minimal inhibition concentrations (MICs) were obtained from 2-fold serial dilutions of the cyclic peptides and authentic daptomycin prepared in microtiter plates as previously described using LB medium containing 74 mg Ca^{2+}/L [57]. Therefore, 80 μL of an overnight culture diluted 1:10000 was added to each well and incubated at 37 °C for 18 h prior to visual determination of MICs.

4.3.4 Enzymatic reduction assays

Enzymatic reduction assays wit Ncp PCP-R and Ncp R and peptidyl-thioester derivatives were carried out in a total volume of 100 µL containing 20 µM ncp PCP-R or ncp R, 250 µM peptidyl-CoA substrate, 1.5 mM NADPH, 10 mM $MgCl_2$, and 10 µM $MnCl_2$ in 50 mM Hepes, 50 mM NaCl at pH 6. All assays were incubated at 25 °C for 1 h. The reactions were stopped by the addition of 1 mL MeOH and stored at –20 °C for 1 h. The supernatant was separated from the precipitant by centrifugation for 15 min at maximum speed. After removing the solvent under vacuum at 30 °C, the remaining pellet was resuspended in 100 µL 10% acetonitrile in water and analyzed by LC-MS on a C18 Nucleodur column (Macherey and Nagel, 125/2 pore diameter of 100 Å, particle size of 3 µm) with the following gradient: 10-80% acetonitrile in water over 25 min at 0.2 mL/min and 45 °C. It was crucial that TFA was not added to the solvents as a modifying agent, as the low pH would destroy the macrocyclic imine.

For kinetic studies the assay was carried out as described above and followed spectrophotometrically (Pharmacia Ultrospec 3100 pro UV/visible spectrophotometer). This direct monitoring is possible, because the reduction of each peptidyl-thioester substrate consumes one equivalent NADPH leading to a decrease in absorption at 340 nm. Following the extinction coefficient 6220 $M^{-1}cm^{-1}$ for NADPH, K_M and k_{cat} values for the reduction reaction were determined.

4.3.5 Imine macrocyclization assay with peptide aldehydes

For the imine cyclization assay 50 µM peptide aldehyde were incubated in a total volume of 100 µL containing 50 mM NaCl, 50 mM Hepes at pH 6 for 2 h at 25 °C. For the cyclization assay with enzyme 5 µM ncp PCP-R was added to the reaction mixture. Assays were immediately analyzed as reported above.

4.3.6 HPLC analysis of HxcO and HcmO flavin cofactors

A 50 µL sample of purified HxcO (30 µM) or HcmO (30 µM) was boiled for 5 min and denatured protein was removed by centrifugation. The flavin present in the supernatant was analyzed by HPLC on a C18ec Nucleodur column (Macherey and Nagel, 250/2, pore diameter of 100 Å, particle size of 3 µm) with the following gradient: 0-70% acetonitrile, 0.1% TFA in water, 0.1% TFA over 30 min at a flow rate of 0.2 mL/min at 40 °C. Product elution was monitored at 445 nm. Additionally, the identity of the cofactor was proven by mass spectrometry.

4.3.7 In vitro 4'-phosphopantetheinylation of ACP

A reaction mixture containing 200 µM fluorescein-CoA/acetyl-CoA, 200 µM ACP, 10 mM $MgCl_2$, and 50 µM recombinant *B. subtilis* 4'-phosphopantetheine transferase (PPTase) Sfp in assay buffer was incubated at 30 °C for 30 min and analyzed directly by LC-ESI-MS. The loading of fluorescein-CoA onto the ACP, which was prepared as previously reported [57, 115], was monitored by measuring the in-gel fluorescence.

4.3.8 Assays with ACP-bound acyl substrates

Acyl-phosphopantetheinylation of the ACP was achieved by incubating the carrier protein with Sfp and acyl-CoA substrates. The reaction mixture was incubated at 30 °C for 30 min and contained 200 µM ACP, 200 µM Acyl-CoA substrate, 2 mM $MgCl_2$, and 50 µM Sfp in a 25 mM Hepes buffer pH 7.5. The solution was desalted using a Micro Bio-Spin 6 column (Bio-Rad).

4.3.8.1 HxcO oxidation/epoxidation assay

A typical reaction mixture (150 µL) for the detection of HxcO epoxidation product was prepared using 100 µM loaded acyl-ACP substrate, 5 µM HxcO and 250 µM FAD in assay buffer. After incubation at 25 °C for 30 min, 10 µg trypsin (Promega) were added to the reaction mixture and incubated for 5 min at 30 °C. Finally, 15 µL formic acid were added and the samples were subjected to HPLC and high-resolution ESI-FTICR-MS analysis was

carried out with an LTQ-FT mass spectrometer (Finnigan, Bremen) using the following gradient: 25-50% acetonitrile, 0.045% formic acid in water, 0.05% formic acid over 30 min at a flow rate of 0.2 mL/min on a Jupiter C4 column (Phenomenex, 150x2 mm, 5 µm) at 40 °C. To achieve maximum sensitivity of the described ESI-FTICR-MS method, the MS experiment was carried out at single-reaction monitoring (SRM) mode of the LTQ mass analyzer. Masses selected for MS-MS are listed in Table 4.2.

Table 4.2: $[M+H]^{2+}$ mass fragments of fatty acid-*S*-Ppan-PCP (Lys^{57}-Arg^{71}) subjected to MS-MS. FA = fatty acid.

Chain length	Saturated FA	Unsaturated FA	Epoxidized FA
C4	1032.5	1030.5	1038.5
C5	1039.5	1037.5	1045.5
C6	1046.5	1044.5	1052.5
C7	1053.5	1051.5	1059.5
C8	1060.5	1058.5	1068.5
C10	1074.5	1072.5	1080.5

To study the kinetics of *(2R,3S)*-2,3-epoxyhexanoic-*S*-ACP formation mediated by HxcO, samples were trypsinized at different time points following initiation of the enzymatic reactions. Reaction volumes were then fractionated and analyzed by HPLC-MS-MS. The percentage of HxcO reaction product tethered to the ACP was plotted as a function of time.

4.3.8.2 HcmO epoxidation assay

Typical incubations (150 µL) for the detection of HcmO epoxidation products were prepared using 100 µM loaded acyl-ACP substrate and 10 µM HcmO, 250 µM FAD and 250 µM NAD(P)H in assay buffer. After 30 min at 25 °C, 10 µg trypsin (Promega) were added and incubated for another 5 min at 30 °C. The tryptic digest was stopped by the addition of 15 µL formic acid and the reaction volumes were analyzed by ESI-FTICR-MS as reported for HxcO assays.

4.3.9 Analysis of ACP-bound products by direct amide ligation

To further characterize the ACP-bound products of HxcO and HcmO reactivities, the undigested reaction mixtures were incubated with a 1000-fold excess of D-Phe-OMe at 60 °C for 2 h. The precipitated proteins were removed by centrifugation. Protein pellets were washed twice with 25 µL assay buffer and the combined fractions were concentrated to 50 µL prior to HPLC-MS analysis.

For epoxide product detection, the reaction volumes were compared to the synthesized standards using the following gradient: 0-60% acetonitrile, 0.1% TFA in water, 0.1% TFA from 0 to 20 min at a flow rate of 0.4 mL/min on a ChiraDex® Gamma column (Merck KGaA, Darmstadt, 250/4, particle size of 5 µm) at 30 °C.
The HPLC-MS analysis of the 2,3-hexenoyl moiety was carried out on a standard C18ec Nucleodur column (Macherey and Nagel, 250/2, pore diameter of 100 Å, particle size of 3 µm) with the following gradient: 0-60% acetonitrile, 0.1% TFA in water, 0.1% TFA over 20 min at 0.2 mL/min and 30 °C.

4.3.10 Assays with chemoenzymatically derived CDA analogs

4.3.10.1 HxcO assay

The reaction mixture contained 100 µM hexanoyl-CDA, 20 µM enzyme, and 60 µM FAD in a total volume of 75 µL. After incubation at 25 °C for 30 min the reaction was quenched by the addition of 15 µL formic acid and directly analyzed by LC-ESI-MS.

4.3.10.2 HcmO assay

The reaction mixture contained 100 µM hex-2-enoyl-CDA, 20 µM enzyme, 60 µM FAD, 100 µM NAD(P)H in a total volume of 75 µL. After incubation at 25 °C for 30 min the reaction was quenched by the addition of 15 µL formic acid and directly analyzed by LC-ESI-MS.

4.3.11 Assays with acyl-CoA substrates

Reaction mixtures for the detection of HxcO oxidation/epoxidation products were prepared using 250 µM hexanoyl-CoA substrate, 5-50 µM HxcO, and 100 µM FAD in assay buffer. Reaction mixtures for the detection of HcmO epoxidation products were prepared using 250 µM hexenoyl-CoA substrate, 10 µM HcmO, 250 µM FAD, and 250 µM NAD(P)H in assay buffer. Incubations were carried out at different temperatures and several periods of time.

4.4 Chemical synthesis

4.4.1 Solid-phase peptide synthesis (SPPS)

The synthesis of the peptide substrates used in this work has been carried out by Fmoc-based solid-phase peptide synthesis (SPPS). In SPPS the peptide chain is assembled by the sequential addition of α-amino and side chain protected amino acid building blocks. During the whole synthesis process, the growing peptide chain is attached to an insoluble polymer via its C-terminus and can be separated from reagents and by-products simply by filtration. Peptide synthesis was carried out on an automated peptide synthesizer (APEX 396 synthesizer, Advanced ChemTech). As solid support 2-chlorotritylchloride resin (Novabiochem, Darmstadt) was used. To prevent side reaction with the functional groups of amino acid side chains the following protection groups were employed: tert-butyl (tBu), trityl (Trt), allyloxycarbonyl (Aloc), tert-butyloxycarbonyl (Boc), and pentamethyldihydro-benzofuran-5-sulfonyl (Pbf).

4.4.1.1 Initiation: Coupling of the C-terminal amino acid to the resin

The first step in SPPS is the loading of the 2-chlorotritylchloride resin with the C-terminal amino acid. The efficiency of this loading reaction is essential for the whole synthesis process, because it will determine the yield and the purity of the final product. Sites on the resin that are not initially acylated can potentially react in later synthesis cycles leading to truncated peptides. To achieve an efficient loading, the resin was swelled in DCM, followed by incubation with 2 eq. of Fmoc protected amino acid and 8 eq. of DIPEA. This non nucleophilic base deprotonates the carboxyl function, which subsequently attacks the 2-chlorotrityl cation and the first amino acid is attached to the resin (Figure 4.1). After 2 h of incubation the solvent was removed by filtration and the resin was washed several times with DCM. Unreacted sites of the resin were capped by using methanol.

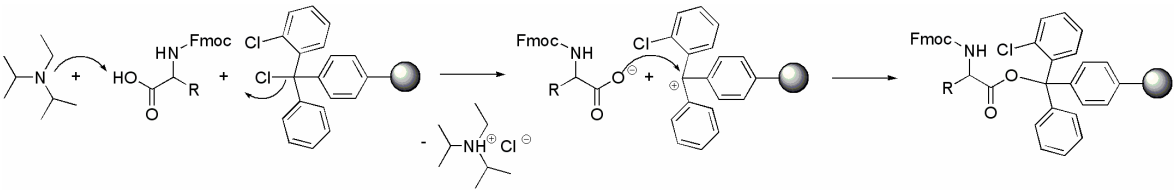

Figure 4.1: Initiation of SPPS. The C-terminal amino acid is loaded onto the 2-chlorotritylchloride resin.

4.4.1.2 Elongation

Elongation of the peptide chain requires deprotection of the N-terminal Fmoc group of the resin bound amino acid or peptide, respectively. The removal was usually achieved under mild basic conditions by the treatment with 15% piperidine in DMF for 20 min. The deprotonation of the fluorene gives an aromatic cyclopentadiene-type intermediate that rapidly eliminates to form the dibenzofulvene and carbon dioxide (Figure 4.2).

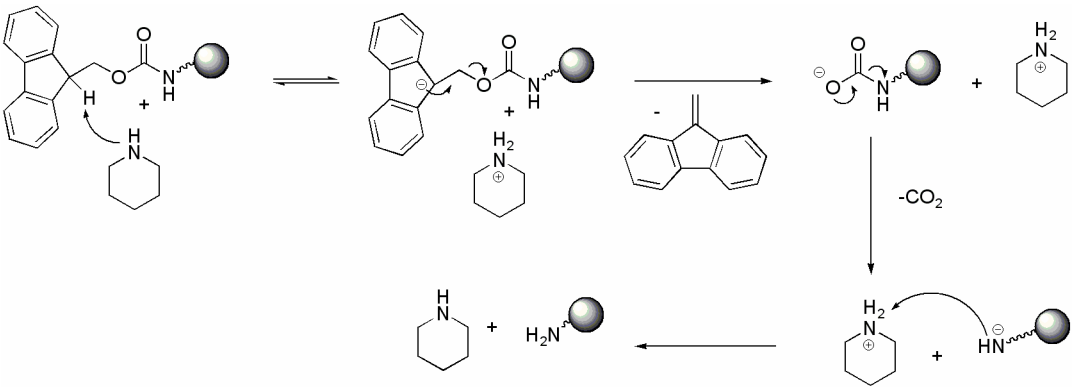

Figure 4.2: Fmoc-group removal reaction.

Peptide bond formation requires the activation of the carboxyl group of the Fmoc-protected amino acid. The *in situ* coupling method that was applied in this work made use of the coupling reagents HBTU and HOBt in DMF. After deprotonation of the carboxyl group by a 10-fold excess of DIPEA it attacks the electrophilic carbenium ion of the acyluronium salt HBTU. A highly reactive tetramethylurea intermediate is generated, which is subsequently converted into the reactive benzotriazole ester in the presence of the nucleophile HOBt. The free N-terminus of the resin bound amino acid/peptide then attacks this intermediate giving rise to the elongated peptide chain. To ensure quantitative reactions, a 3-fold excess of protected amino acid is used.

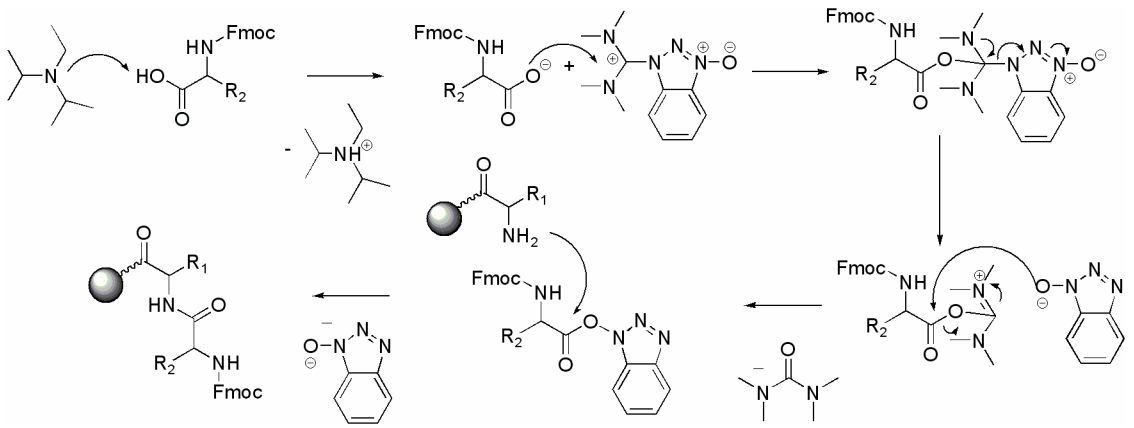

Figure 4.3: Peptide bond formation using HBTU/HOBt.

4.4.1.3 Termination

Cleavage of the mature peptide from the resin was achieved by incubating 2-chlorotrityl resin with TFE/AcOH/DCM (2:7:1). Under these conditions the used side chain protected groups are stable and the protected peptide acids can be selectively released from the resin. Finally the protected peptides were precipitated with hexane.

4.4.2 Synthesis of peptide aldehydes

For the synthesis of peptide aldehydes H-Thr-Gly-NovaSyn® TG resin (Novabiochem) preloaded with leucin or phenylalanine amino aldehydes, respectively, was used (Figure 4.4). The resin was suspended in DMF, left swelling for 30 min and was then suitable for the Fmoc protocol reported above. After assembly of the target sequence protecting groups were removed by treatment with anhydrous TFA (2 x 10 min). The resin was washed with DCM and the product was cleaved from the resin by treatment with AcOH/water/DCM/MeOH (10:5:63:22) for 30 min to obtain the deprotected peptide aldehyde. Purification of the crude product was carried out by semipreparative HPLC (Agilent 1100 system) with a reversed-phase 250/21 Nucleodur 100-5 C18ec column (Macherey and Nagel) using the following gradient: 5-55% of acetonitrile, 0.1% TFA in water, 0.1% TFA was applied over 30 min at 20 ml/min and 25 °C. Identification of the derived peptide aldehydes was achieved by LC-MS (Table 4.6). The purified product was dissolved in DMSO to a final concentration of 10 mM.

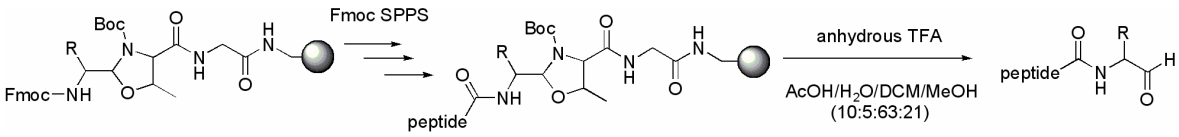

Figure 4.4: Preparation of peptide aldehydes using H-Thr-Gly-NovaSyn® resin.

4.4.3 Synthesis of peptidyl-SNAC and peptidyl-thiophenol substrates

Side-chain protected peptides (1 eq.) were dissolved in DCM, followed by the addition of DCC (2 eq.), HOBt (2 eq.), thiophenol or N-acetylcysteamine (10 eq.). After 30 min a catalytic amount of K_2CO_3 was added and stirring was continued for 2.5 h. After removal of the solvent, the protected peptide thioesters were treated with 2 mL TFA/H_2O/TIPS (95:2.5:2.5) at room temperature for 2 h. Precipitation of the deprotected peptide thioesters was carried out with ice-cold ether (30 mL). After centrifugation the peptide thioesters were dissolved in DMSO and purified by semipreparative HPLC carried out on an Agilent

1100 system with a reversed-phase 250/21 Nucleodur 100-5 C18ec column (Macherey and Nagel). Applied gradients are 20-60% acetonitrile, 0.1% TFA in water, 0.1% TFA for lipopeptide derivatives and 10-70% acetonitrile, 0.1% TFA in water, 0.1% TFA over 30 min at a flow rate of 20 mL/min at 40 °C for nostocyclopeptide peptidyl-SNAC and peptidyl-SPh substrates.

Identification of the peptidyl-SNAC and peptidyl-SPh substrates was achieved by LC-MS (Tables 4.3 and 4.5).

4.4.4 Synthesis of 4'-phosphopantetheine (ppan)

One equivalent of coenzyme A trilithium salt, 0.2 eq. of TCEPxHCl, and 0.5 unit/µmol nucleotide pyrophosphatase (Sigma) were dissolved in Hepes buffer (50 mM, pH 7.5). After incubation at 30 °C for 18 h the mixture was lyophilized and the identity of the products was confirmed by LC-MS.

4.4.5 Synthesis of peptidyl-CoA and peptidyl-ppan substrates

For the preparation of peptidyl-CoA and peptidyl-ppan substrates 1.5 eq. of ppan/CoA, 1.5 eq. of PyBOP, and 4 eq. of K_2CO_3 were added to 1 eq. of the side chain protected peptide and dissolved in THF/water (1:1). The reaction mixture was stirred for 2 h at room temperature and the solvent was removed.

Cleavage of the side-chain protecting groups was carried out using a mixture containing TFA/TIPS/H_2O (95:2.5:2.5). The deprotected peptidyl-ppan/peptidyl-CoA substrates were precipitated in ice-cold diethyl ether and purified by semipreparative HPLC carried out on an Agilent 1100 system with a reversed-phase 250/21 Nucleodur 100-5 C18ec column (Macherey and Nagel). The following gradient was applied: 5-55% of acetonitrile, 0.1% TFA in water, 0.1% TFA over 30 min at a flow rate of 20 mL/min and 25 °C.

Identification of the peptidyl-CoA and peptidyl-ppan substrates was verified by LC-MS (Table 4.5).

4.4.6 Synthesis of acyl-CoA substrates

The synthesis of acyl-CoA derivatives was based on the synthesis of peptidyl-CoA substrates as reported in 4.4.5. Briefly, 1 eq. CoA trilithium salt, 2 eq. of the fatty acid, 1.5 eq. of PyBOP and 4 eq. of K_2CO_3 were dissolved in 4 mL THF/water (1:1) and incubated for 2 h at room temperature. After lyophilization, the resulting white solids were dissolved in water and purified by HPLC (Agilent, 1100 series) on a preparative Nucleodur C18ec column (Macherey and Nagel, 250/2, pore diameter of 100 Å, particle size of 3 µm)

with a gradient of 5-70% acetonitrile, 0.1% TFA in water, 0.1% TFA over 30 min at a flow rate of 20 mL/min. Product elution was monitored at 215 nm and the identity was confirmed by MALDI-TOF MS analysis (Table 4.8).

4.4.7 Synthesis of N-(9-Fmoc)-L-kynurenine

Kynurenine sulfate (306 mg, 1 mmol) and K_2CO_3 (252 mg, 3 mmol) were dissolved in a mixture of acetone (2.5 mL) and water (2.5 mL). After addition of Fmoc-OSu (Novabiochem) (337.3 mg, 1 mmol), the solution was stirred overnight. The mixture was acidified to pH 2 with concentrated hydrochloric acid, and the acetone was removed by rotary evaporation. The product was extracted with chloroform and washed with 0.1 N HCl and water. After drying over anhydrous sodium sulfate, the combined organic phases were evaporated and the product was confirmed by ESI-MS and NMR: Fmoc-L-Kyn m/z 431.1 $[M + H]^+$ (431.2 calc.); ^{1}H-NMR (300 MHz, CD_3OD): δ = 3.46 (dd, $^3J_{CH\beta^h,\ CH\alpha}$ = 4.6 Hz, $^2J_{CH\beta^h,\ CH\beta^t}$ = 17.5 Hz, 1 H, $CH\beta^h$), 3.59 (dd, $^3J_{CH\beta^t,\ CH\alpha}$ = 6.4 Hz, $^2J_{CH\beta^t,\ CH\beta^h}$ = 17.5 Hz, 1 H, $CH\beta^t$), 4.22 (t, $^3J_{\text{Fmoc-CH},\ \text{Fmoc-CH}_2}$ = 7.0 Hz, 1 H, Fmoc-CH), 4.34 (d, $^3J_{\text{Fmoc-CH}_2,\ \text{Fmoc-CH}}$ = 7.0 Hz, 2 H, Fmoc-CH_2), 4.71 (dd, $^3J_{CH\alpha,\ CH\beta^h}$ = 4.6 Hz, $^3J_{CH\alpha,\ CH\beta^t}$ = 6.4 Hz, 1 H, $CH\alpha$), 6.60 (t, $^3J_{\text{CH}_{arom},\ \text{CH}_{arom}}$ = 7.4 Hz, 1 H, CH_{arom}), 6.75 (d, $^3J_{\text{CH}_{arom},\ \text{CH}_{arom}}$ = 8.6 Hz, 1 H, CH_{arom}), 7.27 (m, 3 H, CH_{arom}), 7.36 (m, 2 H, CH_{arom}), 7.64 (d, $^3J_{\text{CH}_{arom},\ \text{CH}_{arom}}$ = 7.4 Hz, 2 H, CH_{arom}), 7.76 (m, 3 H, CH_{arom}).

4.5 Analytical methods

4.5.1 Mass spectrometry

4.5.1.1 MALDI-MS

Matrix Assisted Laser Desorption/Ionization Mass Spectrometry (MALDI-MS) is an analytical method to determine the molecular mass of peptides and proteins in high vacuum. For sample preparation 0.5 µL of peptide sample with 0.5 µL DHB-matrix solution (Agilent Technologies) were mixed, and pipetted onto a metallic probe target and dried under air. The cocrystallized samples were investigated with a "Bruker FLEX III" (Bruker Daltronics, Leipzig).

4.5.1.2 HPLC-MS

High Performance Liquid Chromatography (HPLC) was used to characterize substrate and product by retention time on a chromatography column and by mass. Reversed-phase

chromatography is based on hydrophobic interactions with the unpolar stationary phase (C_{18} or C_8 coated silica gel). Elution is mediated by the unpolar organic solvent acetonitrile which competes with the adsorbed analytical compounds for binding positions. The retention time of the analytical compound is monitored by UV-detection. An electrospray-ionization mass detector allows the mass analysis of liquid compounds at atmospheric pressure. Ionization of the analytical compound was achieved by adding 0.1% TFA. In general, experiments were carried out on an Agilent 1100 system. For the identification of peptide fragments from tryptic digests after enzyme assays, Fourier Transform Ion Cyclotron Resonance-MS was applied (FTICR-MS). FTICR-MS is a high-resolution technique that allows determining the composition of molecules based on their accurate mass. Experiments were carried out on a Finnigan-LTQ-FT-mass spectrometer (Thermo Electron Corp, Bremen).

All substrates and products synthesized during this study were confirmed by HPLC-MS or MALDI-MS:

Table 4.3: Characterization of lipopeptide substrates and products by mass. (n.d. = not detected; * = cyclization via L-Orn; ‡ = cyclization via L-Kyn)

Compound	**Observed mass (calculated mass) $[M+H]^+$ [Da]**		
	Substrate	**Cyclized product**	**Hydrolyzed product**
A54145(Val)	1694.6 (1694.7)	1584.6 (1584.7)	1602.6 (1602.7)
A54145(Ile)	1708.6 (1708.7)	1598.6 (1598.7)	1616.6 (1616.7)
A54145(Kyn)	1784.7 (1784.8)	1675.8 (1675.8)	1692.8 (1692.8)
A54145(Thr_3)	1651.7 (1651.7)	1541.7 (1541.7)	1558.6 (1658.7)
A54145(Thr_5)	1694.7 (1693.8)	1584.7 (1583.8)	1502.7 (1502.8)
A54145(Thr_6)	1693.8 (1693.8)	1583.8 (1583.8)	1601.8 (1601.8)
A54145(NXNG)	1692.8 (1692.8)	1582.8 (1582.8)	1600.8 (1600.8)
A54145(DXNG)	1693.7 (1693.8)	1583.7 (1583.8)	1601.7 (1601.8)
A54145(NXDG)	1693.7 (1693.8)	1583.6 (1583.8)	1601.6 (1601.8)
A54145(DAP)	1692.7 (1692.8)	1583.7 (1583.8)	1601.7 (1601.8)
Dap	1716.8 (1716.7)	1606.8 (1606.7) 1606.8 (1606.7)* 1606.8 (1606.7)‡	1624.6 (1624.7)
Dap-Aloc	1800.7 (1800.7)	n.d.	1691.6 (1691.7)
Dap(DAP)	1701.6 (1701.7)	n.d.	1609.6 (1609.7)

Dap(Thr$_3$)	1672.6 (1672.7)	1562.6 (1562.7)	1580.6 (1580.7)
Dap(Thr$_5$)	1730.6 (1730.7)	1620.6 (1620.7)	1638.6 (1638.7)
Dap(Thr$_6$)	1672.7 (1672.7)	1562.7 (1562.7)	1580.7 (1580.7)
Dap(A54$_{1-6}$)	1701.6 (1701.7)	1691.6 (1691.7)	1709.6 (1709.7)
Dap(A54$_{1-3}$)	1730.7 (1730.7)	1620.6 (1620.7)	1638.7 (1638.7)
CDA(DAP)	1562.3 (1562.6)	n.d.	1471.3 (1470.6)
CDA	1575.4 (1575.6)	1465.4 (1465.6)	1483.4 (1483.6)

Table 4.4: Characterization of semipreparative scale generated cyclic lipopeptides by ESI-MS.

Compound	**Observed mass $[M+H]^+$ [Da]**	**Calculated mass $[M+H]^+$ [Da]**
Dap	1606.8	1606.7
Dap(A54$_{1-6}$)	1691.6	1691.7
Dap(A54$_{1-3}$)	1620.6	1620.7
A54145(Val)	1584.6	1584.7
A54145(Ile)	1598.6	1598.7
A54145(Kyn)	1675.8	1675.8
A54145(DAP)	1583.7	1583.8
A54145(NXNG)	1582.8	1582.8
A54145(DXNG)	1583.7	1583.8
A54145(NXDG)	1583.6	1583.8

Table 4.5: Characterization of ncp peptidyl-thioester substrates by ESI-MS.

Compound	**Observed mass $[M+H]^+$ [Da]**	**Calculated mass $[M+H]^+$ [Da]**
ncpA1	1526.5	1526.3
ncpA2	1560.5	1560.4
ncpCT	1514.5	1514.6
ncpCK	1541.5	1541.5
ncpCD	1528.5	1528.5
ncpS2	1573.5	1573.6
ncpS3	1503.5	1503.4
ncpS4	1518.5	1518.4
ncpS5	1544.5	1544.3

ncpS6	1534.5	1534.6
ncpNL	1510.5	1510.6
ncpNT	1498.5	1498.6
ncpNK	1525.5	1525.5
ncpND	1512.5	1512.6
ncpA1-ppan	1151.5	1151.6
ncpA2-ppan	912.4	912.5
ncpA1-SNAC	1117.5	1117.6
ncpA2-SNAC	878.4	878.5
ncpA1-SPh	903.4	902.8
ncpA2-SPh	869.4	869.4

Table 4.6: Characterization of peptide aldehydes by ESI-MS.

Compound	**Observed mass $[M+H]^+$ [Da]**	**Calculated mass $[M+H]^+$ [Da]**
ncpA1-CHO	761.4	761.4
ncpA2-CHO	795.4	795.4

Table 4.7: Characterization of chemoenzymatically generated CDA by ESI-MS.

Compound	**Observed mass $[M+H]^+$ [Da]**	**Calculated mass $[M+H]^+$ [Da]**
CDA	1466.7	1466.6
EN-CDA	1464.7	1464.5

Table 4.8: Characterization of synthesized acyl-CoA derivatives by MALDI-MS.

Acyl-CoA (chain length is indicated)	**Observed mass $[M+H]^+$ [Da]**	**Calculated mass $[M+H]^+$ [Da]**
C4	838.2	838.1
C5	852.2	852.2
C6	866.1	866.2
C7	880.2	880.2
C8	894.1	894.2
C10	922.2	922.2
C6-EN2	864.1	864.2

C8-EN2	892.2	892.2
C4-EN2 (crotonyl)	836.2	836.1
C6-EN3	864.2	864.2
C6-EN3cis	864.2	864.2

4.5.1.3 Protein fingerprinting

To verify the identity of recombinant proteins mass spectrometry based fingerprinting was applied. Therefore, SDS-PAGE bands from the protein of interest were excised and 200 µL of washing solution were added. After incubation at 37 °C for 30 min, the washing solution was removed and gel bands were dried in vacuo at 37 °C for 30 min. Subsequently, in band proteolytic cleavage was achieved by the addition of 15-20 µL trypsin solution. After incubation for 45 min at 37 °C the excess of trypsin solution was removed and incubated for another 16-18 h under otherwise identical conditions. Finally, the peptide fragments were eluted with 20-25 µL diffusion solution under sonication (45 min, RT). Sample analysis was carried out by nano spray-LC-MS. The obtained fingerprint sequences were applied to the MASCOT database.

Washing solution:

NH_4HCO_3	200 mM
CH_3CN	50% (v/v)

Trypsin solution (adjusted to pH 8.1):

trypsin	0.02 µg/µL
NH_4HCO_3	10% (v/v)
CH_3CN	10% (v/v)

Diffusion solution (adjusted to pH 8.1):

TFA	1% (v/v)
CH_3CN	10% (v/v)

5 Results

5.1 Chemoenzymatic design of acidic lipopeptide derivatives

The acidic lipopeptides, including the clinically approved antibiotic daptomycin, constitute a class of structurally related branched cyclic peptidolactones and peptidolactams synthesized by multimodular NRPSs in nature. In this study, the excised peptide cyclases from the A54145 and daptomycin NRPS systems were shown to be able to catalyze the macrocyclization of peptidyl-thioester substrates, which were chemically generated by solid-phase peptide synthesis (SPPS). Both enzymes showed remarkable substrate tolerance *in vitro* and catalyzed the formation of macrolactones with ring sizes from 9-11 amino acids.

Further, the described chemoenzymatic approach towards derivatives of A54145 and daptomycin enabled the semipreparative production of model compounds. Minimal inhibition concentrations (MICs) were determined and a lipopeptide hybrid with a MIC close to that of chemoenzymatic derived daptomycin, as well as a bioactive macrolactam variant of A54145 were identified. Additionally, the two conserved aspartate residues at positions 7 and 9 were shown to be crucial for antimicrobial potency, suggesting their participation in calcium binding. Together the identified structural elements may be promising sites for the introduction of further modifications. An overview of all synthesized peptide substrates, including their characterization by mass spectrometry, is given in Table 4.3.

5.1.1 Overproduction of dap PCP-TE and A54145 PCP-TE

Dap PCP-TE and *A54145 PCP-TE* gene fragments were cloned and overexpressed in *E. coli* BL21 as described in the Methods section. The recombinant proteins were purified by Ni^{2+}-NTA chromatography and the concentrated proteins were resolved by SDS-PAGE (10%) and visualized by Coomassie stain.

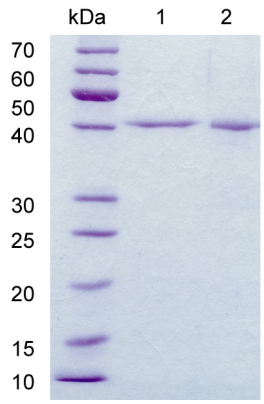

Figure 5.1: Coomassie-stained SDS-PAGE of purified recombinant daptomycin PCP-TE (lane 1, 41.2 kDa) and A54145 PCP-TE (lane 2, 44.5 kDa).

5.1.2 In vitro macrocyclization activity of daptomycin and A54145 cyclases

For the biochemical characterization of the daptomycin and A54145 cyclases linear peptide substrates according to the daptomycin and A54145 peptide sequences were synthesized by SPPS and C-terminally activated with a thiophenol (SPh) leaving group (Figure 5.2). For synthetic reasons, the peptidyl-thioester **Dap** contained L-glutamate at position 12 instead of L-3-methylglutamate, which can be found in the peptide backbone of authentic daptomycin. With regards to the fact, that A54145 occurs in nature as a mixture of two major compounds, containing either valine or isoleucine at the C-terminal position of their peptide sequence, the peptide substrates **A54145(Val)** and **A54145(Ile)** were synthesized. Deviating from the natural A54145 sequence the noncanonical amino acids L-3-O-methylaspartic acid at position 9 and L-3-hydroxyasparagine at position 3 were replaced with L-aspartic acid and L-asparagine, respectively.

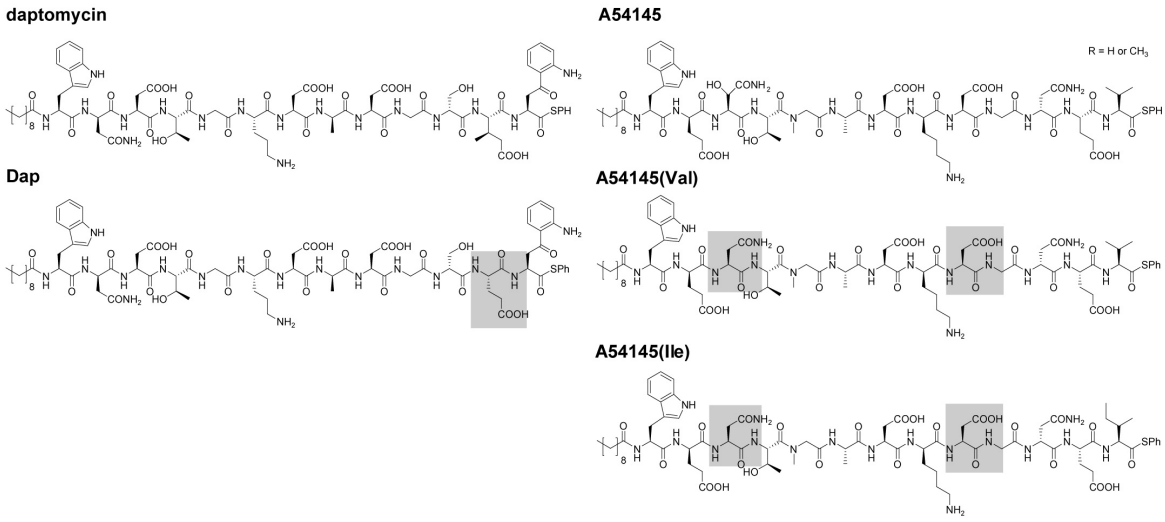

Figure 5.2: Peptidyl-thiophenol substrate analogs of daptomycin and A54145. Amino acid substitutions compared to the naturally occurring compounds are indicated in grey.

The reaction of daptomycin PCP-TE with **Dap** afforded two main products in the HPLC-MS analysis (Figure 5.3). The expected cyclic product (t_R = 34.1 min) was formed along with the hydrolysis product (t_R = 33.3 min) (cyclization-to-hydrolysis ratio of 9:1). The kinetic data for the cyclization of **Dap** catalyzed by daptomycin PCP-TE revealed a K_M value of 50.09 ± 4.48 μM and a k_{cat} of 0.18 ± 0.02 min^{-1}.

In addition to the main product, two minor peaks (t_R = 35.4 min and t_R= 33.4 min) were observed. As shown by MS-MS fragmentation and an orthogonal Aloc-protected **Dap** substrate (see below) these two species arise from the cyclization via alternative side chain nucleophiles, namely the amino group of L-Orn$_6$ or L-Kyn$_{13}$. The non-enzymatic origin of the by-products was evidenced by a negative control experiment with the heat denatured enzyme, in which both species are more apparent than in the enzyme assay (Figure 5.3).

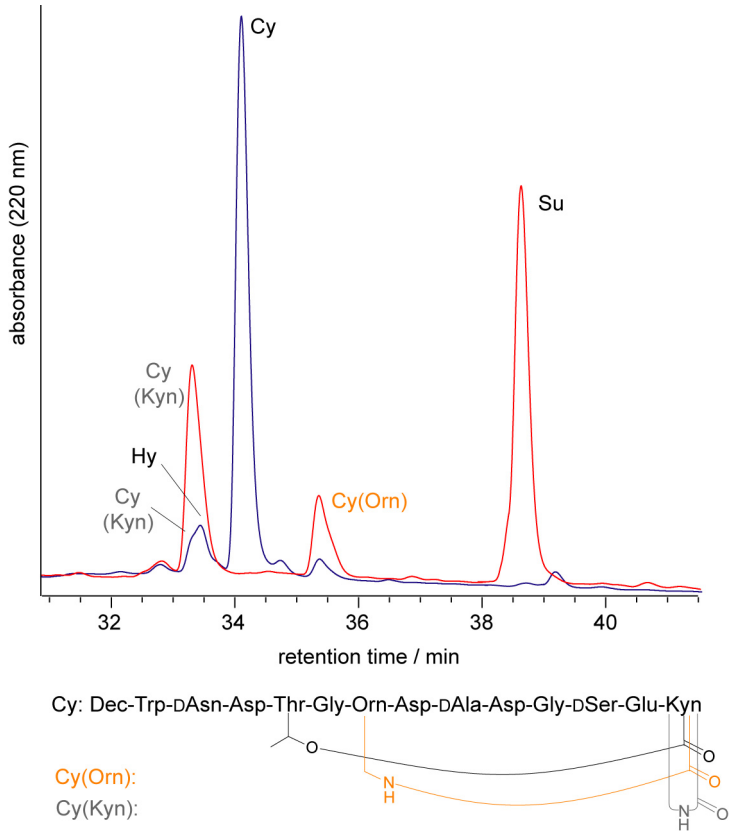

Figure 5.3: Cyclization of the peptidyl-thiophenol substrate Dap by daptomycin cyclase followed by HPLC-MS. The blue trace is the result of the assay with the native enzyme. The red trace corresponds to a negative control with the heat denatured enzyme. Su stands for the chemically synthesized thioester substrate analog and Cy for the cyclized product. Hy indicates hydrolysis; Cy(Kyn) and Cy(Orn) are side-products due to the reaction of the activated C-terminus with the side chain nucleophile of L-ornithine and L-Kyn, respectively.

To prove the identity of the 8-membered macrolactam via Orn$_6$, an orthogonal Aloc side chain protected variant of **Dap**, **Dap-Aloc**, was synthesized. In contrast to **Dap**, for this

substrate the formation of the 8-membered lactam via ornithine was not observed in experiments with and without daptomycin cyclase.

The identity of the other species was proven by MS-MS fragmentation (Figure 5.4). In the case of the 10-membered macrolactone via Thr_4, a fragment containing the intramolecular ester bond was detected directly (Figure 5.4 A).

The kynurenine cycle **Cy(Kyn)** was identified by comparison of its fragmentation pattern with the fragmentation pattern of the **Dap** hydrolysis product **Hy** (Figure 5.4 B). While **Hy** shows the y_1-fragment m/z = 209.1, indicating the C-terminal carboxyl function, for the 7-membered lactam via Kyn, the y_1-fragment m/z = 209.9 was not detected.

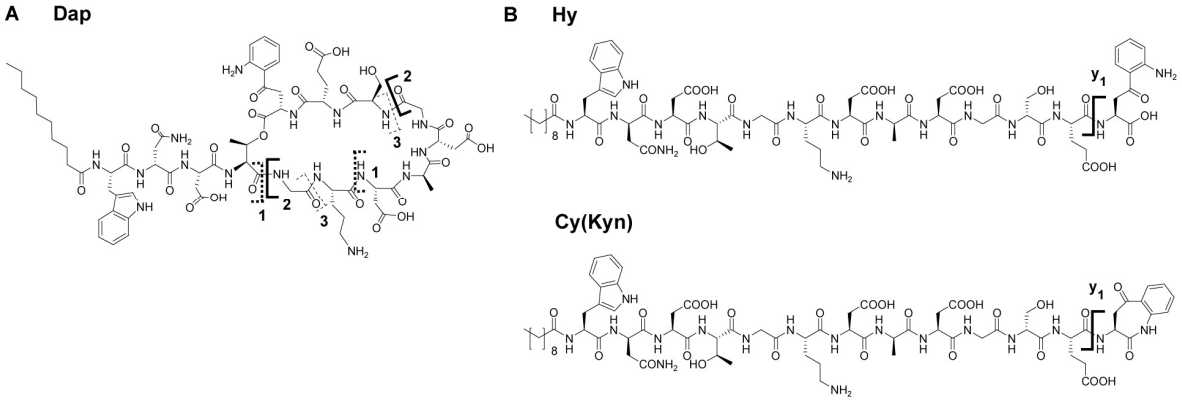

A

compound	molecular formula	species	observed mass of fragments (calculated mass) [Da]
decapeptide lactone of **Dap**	$C_{64}H_{90}N_{15}O_{25}$	$[M+H]^+$	**1** 1435.6 (1435.6)
	$C_{20}H_{32}N_7O_{10}$		**2** 530.3 (530.2)
	$C_{53}H_{72}N_{11}O_{17}$		**3** 1134.5 (1134.5)

B

hydrolysis **Hy** observed mass (calculated mass) $[M+H]^+$ [Da]		cyclization via Kyn_{13} **Cy(Kyn)** observed mass (calculated mass) $[M+H]^+$ [Da]	
y_1	y_1-H_2O	y_1	y_1-H_2O
209.1 (209.1)	191.1 (191.1)	191.1 (191.1)	n.d

Figure 5.4: MS-MS fragmentation of products derived from Dap. A: MS-MS fragmentation of the decapeptide lactone (cyclization via L-Thr_4). Fragments arising from the cleavage of two bonds (1-3) are shown. The patterns giving rise to the above listed fragments are illustrated by solid and dotted lines. B: Depiction of the y_1-fragment of the hydrolysis product Hy and the 7-membered kynurenine cycle Cy(Kyn).

Analogously, the reaction of A54145 cyclase with **A54145(Val)** led to the formation of the expected cyclic product (t_R = 33.0 min), which was identified by ESI-MS (Figure 5.5). The flux towards hydrolysis (t_R = 31.9 min) was remarkably low, revealing a cyclization-to-hydrolysis ratio of 12:1.

After incubation of **A54145(Ile)** with A54145 cyclase, the cyclization product was detected (t_R = 33.9 min) and the occurrence of the undesired hydrolysis product (t_R = 32.9 min) was as low as that for **A54145(Val)** with a cyclization-to-hydrolysis ratio of 12:1 (Figure 5.5). The kinetic data obtained for A54145 PCP-TE revealed a K_M value of 80.17 ± 7.70 μM and a k_{cat} of 0.22 ± 0.01 min^{-1} with **A54145(Ile)** and a K_M value of 76.64 ± 8.60 μM and a k_{cat} of 0.24 ± 0.02 min^{-1} with **A54145(Val)**.

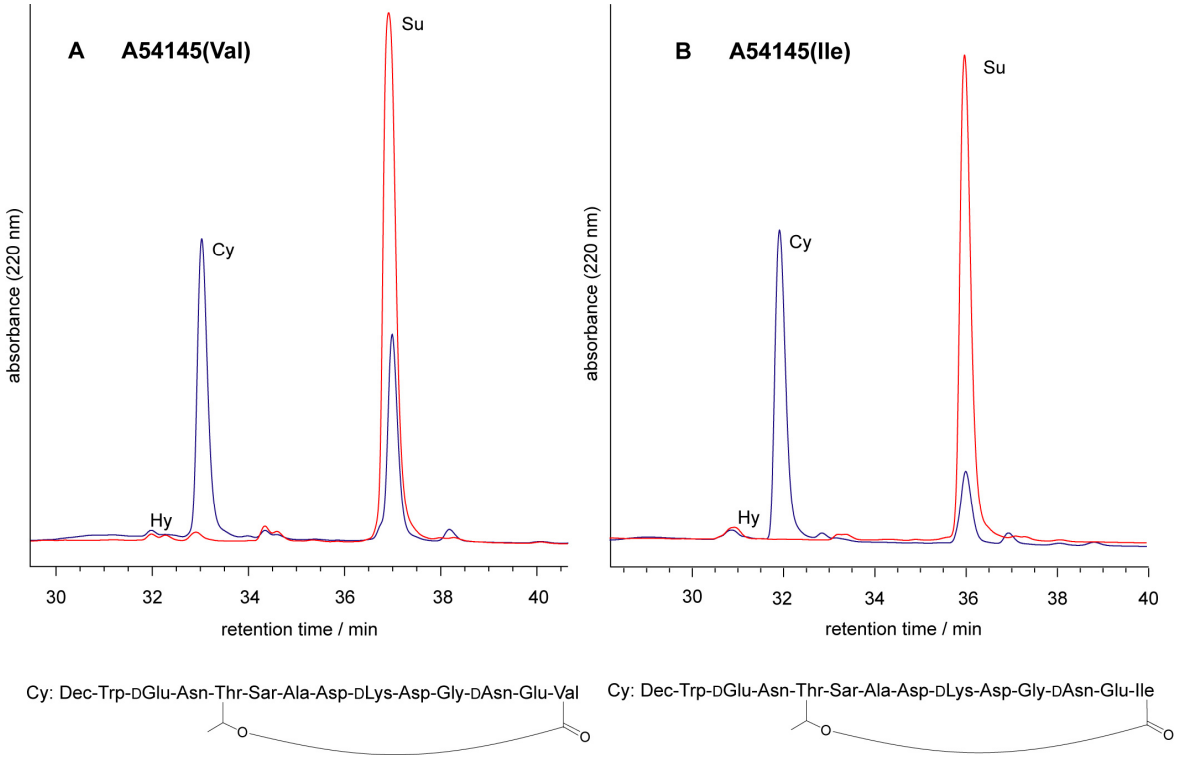

Figure 5.5: Cyclization of the peptidyl-thioester substrates A54145(Val) (A) and A54145(Ile) (B) by A54145 cyclase followed by HPLC-MS. Red traces represent the enzyme assay. Blue traces correspond to a negative control assay with the heat denatured enzyme. Su stands for the chemically synthesized thioester substrate analog and Cy for the cyclized product. Hy indicates hydrolysis.

The identity of the observed species was confirmed by MS-MS fragmentation. For both substrates cyclization was shown to occur via threonine at position 4, leading to the desired 10-amino acid macrolactone (Figure 5.6).

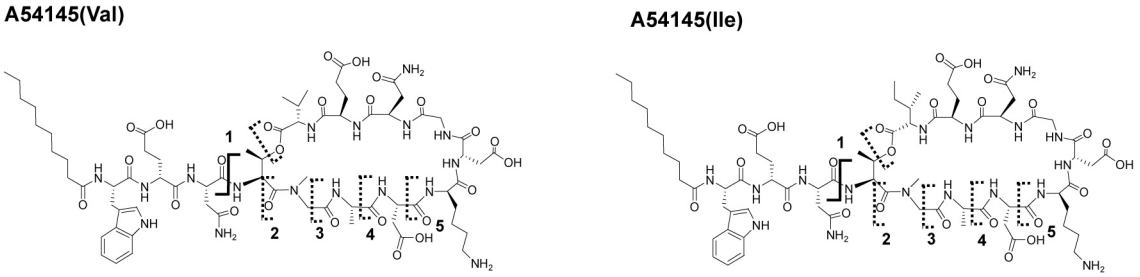

compound	molecular formula	species	observed mass of fragments (calculated mass) [Da]
decapeptide lactone **A54145(Val)**	$C_{40}H_{64}N_{12}O_{18}^{+}$	$[M+H]^{+}$	**1** 1001.5 (1001.5)
	$C_{36}H_{60}N_{11}O_{17}^{+}$		**2** 918.5 (918.4)
	$C_{33}H_{55}N_{10}O_{16}^{+}$		**3** 847.4 (847.4)
	$C_{30}H_{50}N_{9}O_{15}^{+}$		**4** 776.4 (776.3)
	$C_{26}H_{45}N_{8}O_{12}^{+}$		**5** 661.4 (661.3)
decapeptide lactone **A54145(Ile)**	$C_{41}H_{66}N_{12}O_{18}^{+}$		**1**.1015.5 (1015.5)
	$C_{37}H_{62}N_{11}O_{17}^{+}$		**2** 932.4 (932.4)
	$C_{34}H_{57}N_{10}O_{16}^{+}$		**3** 861.4 (861.4)
	$C_{31}H_{52}N_{9}O_{15}^{+}$		**4** 790.3 (790.3)
	$C_{27}H_{47}N_{8}O_{12}^{+}$		**5** 674.4 (675.3)

Figure 5.6: MS-MS fragmentation of products derived from A54145(Val) and A54145(Ile). Fragments arising from single bond cleavage (1) or simultaneous cleavage of two bonds (2-5) are shown. The patterns giving rise to the above listed fragments are illustrated by solid lines (1) and dotted lines (2-5). Evidence for the connection via L-Thr$_4$ is given due to the fact that the alternative side chain nucleophile L-Lys$_6$ can not lead to the fragments (1-5).

5.1.3 Variation of the ring size

Next, we addressed the question whether daptomycin and A54145 cyclases are able to catalyze the formation of macrolactones with different ring sizes. Therefore, six peptidyl-thioester substrates, **Dap(Thr$_3$)**, **Dap(Thr$_5$)**, **Dap(Thr$_6$)**, **A54145(Thr$_3$)**, **A54145(Thr$_5$)**, and **A54145(Thr$_6$)**, were synthesized (Figure 5.7). The cycle-forming L-threonine, originally found at position 4 of the daptomycin and A54145 peptide backbone, was placed at amino acid position 3, 5, or 6, respectively, while L-alanine occupied position 4 of those peptidyl-thioester substrates. Consequently, after cyclization, a macrolactone consisting of 11, 9, or 8 amino acids should be formed.

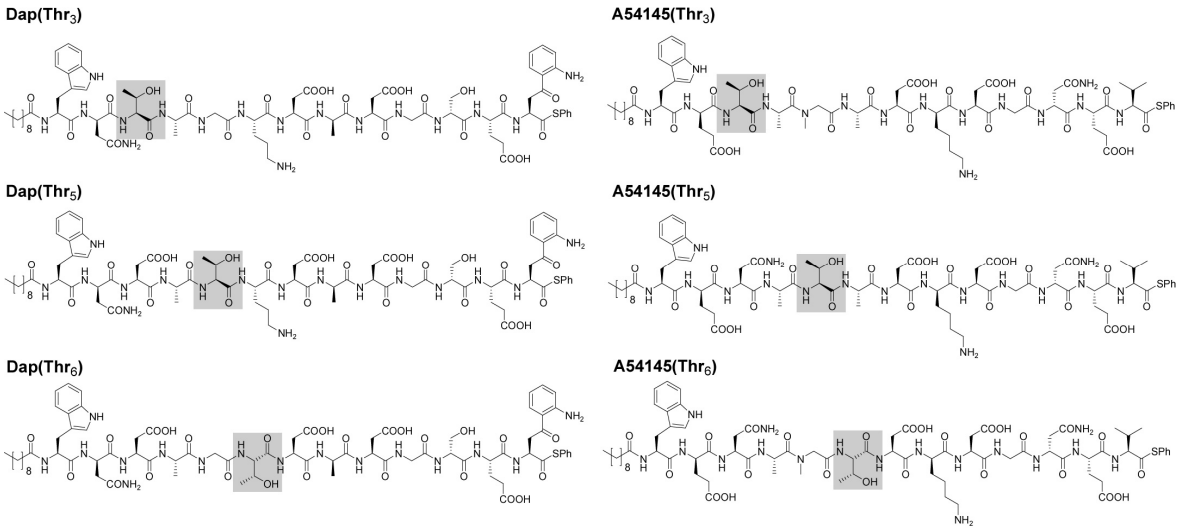

Figure 5.7: Peptidyl-thiophenol substrates with the cycle forming L-threonine side chain nucleophile at position 3, 5, and 6, respectively. Threonine side chains are indicated in grey.

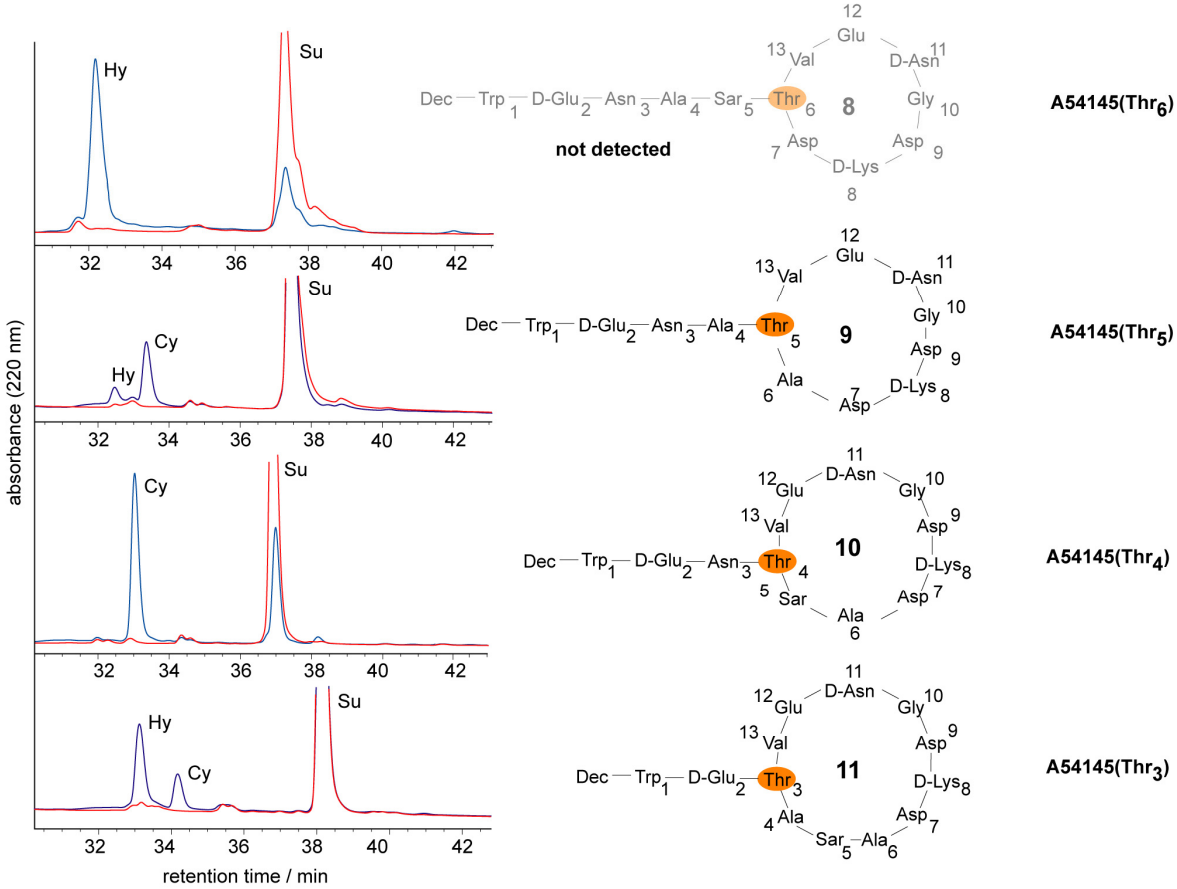

Figure 5.8: Formation of 9-11 amino acid cyclic macrolactones mediated by A54145 cyclase. Left: HPLC analysis of the cyclization reaction. Right: peptide sequences of the assayed thioester substrates; the ring size and the cycle-forming threonine are highlighted. Su stands for the chemically synthesized thioester substrate analog and Cy for the cyclized product. Hy indicates hydrolysis.

As shown in Figure 5.8, **A54145(Thr$_3$)** was cyclized (t_R = 34.2 min), but hydrolysis (t_R = 33.1 min) was favored (cyclization-to-hydrolysis ratio of 1:3). Branch point

movement of one amino acid position was also tolerated in the case of **A54145(Thr$_5$)** in forming the nonapeptide lactone (t_R = 33.4 min) after incubation with A54145 PCP-TE. Interestingly, the occurrence of hydrolysis (t_R = 32.5 min) was decreased compared to that of **A54145(Thr$_3$)**, revealing the cyclization-to-hydrolysis ratio of 4:1. In contrast to the reaction with **A54145(Thr$_3$)** and **A54145(Thr$_5$)**, attempts to cyclize **A54145(Thr$_6$)** with A54145 PCP-TE resulted exclusively in hydrolysis of the peptide thioester substrate (t_R = 32.3 min) and did not lead to the eight-membered lactone.

Assaying **Dap(Thr$_3$)** and **Dap(Thr$_5$)** for cyclization revealed that both substrates were cyclized (t_R = 34.9 min and t_R = 34.6 min), indicating that branch point movement of one amino acid was also tolerated by Dap PCP-TE. Incubation of **Dap(Thr$_6$)** with Dap PCP-TE led only to the hydrolysis product (t_R = 32.4 min). In contrast to the results with A54145 PCP-TE, the formation of the macrolactones derived from **Dap(Thr$_3$)** and **Dap(Thr$_5$)** was accompanied by a stronger occurrence of hydrolysis (Figure 5.9).

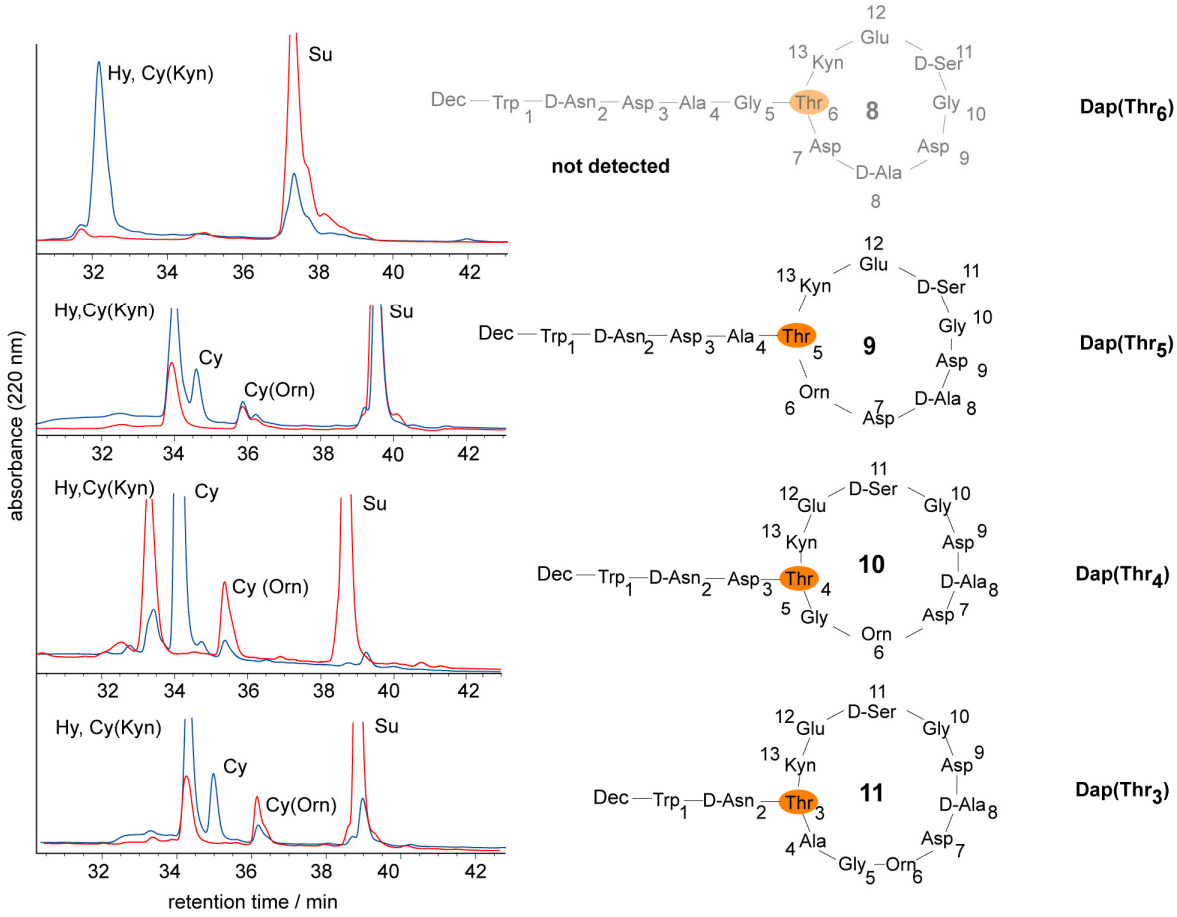

Figure 5.9: Formation of 9-11 amino acid cyclic macrolactones mediated by daptomycin cyclase. Left: the HPLC analysis of the cyclization reaction. Right: peptide sequences of the assayed thioester substrates; the ring size and the cycle-forming threonine are highlighted. Su stands for the chemically synthesized thioester substrate analog and Cy for the cyclized product. Hy indicates hydrolysis. Cy(Kyn) and Cy(Orn) are side products due to the reaction of the activated C-terminus with the side chain nucleophile of L-ornithine and L-Kyn, respectively.

5.1.4 Macrolactam formation

All members of the acidic lipopeptide family have macrocyclic structures in order to constrain their biological active form. Interestingly, this structural constraint is not always achieved via the formation of a macrolactone as for daptomycin and A54145 since friulimycin [116], amphomycin [117], and laspartomycin [95] contain a 10-membered macrolactam (Figure 5.10).

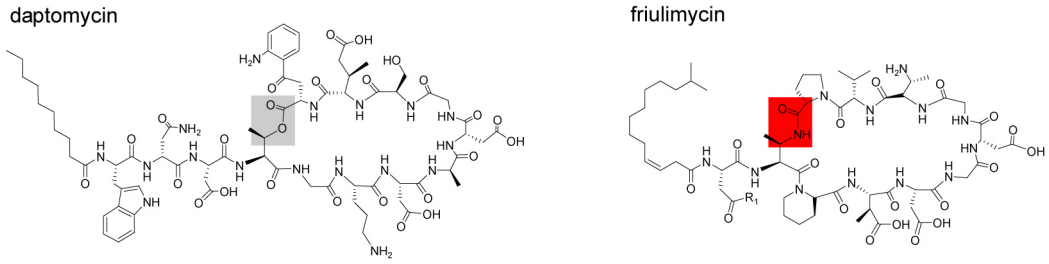

Figure 5.10: The conserved ten-membered macrocyclic ring of lipopeptides can either be achieved by the formation of a macrolactone (daptomycin) or -lactam (friulimycin).

To explore the ability of the recombinant cyclases of A54145 and daptomycin to catalyze the formation of macrolactams, the three peptidyl-thioester substrate analogs **Dap(DAP)**, **A54145(DAP)**, and **CDA(DAP)** were synthesized carrying the cyclization nucleophile L-diaminopropionate (DAP) instead of L-threonine at position 4 or 2 of their peptide sequence (Figure 5.11).

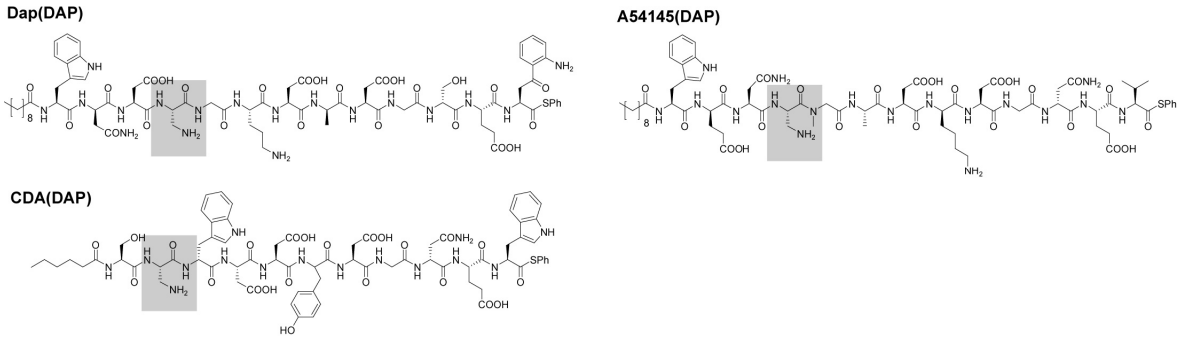

Figure 5.11: Peptidyl-thiophenol substrates containing diaminopropionate (DAP) instead of L-Thr as cyclization nucleophile.

Remarkably, **A54145(DAP)** was cyclized efficiently by A54145 PCP-TE (t_R = 32.3 min) as shown in Figure 5.12. The cyclization reaction revealed a very low flux toward hydrolysis (t_R = 30.9 min) (cyclization-to-hydrolysis ratio of 12:1) in analogy to the macrolactonization reaction of the peptidyl-thioester substrates **A54145(Val)** and **A54145(Ile)**. To confirm the amide linkage between DAP and the C-terminal amino acid of A54145, MS-MS fragmentation clearly identified that the observed macrolactam is

formed via DAP_4 and Ile_{13} (Figure 5.13). In contrast to this result, no cyclization of **Dap(DAP)** or **CDA(DAP)** was observed after incubation with either the daptomycin or CDA cyclization catalyst. Additional attempts to cyclize **Dap(DAP)** and **CDA(DAP)** with A54145 PCP-TE also failed.

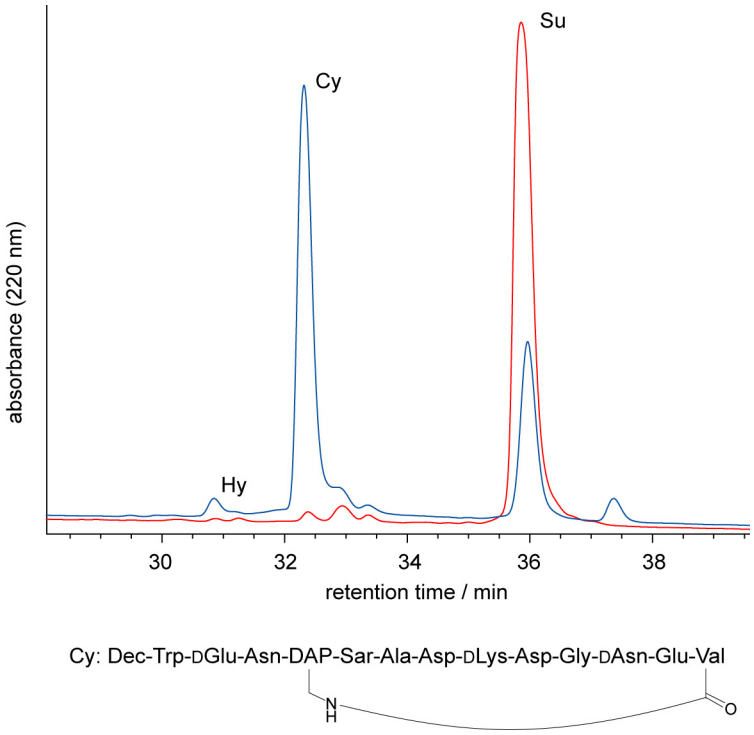

Figure 5.12: Cyclization of A54145(DAP) with A54145 cyclase leads to the formation of a macrolactam analog of A54145 analyzed by HPLC-MS. Shown are the enzyme assay (blue trace) and the negative control with the heat denatured enzyme (red trace). Su is the chemically synthesized peptide substrate, Cy the cyclized product. Hy indicates hydrolysis.

A54145(Ile)

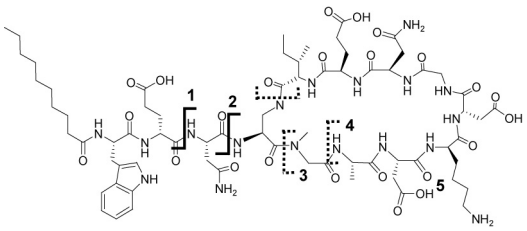

compound	molecular formula	species	observed mass of fragments (calculated mass) [Da]
decapeptide lactone of **A54145(DAP)**	$C_{44}H_{72}N_{15}O_{19}^+$	$[M+H]^+$	**1** 1114.5 (111.4.5)
	$C_{40}H_{66}N_{13}O_{17}^+$		**2** 1000.5 (1000.5)
	$C_{37}H_{60}N_{11}O_{16}^+$		**3** 914.4 (914.4)
	$C_{34}H_{55}N_{10}O_{15}^+$		**4** 843.4 (843.4)

Figure 5.13: MS-MS fragmentation of the decapeptide lactone cyclized via L-DAP_4. Shown are fragments arising from single bond cleavage (1) and (2), or simultaneous cleavage of two bonds (3) and (4). The patterns giving rise to the above listed fragments are illustrated by solid and dotted lines. The intensity of fragments (3) and (4) is much lower than for (1) and (2), indicating that branch point is L-DAP at position 4, since cleavage of single bond is much more likely than simultaneous cleavage of two bonds.

5.1.5 Enzymatic cross reactivity

To gain further information about the substrate specificity of daptomycin and A54145 cyclases the ability of these enzymes to cyclize the peptidyl-thioester substrate analogs of daptomycin (**Dap**), A54145 (**A54145(Val)**), and CDA (**CDA**) was examined. In addition to this, the substrate specificity of the previously characterized CDA cyclase was evaluated with these three peptidyl-substrates. Table 5.1 summarizes the results, including cyclization-to-hydrolysis ratios. As shown before, each recombinant cyclase was able to catalyze its associated substrate analog. Interestingly, A54145 PCP-TE cyclized **Dap** and Dap PCP-TE was able to cyclize **A54145(Val)**. On the other hand, only hydrolysis was observed for the substrate analog **CDA** after incubation with A54145 or daptomycin cyclase, respectively. It was previously shown that CDA PCP-TE is able to cyclize **Dap** [118]; **A54145(Val)** in contrast was not converted after incubation with CDA cyclase. Remarkably, the cyclization-to-hydrolysis ratio for **Dap** with A54145 PCP-TE (cyclization-to-hydrolysis ratio of 10:1) was as high as that for the naturally associated pair of cyclase and substrate analog (cyclization-to-hydrolysis ratio of 9:1). Further, the A54145 analog **A54145(Val)** was cyclized with less than 10% hydrolysis (cyclization-to-hydrolysis ratio of 12:1) by A54145 PCP-TE, revealing the excellent *in vitro* activity of this recombinant TE domain.

Table 5.1:Substrate specificity of lipopeptide cyclases with cyclization-to-hydrolysis ratio.

	Dap PCP-TE	A54145 PCP-TE	CDA PCP-TE
Dap	9:1	10:1	2:1
A54145	5:1	12:1	no turnover
CDA	hydrolysis	hydrolysis	6:1

5.1.6 Structure-activity studies

To identify structural features of the acidic lipopeptides that are important for antibacterial activity, a small library consisting of ten peptidyl-thioester substrates (**Dap**, **A54145(Val)**, **A54145(Ile)**, **A54145(Kyn)**, **Dap(A54$_{1-3}$)**, **Dap(A54$_{1-6}$)**, **A54145(DAP)**, **A54145(NXDG)**, **A54145(DXNG)**, and **A54145(NXNG)**) was synthesized (Figure 5.14 and 5.15).

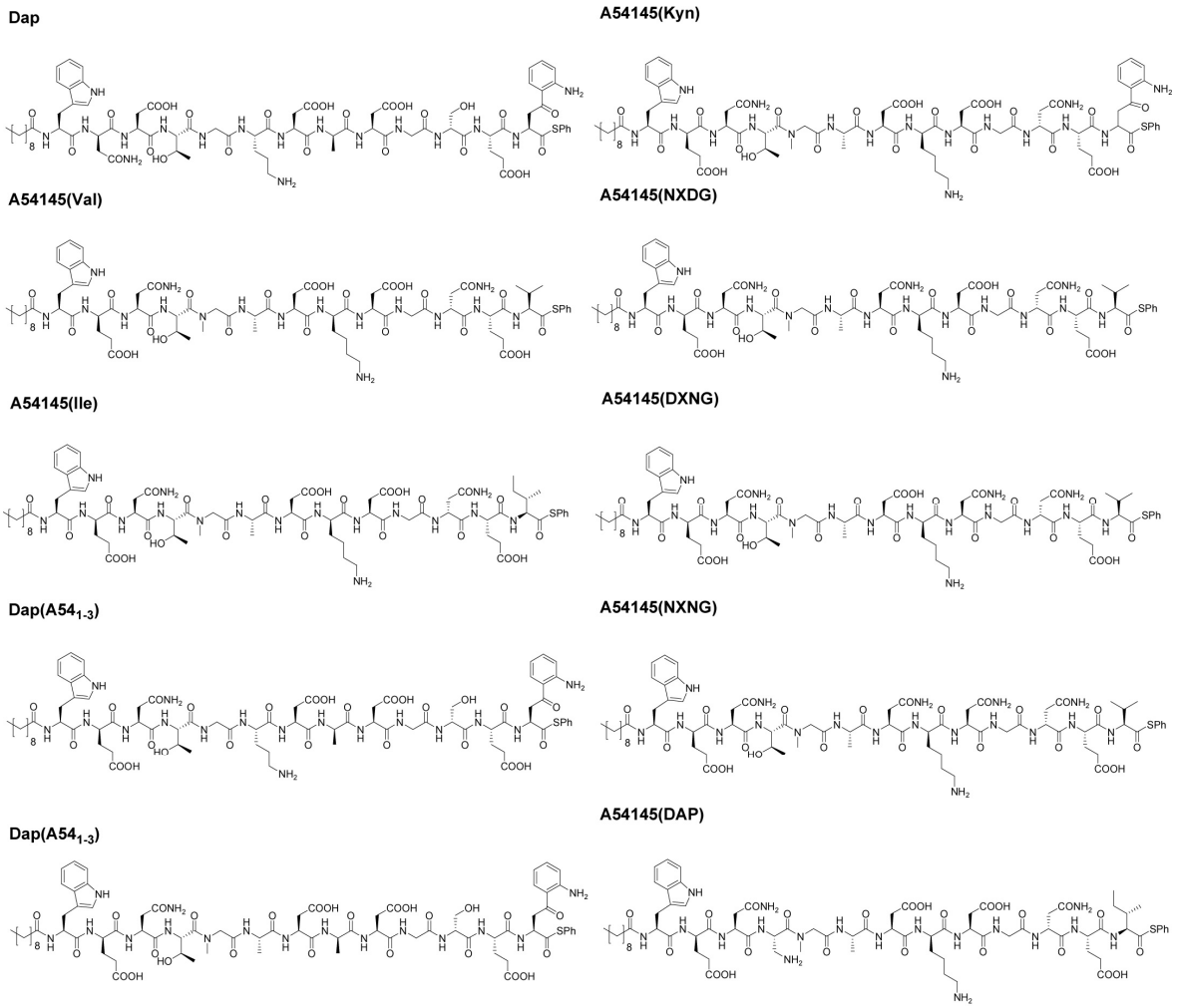

Figure 5.14: Peptidyl-thiophenol substrates for semipreparative macrocyclization and minimal inhibition concentration (MIC) determination.

Based on the results obtained when testing enzymatic cross reactivity, A54145 and daptomycin PCP-TE were found to be the most efficient cyclization catalysts for these substrates. After enzymatic cyclization in a semipreparative scale, the obtained products were purified with reversed-phase HPLC and checked for purity by HPLC-MS (Table 4.4). Subsequently, antibacterial activity was measured by determining the minimal inhibition concentration (MIC) against *B. subtilis* PY79. In this strain, the own production of secondary metabolites is knocked-out to prevent cooperative effects with the tested compound.

Figure 5.15: Derivatives of daptomycin and A54145 tested for antimicrobial activity. The macrocyclic compounds were derived from peptidyl-thioester substrates after incubation with A54145 or daptomycin cyclase, respectively. Amino acids from the daptomycin peptide sequence are indicated in orange, those from A54145 peptide sequence in blue. Substitution of acidic amino acids with Asn is indicated in red. The macrolactam analog of A54145 contains DAP as the cycle forming amino acid side chain instead of threonine, as marked in grey.

Table 5.2: Minimal inhibition concentrations (MICs) of the lipopeptides shown in Figure 5.15.

Compound	MIC_{90} (µg/mL) at 73.6 mg Ca^{2+}/L
authentic daptomycin	2
Dap	11
A54145(Val)	200
A54145(Ile)	25
A54145(Kyn)	15
Dap($A54_{1-3}$)	20
Dap($A54_{1-6}$)	20
A54145(DAP)	25
A54145(NXDG)	>900
A54145(DXNG)	>900
A54145(NXNG)	>900

In comparison to authentic daptomycin with a MIC of 2 μg/mL, the cyclic peptide **Dap** (at position 12, glutamate is incorporated instead of 3-methylglutamate) displayed a MIC value of 11 μg/mL (Table 5.2).

Since naturally occurring A54145 variants differ at position 13, the peptidolactones **A54145(Val)** and **A54145(Ile)** were generated. Interestingly, the MIC value of **A54145(Ile)** was 25 µg/mL, while **A54145(Val)** was less effective against *B. subtilis*, revealing a MIC of 200 μg/mL. The A54145 analog **A54145(Kyn)** displayed a MIC of 15 μg/mL that comes close to chemoenzymatic derived **Dap**. With regard to the fact that both compounds differ only in one amino acid position, these results underline the great importance of single side chain substitutions for bactericidal activity.

Additionally, two hybrid molecules of A54145 and daptomycin were synthesized (Figure 5.15). To explore the relevance of the exocyclic amino acids, a peptidyl-thioester substrate based on the natural daptomycin peptide sequence carrying the three N-terminal amino acids of A54145, **Dap(A54$_{1\text{-}3}$)**, was designed. Surprisingly, the exchange of the amino acid tail did not crucially affect bioactivity, indicating that these residues are not substantial for antimicrobial behavior. To better approximate A54145, the bioactivity of cyclized **Dap(A54$_{1\text{-}6}$)**, a daptomycin/A54145 hybrid containing the amino acids 1-6 of A54145 and 7-13 of daptomycin's peptide's sequence, was further examined. Compared to **Dap(A54$_{1\text{-}3}$)** the MIC for **Dap(A54$_{1\text{-}6}$)** did not change significantly.

The antibacterial activity of **A54145(DAP)**, which has been cyclized by A54145 PCP-TE, was characterized by a MIC value of 25 μg/mL and is in good agreement with the MIC value of the macrolactone **A54145(Ile)**.

Finally, to prove the significance of acidic amino acid residues for the antibacterial behavior of A54145, three peptidolactones, **A54145(NXDG)**, **A54145(DXNG)**, and **A54145(NXNG)** were synthesized and tested as reported above. Single deletion of aspartic acid as well as the double deletion of both aspartate residues led to the total loss of antibacterial activity (Table 5.2).

5.2 Peptide macrocyclization triggered by the nostocyclopeptide reductase domain: the self-assembly of a macrocyclic imine.

Many biologically active natural products have macrocyclic structures. In nonribosomal peptides (NRPs) macrocyclization is commonly achieved via the formation of intramolecular ester or amide bonds catalyzed by thioesterase domains during biosynthesis. A unique and so far unknown type of peptide cyclization occurs in the nostocyclopeptide (ncp), a macrocyclic imine produced by the terrestrial cyanobacterium *Nostoc* sp. ATCC53789 [14].

The next paragraph deals with the biochemical characterization of the reductive imino bond formation triggered by the C-terminal reductase domain ncp R from the ncp biosynthetic system. During these studies, it could be shown that the reductive release of a linear peptide aldehyde is followed by the spontaneous formation of a relatively stable imino head-to-tail linkage. This is the first time that such a type of imine macrocyclization induced by the reductive release of reactive peptide aldehydes has been investigated.

5.2.1 Overproduction of ncp PCP-R and ncp R

The gene fragments *ncp PCP-R* and *ncp R* of the nostocyclopeptide biosynthetic gene cluster were cloned and overexpressed in *E. coli* BL21 as described in the Methods section. The recombinant proteins were purified by Ni^{2+}-NTA chromatography and the concentrated proteins were resolved by SDS-PAGE (12%) and visualized by Coomassie-stain.

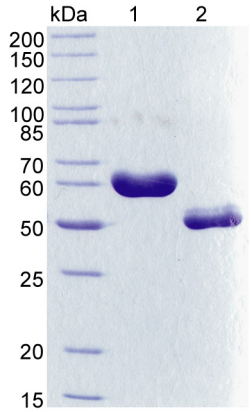

Figure 5.16: Coomassie-stained SDS-PAGE of purified recombinant ncp PCP-R (lane 1, 58.6 kDa) and ncp R (lane 2, 48.6 kDa).

5.2.2 *In vitro reductase activity of ncp PCP-R and ncp R*

In order to characterize the role of the ncp R domain in imine macrocyclization, the reductase activity of ncp PCP-R was tested *in vitro* with peptidyl-thioester substrates that were generated via SPPS (Figure 5.17).

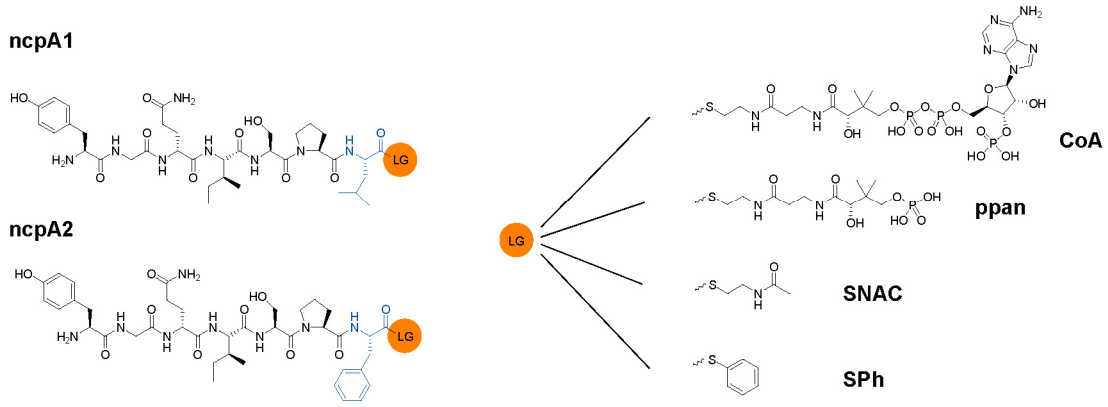

Figure 5.17: Peptidyl-thioester substrates used for the biochemical characterization of ncp PCP-R. The C-terminus is activated with a thioester leaving group (LG): coenzyme A (CoA), phosphopantetheine (ppan), N-acetylcysteamine (SNAC), or thiophenol (SPh).

For synthetic reasons the naturally occurring 4-methylproline was replaced with proline. Since the ncp occurs in nature as a mixture of two compounds that differ in the C-terminal amino acid position, the Leu_7 and Phe_7 variants **ncpA1** and **ncpA2** were synthesized. To achieve enzymatic recognition, the linear peptide substrates were C-terminally activated with four different leaving groups such as thiophenol, SNAC, ppan, and CoA. These substrate analogs mimic the natural situation where the fully assembled peptide chain is thioester-bound to the PCP of the last module.

HPLC-MS analysis of the assay with **ncpA1** and **ncpA2** revealed product formation for peptidyl-CoA substrates in the presence of NADPH (Figure 5.18). NADH was not accepted as electron donor. Mass analysis confirmed that the two linear substrate mimics **ncpA1** and **ncpA2** were converted mainly into the corresponding cyclic imines (t_R = 15.2 min and t_R = 15.6 min) and only traces of **ncpA1** and **ncpA2** aldehydes were detected.

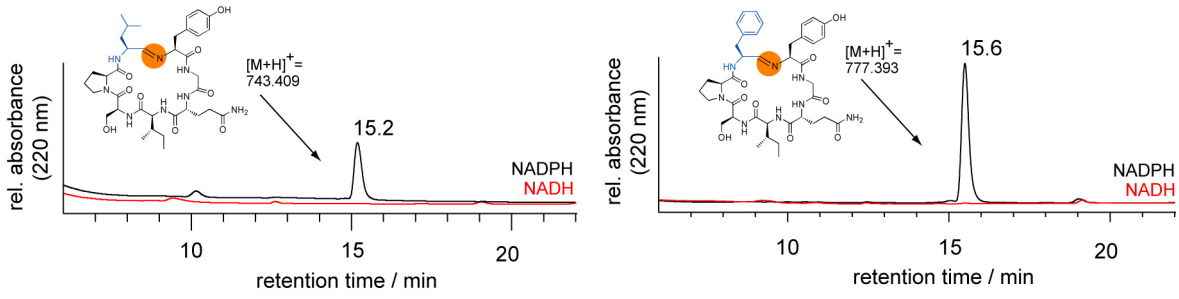

Figure 5.18: HPLC-MS analysis of the ncp PCP-R activity assay.

In contrast to CoA- and ppan-activated substrates, thiophenol and SNAC were not suited as leaving groups.

The kinetic rates of the peptidyl-CoA reduction mediated by ncp PCP-R were determined spectrophotometrically. This direct monitoring is possible, because the reduction of each substrate molecule is accompanied by the consumption of one equivalent NADPH leading to a decrease in absorption at 340 nm. Following the extinction coefficient 6220 $M^{-1}cm^{-1}$ for NADPH, the below listed K_M and k_{cat} values were determined (Table 5.3).

Remarkably, ncp PCP-R was the first recombinant R domain excised from NRPSs that exhibited multiple turnover reactivity *in vitro*. Nevertheless, the alone standing R domain displayed significantly lower catalytic activity. Therefore, all subsequent experiments were performed with recombinant ncp PCP-R.

Table 5.3: Kinetic parameters for peptidyl-CoA reduction by ncp PCP-R.

Substrate	K_M (µM)	k_{cat} (min^{-1})	k_{cat} / K_M ($min^{-1}mM^{-1}$)
ncpA1	101.90 ± 14.48	9.77 ± 1.18	89.65 ± 6.33
ncpA2	102.52 ± 10.48	6.19 ± 0.89	59.34 ± 8.48

5.2.3 Imine self-assembly via peptide aldehyde formation

To investigate the role of the ncp R domain in imino bond formation, linear peptide aldehydes, **ncpA1-CHO** and **ncpA2-CHO** with sequences identical to **ncpA1** and **ncpA2** were chemically synthesized (Table 4.6 and Figure 5.19).

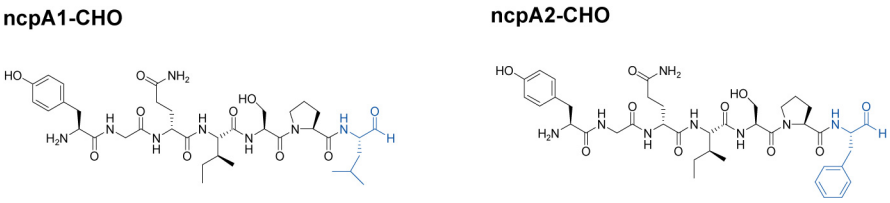

Figure 5.19: Peptide aldehydes with sequences of ncpA1 and ncpA2.

NcpA1-CHO and **ncpA2-CHO** were incubated in aqueous buffer solution at pH 7 with and without the recombinant ncp PCP-R under otherwise identical conditions. In both cases, the formation of the macrocyclic imine (t_R = 15.2 min and t_R = 15.6 min) was detected in identical amounts (Figure 5.20). These results were significant, as they demonstrated that the macrocyclization of the linear heptapeptide aldehydes was not influenced by recombinant ncp PCP-R. With this experiment, the imine formation was

uncoupled from the R domain mediated reductive release, demonstrating that this type of macrocyclization can occur enzyme-independent.

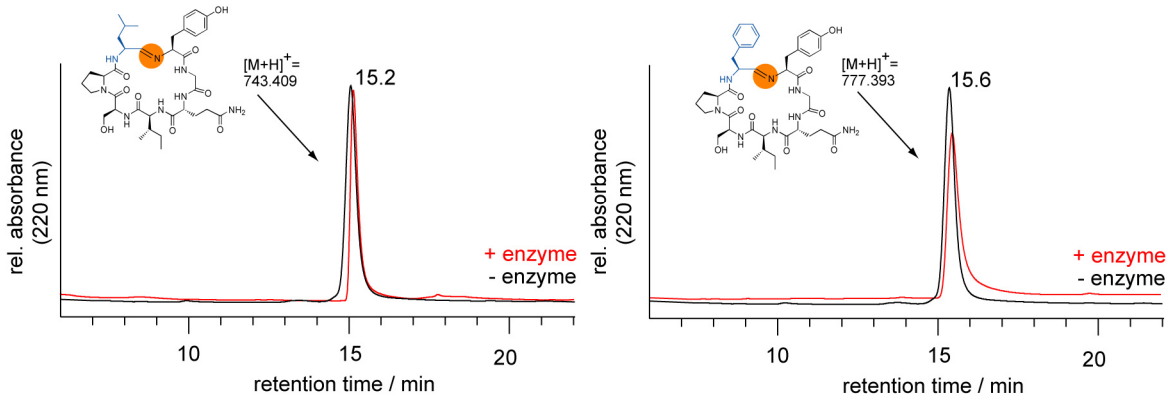

Figure 5.20: Cyclization assay with the chemically synthesized peptide aldehydes ncpA1-CHO (left) and ncpA2-CHO (right). The formation of the macrocyclic imines is not dependent on the recombinant reductase ncp PCP-R.

5.2.4 Alanine scan

To identify structural elements of the ncp peptide sequence that are important for the imine self-assembly, an alanine scanning mutagenesis was performed. Therefore, several peptidyl-CoA substrates were synthesized according to the **ncpA2** sequence. In each substrate, one single amino acid at positions 2-6, respectively, was substituted by L-alanine, while all other amino acids remained conserved (Table 4.5 and Figure 5.21).

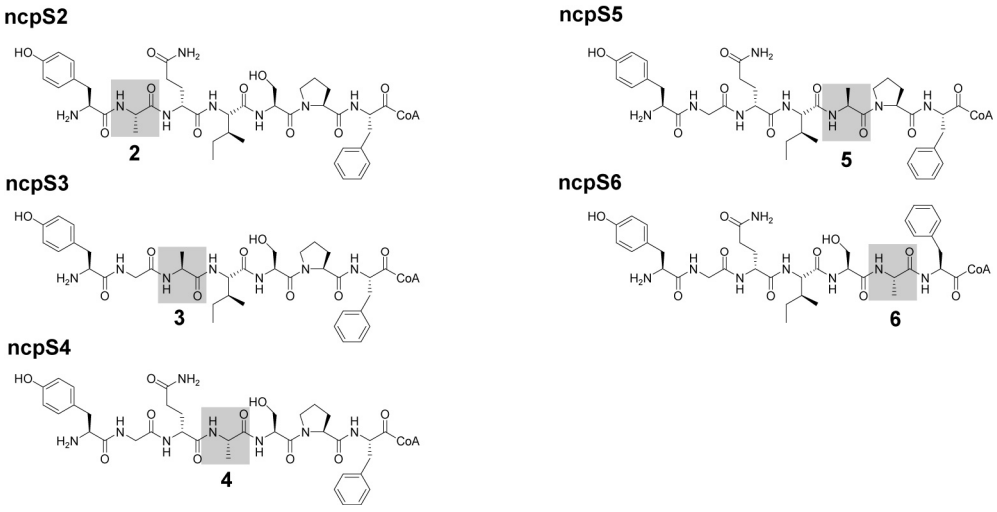

Figure 5.21: Peptidyl-CoA substrates used for the alanine scan experiment. Amino acid substitutions are indicated in grey.

Incubation with the recombinant ncp PCP-R revealed that all synthesized substrates were enzymatically reduced to the corresponding peptide aldehydes. The imine self-assembly was observed for **ncpS4**, **ncpS5**, and **ncpS6**. Replacement of D-Gln_3 and Gly_2 instead, as realized in the substrates **ncpS2** and **ncpS3,** had significant influence on macrocycle formation by reducing imine formation to less then 5% based on the comparison of the intensity of the observed mass signals (Figure 5.22 and Table 5.4).

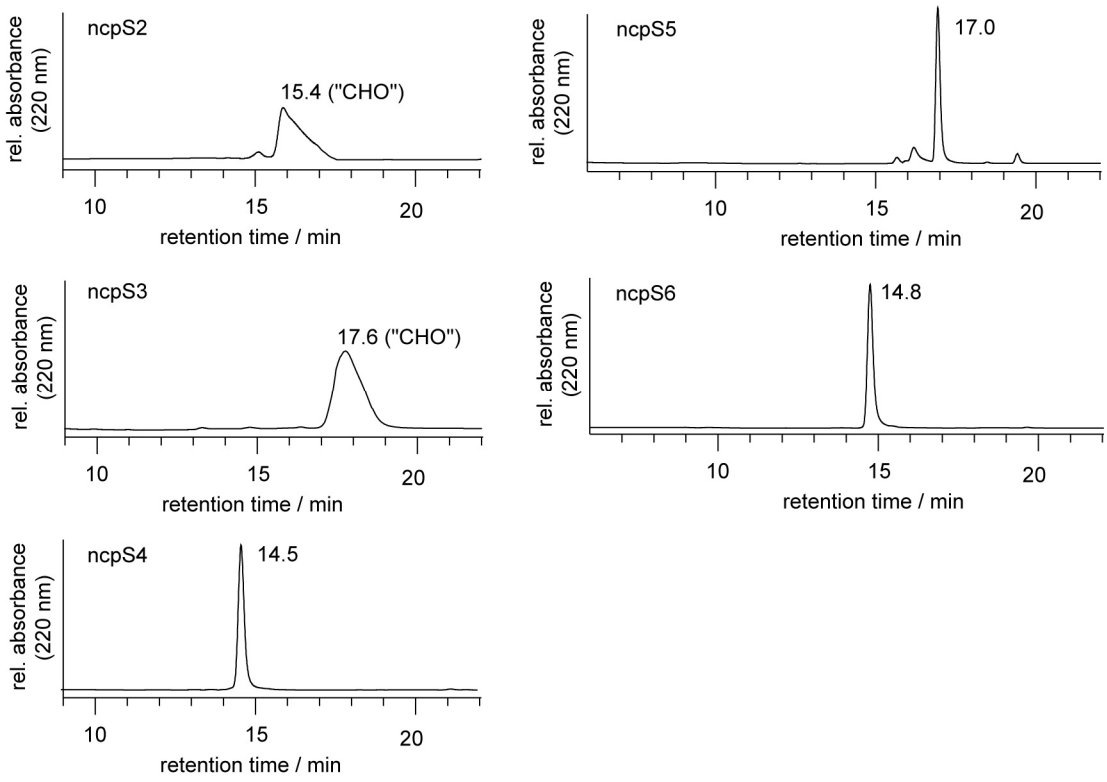

Figure 5.22: HPLC-MS analysis of the alanine scan experiment. TFA was not added to the solvent as a modifying agent as the low pH would destroy the macrocyclic imine. Therefore, linear peptide aldehydes ncpS2 and ncpS3 elute as bright signals, instead of defined peaks.

Table 5.4: Results of the alanine scan experiment with masses of the observed products. Calculated masses are given in brackets. n.d. = not detected.

Compound	Retention time (t_R)	Cyclic imine $[M+H]^+$ [Da]	Retention time (t_R)	Peptide aldehyde $[M+H]^+$ [Da]
ncpS2	15.4	790.4 (790.4) (<5%)	15.4	808.4 (808.4)
ncpS3	17.6	720.3 (720.4) (<5%)	17.6	738.4 (738.4)
ncpS4	14.5	735.4 (735.4)	n.d.	
ncpS5	17.0	761.4 (761.4)	n.d.	
ncpS6	14.8	751.5 (751.4)	n.d.	

5.2.5 Substrate specificity of ncp PCP-R

According to previous studies on TE domain mediated peptide cyclization, an important role for the C- and the N-terminal amino acids was anticipated. However, ncp occurs in nature as a mixture of two compounds, ncpA1 and ncpA2, that differ in the C-terminal position, which can be occupied by either phenylalanine or leucine. Despite these aromatic and aliphatic amino acids, substrates containing threonine, lysine, or aspartate at this position were prepared. In other peptidyl-CoAs phenylalanine remained at the C-terminus, while the N-terminal tyrosine was substituted with threonine, lysine, aspartate or leucine, respectively (Table 4.5 and Figure 5.23).

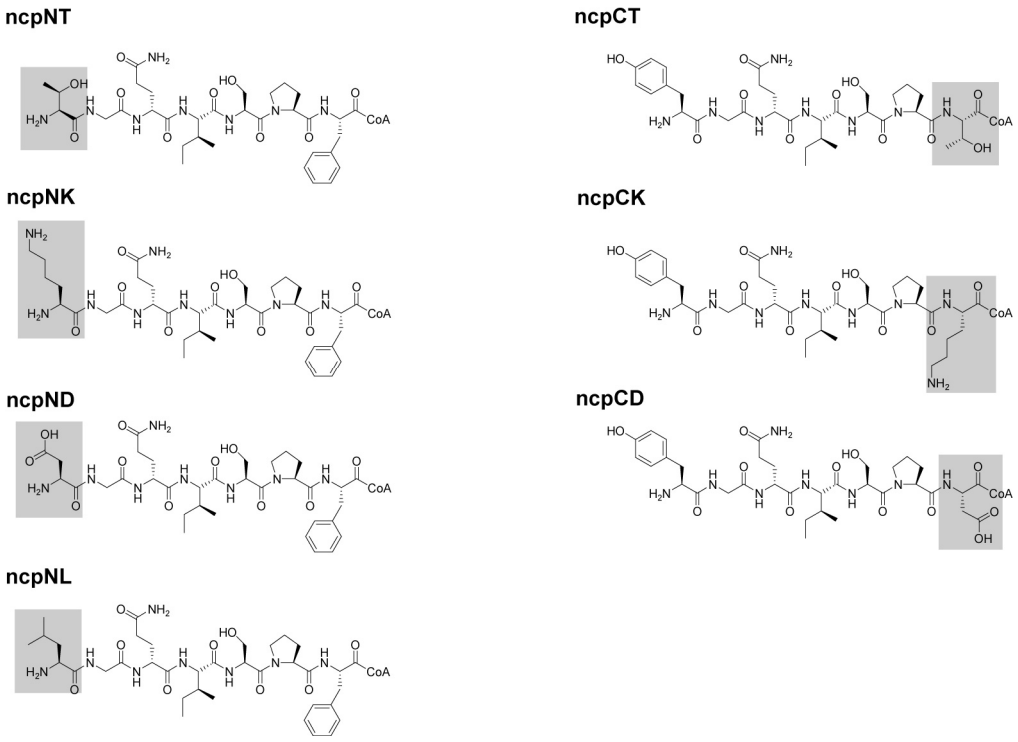

Figure 5.23: Peptidyl-CoA substrates with modified N- and C-termini. Substituted amino acid positions are indicated in grey.

Remarkably, ncp R reduced all modified peptidyl-CoA substrates, although those carrying aspartate or lysine either at the C- or N-terminus were not capable of imine-cycle formation (Figure 5.24 and Table 5.5).

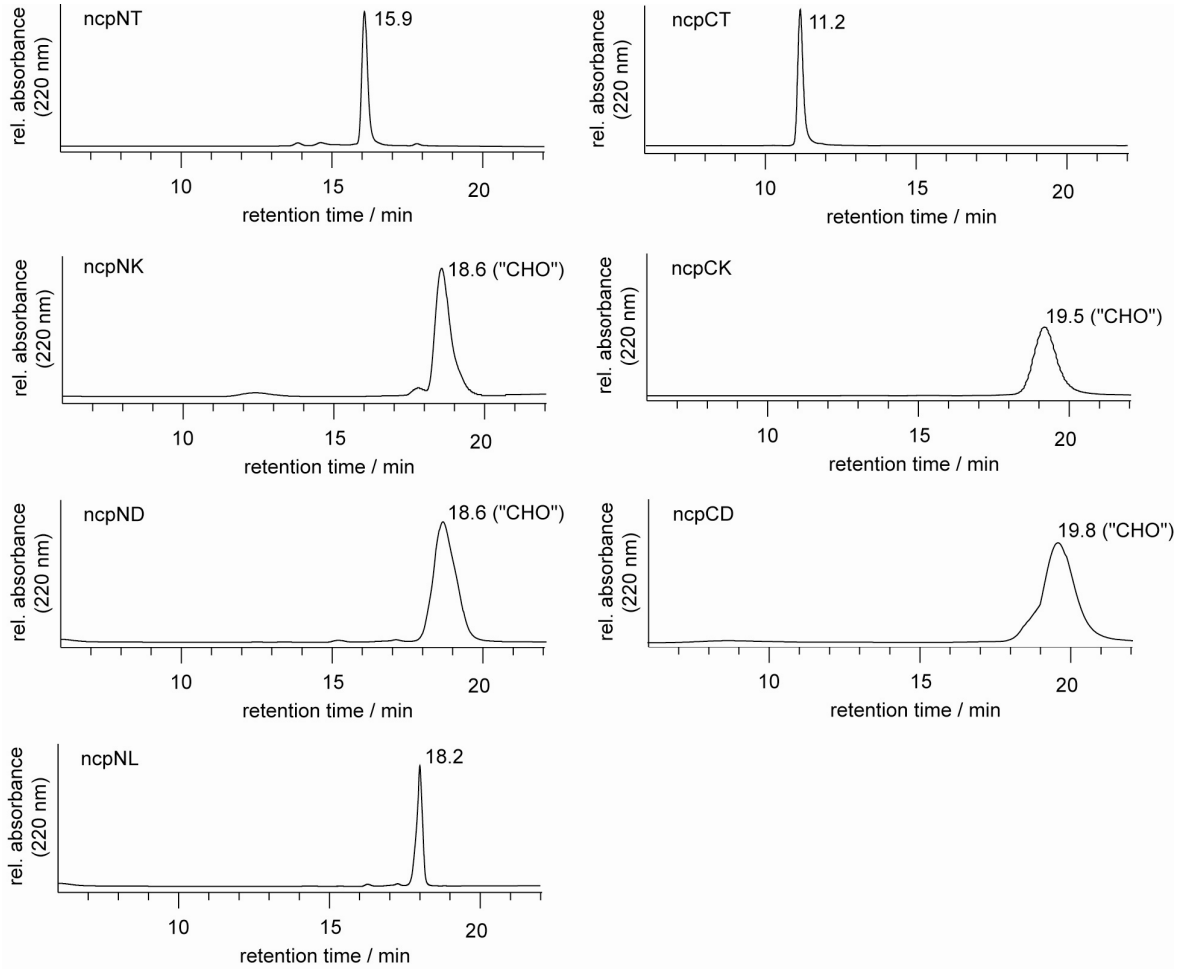

Figure 5.24: HPLC chromatograms of experiments evaluating the substrate specificity of ncp PCP-R for the C- and the N-terminal amino acids.

Table 5.5: Results of C- and N-terminal substitutions with masses of the observed products. Calculated masses are given in brackets.

Compound	Retention time (t_R)	Cyclic imine $[M+H]^+$ [Da]	Peptide aldehyde $[M+H]^+$ [Da]
ncpCT	11.2	731.4 (731.4)	n.d.
ncpCK	19.5	n.d.	776.4 (776.4)
ncpCD	19.8	n.d.	763.4 (763.4)
ncpNT	15.9	715.5 (715.6)	n.d.
ncpNK	18.6	n.d.	761.2 (761.4)
ncpND	18.6	n.d.	747.5 (747.7)
ncpNL	18.2	724.7 (724.7)	n.d.

5.3 Fatty acid tailoring during lipopeptide biosynthesis

A structural key feature of lipopeptide antibiotics, such as daptomycin, CDA, and A54145, is the eponymous long chain fatty acid, which is invariably attached to the N-terminus of the cyclic peptide core. Straight and branched chain fatty acids that can significantly differ in the degree of saturation and the oxidation state are frequently found and contribute to the high structural diversity of this class of compounds. In particular, the lipid portion has a high impact on the biological properties of these molecules, since antimicrobial behavior and toxicity are dramatically affected by the nature of the incorporated fatty acid group [95, 98].

To gain a better understanding of the mechanisms underlying the generation of the diverse fatty acid building blocks, the enzymatic tailoring steps leading to the *trans*-2,3-epoxyhexanoyl moiety found in CDA were reconstituted *in vitro*. Therefore, different scenarios with acyl-CoA substrates, acyl-CoAs loaded onto an ACP, and chemoenzymatically derived CDA were tested. During these studies a new experimental approach utilizing an amide ligation reaction was developed, which was crucial to assign the stereochemistry of the acyl carrier protein (ACP)-bound reaction intermediates. The application of this mild and versatile method enabled the detailed characterization of the two fatty acid tailoring enzymes HxcO and HcmO from the CDA biosynthetic pathway.

5.3.1 Overproduction of SCO3249

Similar to the synthesis of NRPs and PKs, the assembly of fatty acids catalyzed by fatty acid synthases (FASs) occurs on carrier proteins (CPs), to which the substrates, reaction intermediates and products are covalently tethered during biosynthesis [30]. SCO3249 of the CDA cluster, in the following referred to as ACP, showed strong sequence homology to CPs from other NRPSs and PKSs and was likely to be involved in the biosynthesis of the CDA lipid portion.

The N-terminally His_7-tagged ACP was overproduced in *E. coli* BL21(DE3) and purified as described in the Methods section. The identity of the expressed protein was proven by mass spectrometry and SDS-PAGE (Figure 5.25).

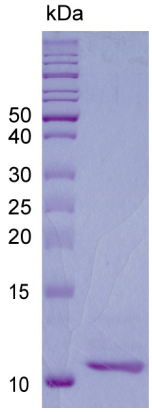

Figure 5.25: Coomassie-stained SDS-PAGE (15%) of purified ACP (11.5 kDa).

5.3.2 Characterization of SCO3249 as an acyl carrier protein

To test whether ACP could be loaded *in vitro*, the recombinant protein was incubated with the 4'-phosphopantetheine transferase (PPTase) Sfp from *B. subtilis* and fluorescein-CoA. The 4'-phosphopantetheinylation of ACP was monitored by the in-gel fluorescence of the loading mixture (Figure 5.26 A); positive and negative control experiments are shown. Additionally, the loading with fatty acid CoA-substrates to the ACP was verified by mass spectrometry (Figure 5.26 B).

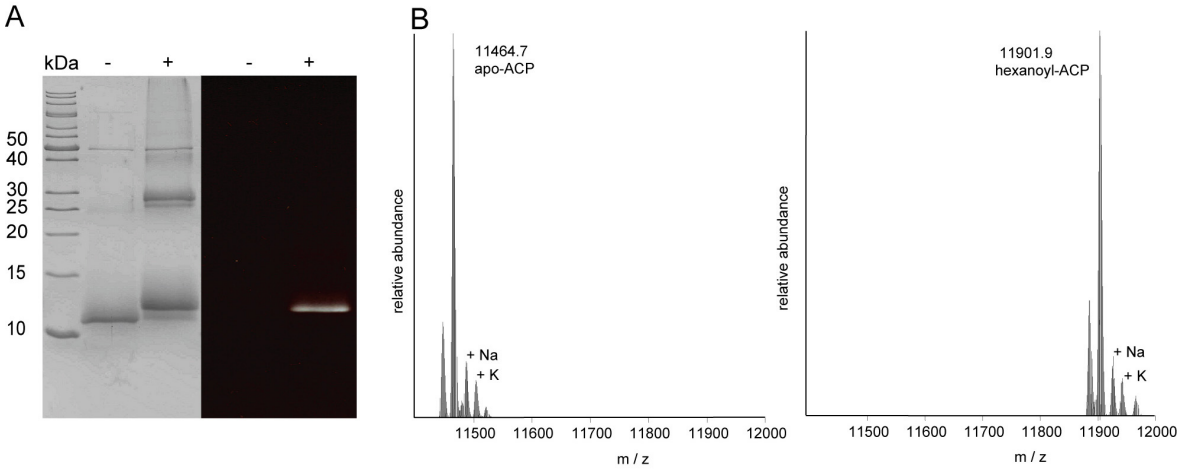

Figure 5.26: *In vitro* phosphopantetheinylation of apo-ACP. A: Coomassie-stained SDS-PAGE (left) and in-gel-fluorescence (right) of the ACP loading mixture with (+) and without (-) Sfp (28 kDa), the phosphopantetheine transferase from *B. subtilis*. B: FTMS broad band spectrum of ACP before (c.m.: 11464.7) and after (c.m.: 11901.9) loading with hexanoic acid.

5.3.3 *Overproduction of HxcO and HcmO*

The *hxcO* and *hcmO* gene fragments of the CDA *fab* operon were cloned and overexpressed in *E. coli* BL21(DE3). Ni^{2+}-NTA chromatography gave ~1.0 mg pure protein per liter of culture. The identity of the proteins was confirmed by mass spectrometry and SDS-PAGE (Figure 5.27).

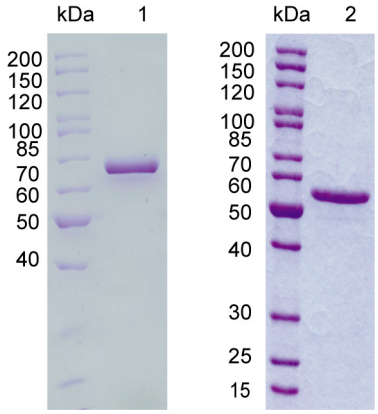

Figure 5.27: Coomassie-stained SDS-PAGE (10%) of purified HxcO (lane 1, 66.8 kDa) and HcmO (lane 2, 47.0 kDa).

5.3.4 *HxcO and HcmO cofactor analysis*

For the identification of HxcO and HcmO cofactors, an overview absorbance spectrum was recorded for both proteins. HxcO was colorless and showed no spectral absorbance typical for the flavin cofactor. In contrast to HxcO, HcmO was bright yellow in color and showed absorption maxima at 377 and 450 nm, which is characteristic for FAD (Figure 5.28 B).

To further specify the nature of the observed flavin cofactor, protein samples of HxcO and HcmO were heat denatured and the supernatants were applied to HPLC-MS analysis (Figure 5.28 A). For HxcO and HcmO, FAD was shown to be the electron accepting cofactor.

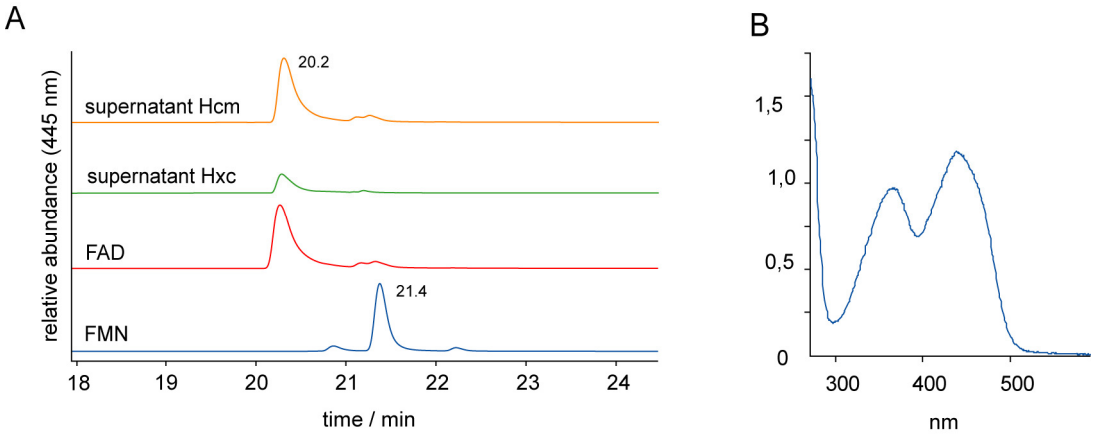

Figure 5.28: A: HPLC analysis of HxcO and HcmO cofactor. B: The UV-visible spectrum of HcmO shows the typical flavin absorption maxima at λ_{max} = 377 and 450 nm.

5.3.5 Characterization of HxcO as a fatty acid-S-ACP oxidase with intrinsic epoxidase activity

HxcO shows sequence homology in the range of 30% to several members of the acyl-CoA dehydrogenase/oxidase superfamily that catalyze double bond formation between C-2 and C-3 of their thioester substrates [119]. Based on the sequence homology, it was also postulated that HcmO is responsible for the oxidation of a hexanoyl-CoA substrate to 2,3-hexenoyl-CoA [104]. Alternatively, different scenarios with an ACP-bound HxcO substrate or the possibility that the oxidation occurs at the state of the already assembled CDA molecule, are conceivable. Accordingly, *in vitro* assays to examine all three possible routes were conducted (Figure 5.29).

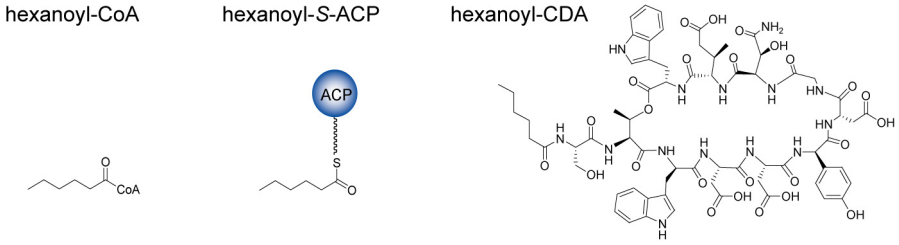

Figure 5.29: Possible substrates for the tailoring enzyme HxcO from the CDA biosynthetic pathway: hexanoyl-CoA, hexanoyl-*S*-ACP, and hexanoyl-CDA.

To test if acyl-CoAs are the physiological substrates of HxcO, the purified enzyme was assayed with synthetic hexanoyl-CoA under a variety of assay conditions typical for acyl-CoA dehydrogenases and oxidases [120, 121]. No oxidation products were detected by HPLC-MS. Additional substrates with a chain length from 4-10 C-atoms (Figure 5.30 and Table 4.8) were tested, but did not reveal the enzymatic introduction of a double bond.

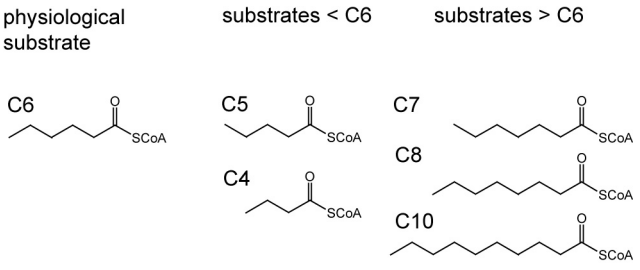

Figure 5.30: Acyl-CoA substrates used for the biochemical characterization of HxcO.

Analogously, experiments with a macrocyclic CDA analog, **hexanoyl-CDA**, were carried out. **Hexanoyl-CDA** (Table 4.7) was generated chemoenzymatically by the use of CDA

cyclase as reported previously [56]. *In vitro* assays clearly evidenced that fatty acid oxidation by HxcO does not occur in the state of the mature CDA molecule.

Next, Sfp, which had previously been shown to be promiscuous for the *in vitro* phosphopantetheinylation of various acyl- and peptidyl-CoA substrates onto carrier proteins [122], was employed to assay the alternative ACP-mediated pathway. The required hexanoyl-ACP substrate was prepared and incubated with HxcO. After tryptic digest, the samples were subjected to HPLC high-resolution FT-MS to analyze product formation. In a so called ppan ejection assay [123], the ACP fragment with the covalently attached enzyme product is subjected to tandem mass spectrometry (MS-MS), which leads to the elimination of the product-ppan arm from the ACP fragment that is subsequently analyzed (Figure 5.31 A).

The ppan ejection assay of samples obtained from negative control reaction volumes without the enzyme resulted in the observation of a 1734.8 Da signal corresponding to the active site ACP fragment (Lys^{57}-Arg^{71}) without the ppan arm that was cleaved off during gas-phase fragmentation. Additionally, a fragment ion of 359.2 Da was detected, which is consistent with the calculated mass of the hexanoyl-ppan MS-MS fragmentation product (Figure 5.31 B). After incubation with HxcO, a fragment ion of 373.2 Da (Figure 5.31 C) and a second signal of 357.2 Da (Figure 5.31 D) with ~15% intensity compared to the 373.2 Da signal, could be detected. These masses are consistent with the calculated masses of the hex-2-enoyl-ppan (357.2 Da) and the epoxyhexanoyl-ppan (373.2 Da) fragmentation products. HxcO showed no conversion of the unsaturated fatty acid-*S*-ACP in the presence of FAD and NAD(P)H cofactors, which are commonly used for the generation of $FADH_2$ by flavin-dependent monooxygenases. This suggests that HxcO generates $FADH_2$ *in situ* by the oxidation of the saturated fatty acid substrate. The reduced cofactor is then the reactive species for the epoxidation reaction.

To proof whether the unexpected epoxyhexanoyl-product, which was predominantly found (~85%), is of enzymatic origin or caused by H_2O_2 formed *in vitro* during the reoxidation of $FADH_2$, catalase was added to the assay in different concentrations. Further, reaction buffers with different pH values in the range from 5-9 were tested to decompose potentially formed H_2O_2. No influence on product formation was observed. Therefore, epoxyhexanoyl-*S*-ACP was clearly identified to be the main product of HxcO. HxcO displayed epoxide formation (Figure 5.32) with a $k_{obs} = 0.3\ min^{-1}$, whereas double bond formation did not increase over the examined period of time.

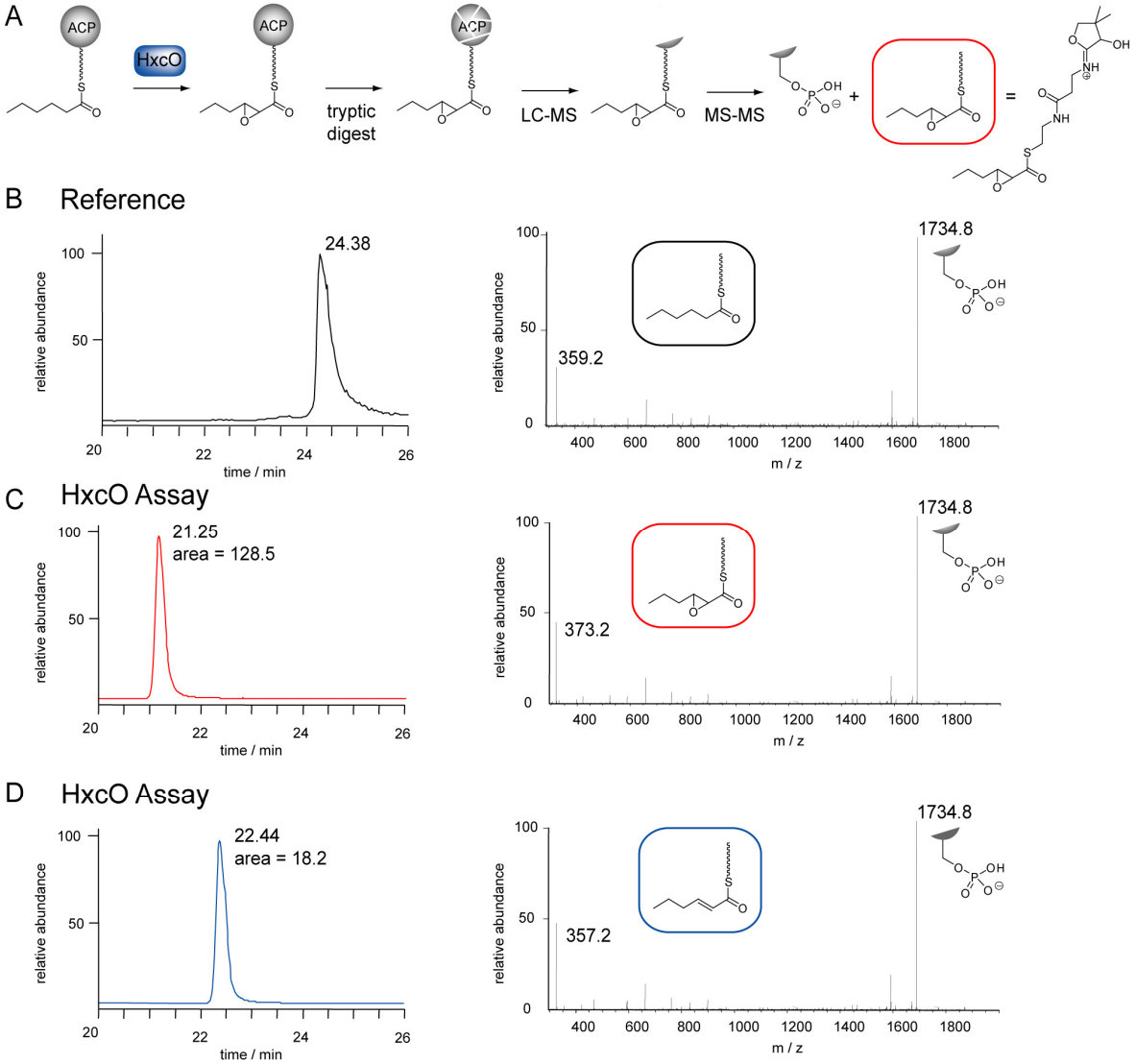

Figure 5.31: HxcO assay with hexanoyl-*S*-ACP. A: Experimental setup. HxcO reaction products were digested with trypsin and subjected to HPLC prior to tandem FTMS spectrometry. B: Single reaction monitoring (SRM; 1046.5→[1732.30-1737.30]) of hexanoyl-*S*-ACP (Lys^{57}-Arg^{71}) and MS-MS data of the ppan ejection assay resulting from a reference assay without HxcO. C: SRM (1054.5→[1732.30-1737.30]) of epoxyhexanoyl-*S*-ACP (Lys^{57}-Arg^{71}) and MS-MS data of the ppan ejection assay resulting from a HxcO assay. D: SRM (1046.5→[1732.30-1737.30]) of hex-2-enoyl-*S*-ACP (Lys^{57}-Arg^{71}) and MS-MS data of the ppan ejection assay resulting from a HxcO assay. This HxcO side product is formed in ~15% compared to epoxyhexanoyl-*S*-ACP (indicated by areas in C and D).

The substrate specificity of HxcO was evaluated with additional linear fatty acids (4-10 C-atoms) loaded onto ACP (Figure 5.30). As with the physiological substrate, these reactions revealed the formation of an enoyl product paired and a fragment ion with a mass of +16 compared to the enoyl product as the most apparent species (~85%).

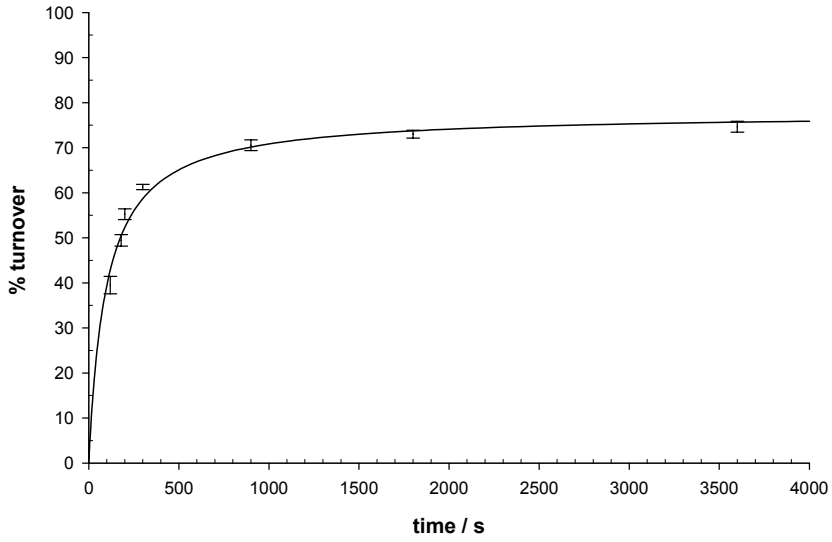

Figure 5.32: Kinetics of *(2R,3S)*-2,3-epoxyhexanoic-*S*-ACP formation mediated by HxcO. Samples were trypsinized at different time points following initiation of the enzymatic reactions, and were then fractionated and analyzed by HPLC-MS-MS. The percentage of HxcO reaction product tethered to the ACP is plotted as a function of time.

5.3.6 Characterization of HcmO as a fatty acid-S-ACP epoxidase

HcmO shows amino acid homology to the diverse class of flavin-dependent monooxygenases, particularly salicylate hydroxylases [124] and the zeaxanthin epoxidases [125] in the range of 40% and 30%, respectively. To determine whether HcmO acts on ACP-bound hexenoyl-substrates, on coenzyme A thioesters, or on the mature CDA all three possibilities were assayed.

In analogy to HxcO, HcmO did not epoxidize hexenoyl-CoA and chemoenzymatically generated **hex-2-enoyl-CDA** (Table 4.8). In order to test ACP-bound substrates, a hexenoyl-moiety was loaded onto the ACP with Sfp and subsequently incubated with HcmO at a 25-fold molar excess of NAD(P)H and FAD. Subsequent FTMS of the proteolytic mixture resulting from tryptic digest was used to characterize HcmO reactivity (Figure 5.33 A). The ppan ejection assay of samples obtained from negative control reaction volumes without the enzyme resulted, in addition to the 1734.8 Da signal corresponding to the active site ACP fragment (Lys^{57}-Arg^{71}) without the ppan arm, in a fragment ion of 357.2 Da, which is consistent with the calculated mass of the hex-2-enoyl-ppan MS-MS fragmentation product (Figure 5.33 B). The HcmO reaction revealed the formation of the fragment ions of the active site ACP(Lys^{57}-Arg^{71}) without the ppan arm (1734.8 Da) accompanied by the epoxy acid ppan product (373.2 Da), both resulting from MS-MS fragmentation (Figure 5.33 C). A hexanoyl-*S*-ACP substrate could not be converted into the epoxide product by HcmO.

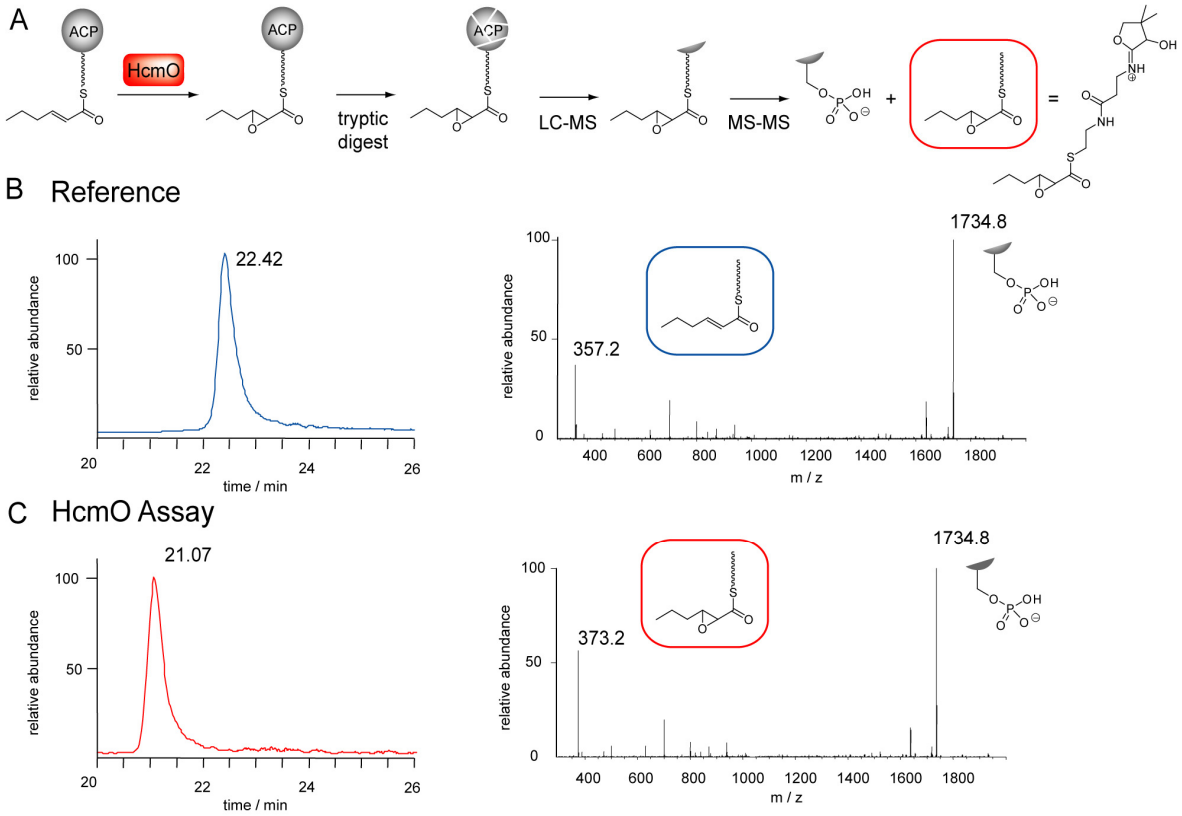

Figure 5.33: HcmO assay with hexanoyl-*S*-ACP. A: Experimental setup. HcmO reaction products were digested with trypsin and subjected to HPLC and tandem FTMS spectrometry. B: Single reaction monitoring (SRM; 1046.5→[1732.30-1737.30]) corresponding to the hex-2-enoyl-*S*-ACP (Lys^{57}-Arg^{71}) and MS-MS data of the ppan ejection assay from a reference without HcmO. C: SRM (1054.5→[1732.30-1737.30]) of the HcmO reaction product 2,3-epoxyhexanoyl-*S*-ACP (Lys^{57}-Arg^{71}) and MS-MS data of the ppan ejection assay.

The substrate specificity of HcmO was assessed with additional enoyl-ACP substrates (Table 4.8 and Figure 5.34). Whereas variations of the position and the configuration of the double bond were not tolerated, a crotonyl-moiety with a chain length shorter than the physiological C_6 substrate was accepted. HcmO was able to epoxidize the hexenoyl-substrate utilizing both NADH and NADPH cofactors.

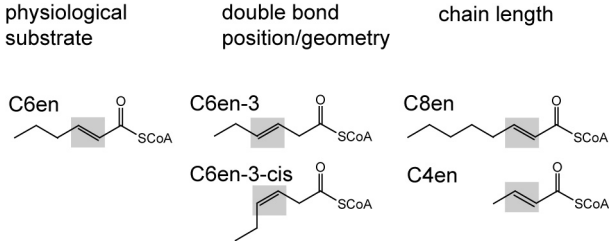

Figure 5.34: Acyl-CoA substrates used for the biochemical characterization of HcmO.

5.3.7 Stereochemical assignment of HxcO and HcmO reaction products via direct amide ligation

To further characterize the ACP-bound epoxide products formed by HxcO and HcmO, an HPLC-based comparison with synthetic standards was envisioned. Therefore, conditions that would allow the efficient transformation of the modified fatty acid-*S*-ACPs into derivatives of smaller size, which would then in turn be analyzed by HPLC, had to be established. Initial experiments using an excess of a simple amine, such as benzylamine, showed that this approach was indeed valid (Figure 5.35 A).

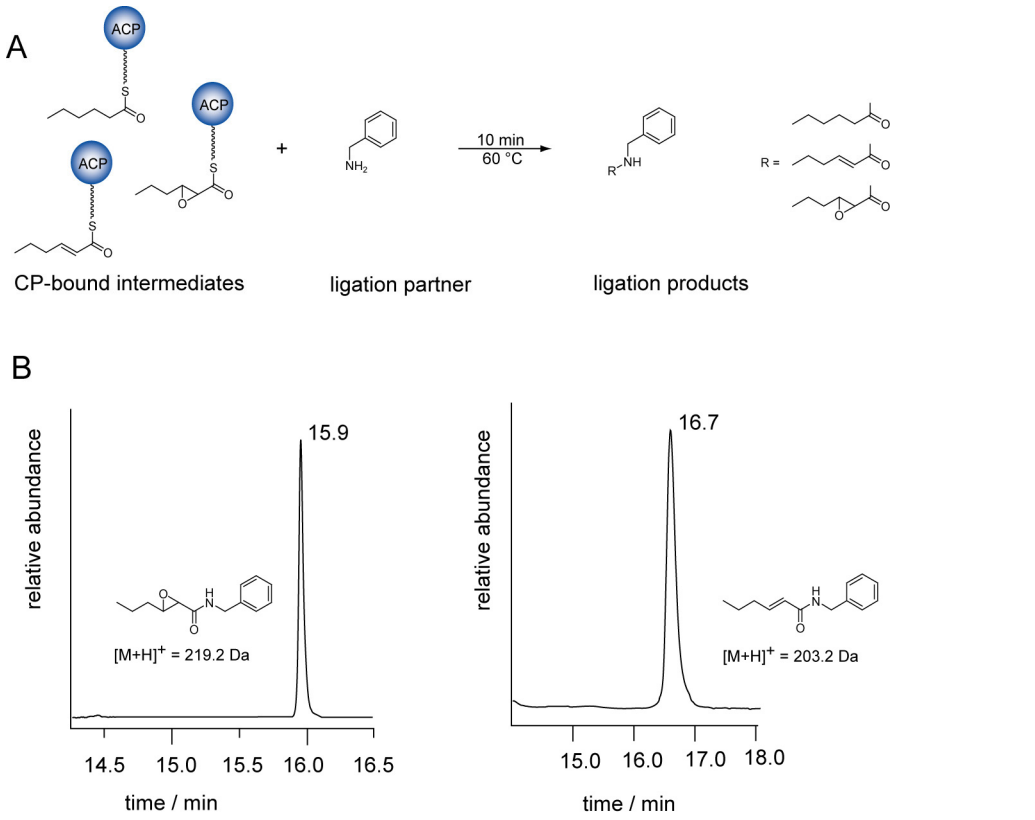

Figure 5.35: A: Cleavage of ACP-bound thioesters with a nucleophile (benzylamine) allows the comparison of enzymatic reaction products with synthetic standards. B: Amide ligation products of HxcO reactions and benzylamine analyzed by HPLC-MS. Shown are extracted ion chromatograms (EICs).

For example, after incubation of an HxcO assay with benzylamine, LC-MS analysis of the reaction mixture showed the formation of the expected mass for the amide ligation products (Figure 5.35 B). However, it was not possible to determine the stereochemistry of the epoxide formed by HxcO by comparison with a synthetic standard as the two enantiomeric benzylamides (2*S*,3*R* and 2*R*,3*S*) showed the same retention time using a chiral cyclodextrin-based HPLC-column.

Therefore, chiral ligation partners, such as D-α-methylbenzylamine, (*S*)-2-phenyl-1-propylamine, and D-Phe-OMe were tested instead. In this case, the possible products are diastereomeric instead of enantiomeric, and therefore supposed to be separate from each other more easily by HPLC analysis.

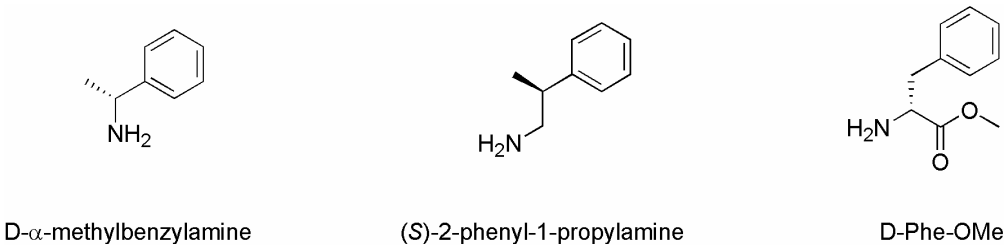

Figure 5.36: Chiral amines used as ligation partners for the cleavage of ACP-bound substances.

Accordingly, in cooperation with Dr. Markus Oberthür (Philipps-Universität Marburg) a racemic mixture of 2,3-epoxyhexanols **4**/**5** was oxidized with $RuCl_3/NaIO_4$ [126] and the resulting carboxylic acids **6**/**7** were coupled with different chiral amines using EDCI/HOBt (Figure 5.37). [1]

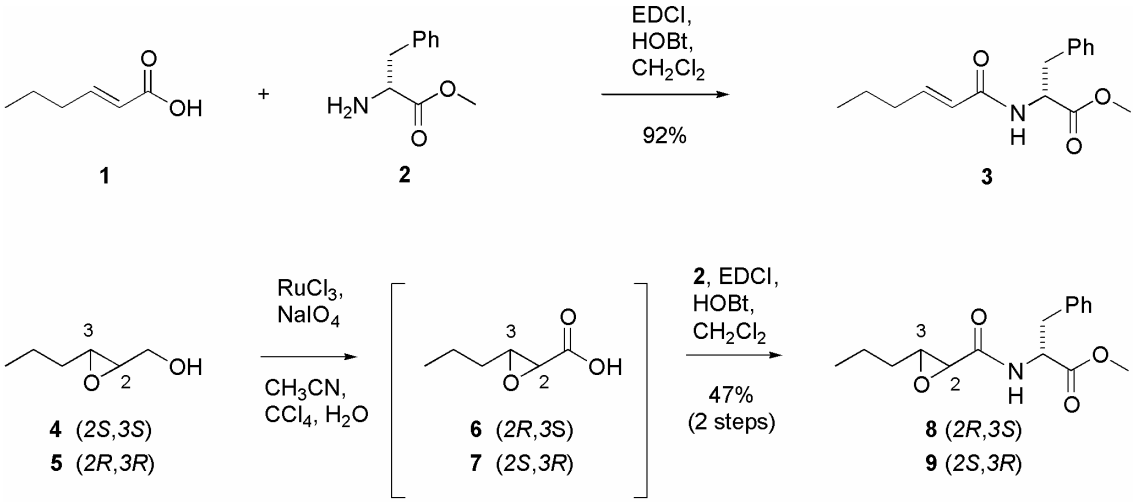

Figure 5.37: Synthesis of chemical standards. EDCI = 1-(3-dimethylaminopropyl)-3-ethylcarbodiimide hydrochloride, HOBt = 1-hydroxybenzotriazole monohydrate.

Best results in terms of separation of the reaction products were obtained using the amino acid derivative D-Phe-OMe (**2**) as a ligation partner and a chiral column for the HPLC analysis of the diastereomeric mixture of amides **8** and **9** (Figure 5.37). In order to establish the exact stereochemistry of amides **8** and **9**, one of the stereoisomers,

[1] The described syntheses were carried out by Dr. Markus Oberthür. Experimental details and analytical data are given in: Kopp et al. (2008). Harnessing the chemical activation inherent to carrier protein-bound thioesters for the characterization of lipopeptide fatty acid tailoring enzymes. *J. Am. Chem. Soc.*, online.

i.e. amide **8**, was synthesized selectively. For this purpose, enantiomer **4**, obtained by Sharpless epoxidation of hex-2-enol [127], was oxidized [126] and coupled with D-Phe-OMe **2** to provide the (*2R,3S*)-configured amide **8** (>90% ee, Figure 5.37). Comparison of the HPLC retention time of stereoisomer **8** with the two peaks obtained from the diastereomeric mixture **8**/**9** then led to the structural assignments shown in Figure 5.38.

The HPLC analysis of HxcO reaction products utilizing D-Phe-OMe as the nucleophilic amide ligation partner established that the HxcO reaction product has the *(2R,3S)*-configuration (Figure 5.38 A). The formation of the 2,3-hexenoic acid side product, which occurred only to a minor extent, was also proven by comparison with the synthetic standard **3**, which was obtained by EDCI/HOBt-mediated coupling of hex-2-enoic acid (**1**) and D-Phe-OMe (**2,** Figure 5.37).

Further, the ensuing application of the established amide ligation strategy enabled the comparison of the HcmO reaction product with synthetic standards (Figure 5.38 B) and proved the formed product to be *(2S,3R)*-2,3-epoxyhexanoic acid.

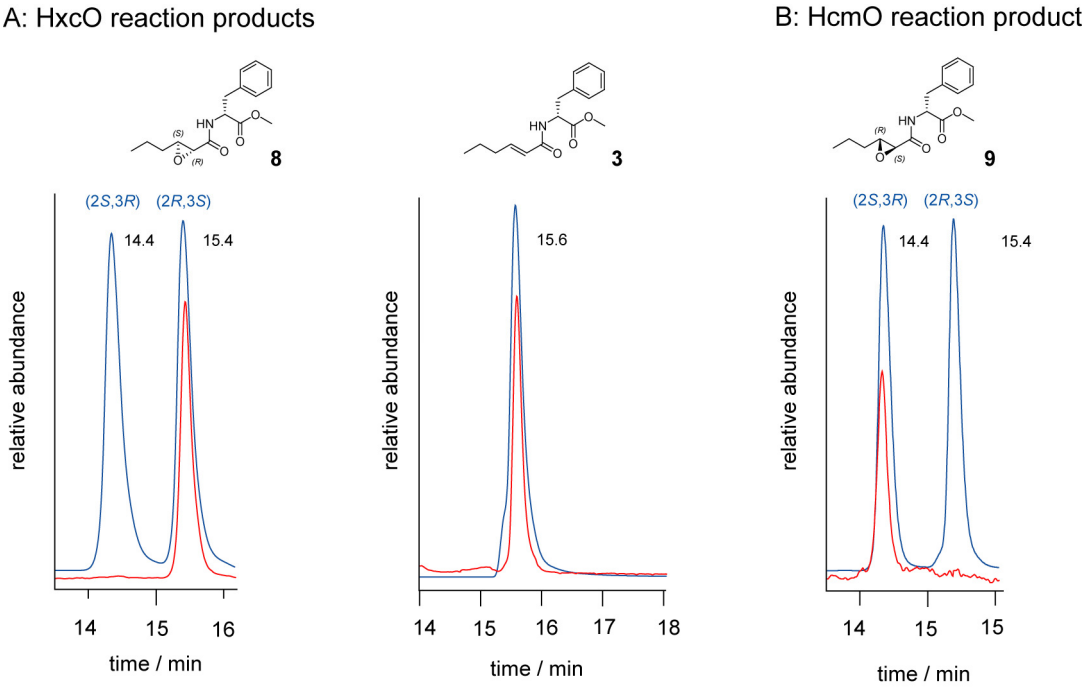

Figure 5.38: Comparison of HxcO and HcmO reaction products with synthetic standards by direct amide ligation. Cleavage of ACP-bound thioesters with a nucleophile (D-Phe-OMe) allows the analysis of enzymatic reaction products by HPLC-MS. A: Amide ligation products of HxcO reactions coelute with the (2*R*,3*S*)-2,3-epoxyhexanoyl-D-Phe-OMe standard 8 ($[M+H]^+$ = 291.1). The HxcO side product was proven to be identical with the synthetic hexenoyl amide 3 ($[M+H]^+$ = 275.1). B: The HcmO reaction product coelutes with the (2*S*,3*R*)-2,3-epoxyhexanoic acid 9 ($[M+H]^+$ = 291.1). Shown are extracted ion chromatograms (EICs).

6 Discussion

6.1 Chemoenzymatic design of acidic lipopeptide hybrids

Natural products play an important role in modern medicine, which is exemplified by the fact that most antibiotics and anticancer drugs in human use are derived from such compounds [97, 128]. Recently, acidic lipopeptide antibiotics, including the clinically approved daptomycin, have received significant attention and different strategies for the derivatization of these compounds have been developed [98, 129, 130]. However, modification of the daptomycin scaffolds has been restricted to two sites so far, namely the α-amino group of L-Trp_1 and the δ-amino group of L-Orn_7.

In nature, macrocyclization of nonribosomal lipopeptides is catalyzed by TE domains, the C-terminal catalytic unit of NRPSs. In the herein described chemoenzymatic approach, the excised TE domains from the daptomycin and A54145 systems have been shown to retain cyclization activity towards chemically prepared peptidyl-thioesters with relaxed substrate specificity. Together with powerful SPPS, that enables the rapid generation of linear peptides, these viable cyclization catalysts make the class of lipopeptide antibiotics more readily accessible for derivatization.

Several analogs of daptomycin and A54145 have been chemoenzymatically prepared to explore the relatively sparse known structure-activity relationship (SAR) of this class of compounds. Altogether a small library of ten peptidyl-thiophenol substrates was cyclized efficiently by daptomycin and A54145 cyclases and the significance of specific amino acid residues for antimicrobial activity became evident. In summary, the chemoenzymatic approach described herein provides new opportunities to develop novel molecules related to daptomycin with an improved or modified spectrum of activity.

6.1.1 Biochemical characterization of daptomycin and A54145 cyclases

On the basis of sequence information derived from acidic lipopeptide biosynthetic gene clusters [9, 105], daptomycin and A54145 cyclases were expressed and purified together with their adjacent PCP domains. Notably, both isolated enzymes were active as macrocyclization catalysts when tested with peptidyl-thiophenol analogs of their natural substrates, **A54145(Val)**, **A54145(Ile)**, and **Dap**.

In general, enzymatic peptide cyclization mediated by NRPS cyclases can be limited by low yields due to the occurrence of hydrolysis of the enzyme-bound peptidyl-residue, the so called acyl-O-TE intermediate (Figure 6.1) [131, 132]. Previous studies with excised

NRPS cyclases from the tyrocidine [131] and pristinamycin [62] synthetases revealed cyclization-to-hydrolysis ratios of 1:1 and 3:1, respectively, for their natural substrate analogs, which is typical for isolated TE domains. In contrast to this, A54145 and daptomycin cyclases show extraordinary cyclization-to-hydrolysis ratios of 12:1 and 9:1 towards peptidyl-thiophenol analogs of their natural substrates, enabling the formation of the desired macrolactones with less than 10% hydrolysis. Therefore, these two enzymes are suitable cyclization catalysts for the rapid synthesis of daptomycin derivatives in a semipreparative scale.

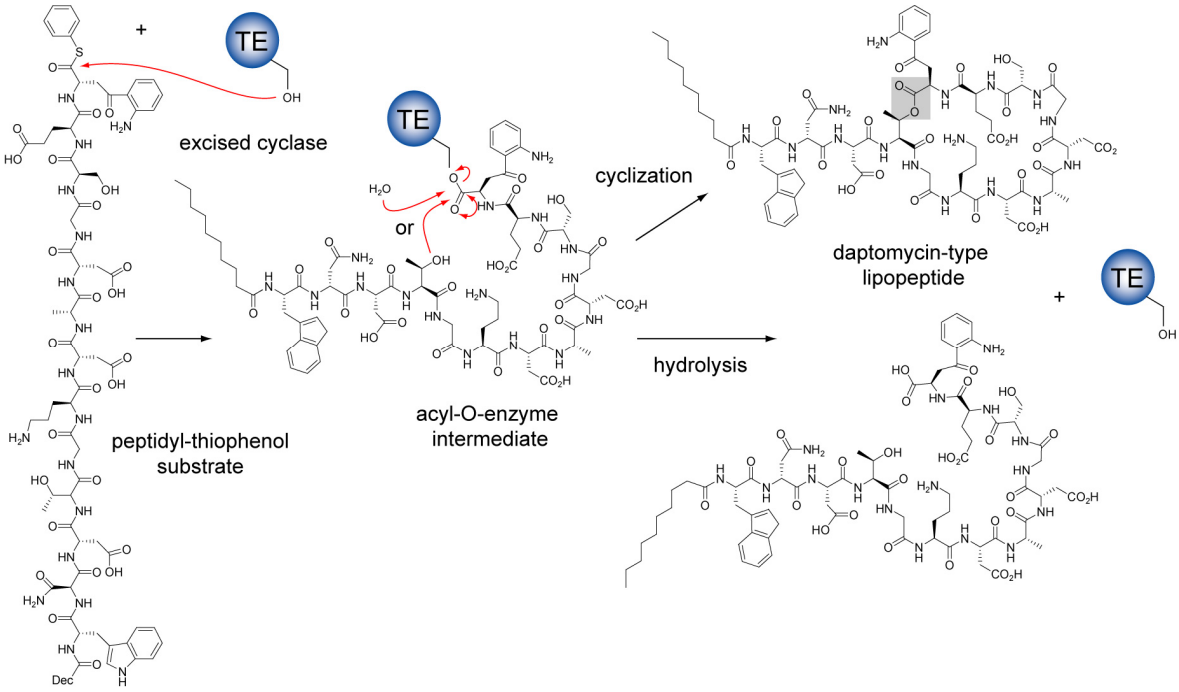

Figure 6.1: Enzymatic peptide cyclization by excised NRPS cyclases. The desired macrolactone formation competes with the attack of an external water nucleophile that leads to hydrolysis of the acyl-O-TE intermediate.

To further explore the utility of these two enzymes for peptide cyclization, thiophenol substrate analogs with the cyclization nucleophile L-threonine at different amino acid positions were tested. Thus, lipopeptide analogs with different ring sizes were expected. Our experiments showed that macrocyclic rings containing nine and eleven amino acids can be generated by A54145 and daptomycin cyclases (Figure 6.2). Unfortunately, the relocation of the cyclization nucleophile leads to a simultaneous increase in substrate hydrolysis, which significantly limits the yields of the obtained macrolactones. For substrates designed to yield an 8-membered macrocyclic ring intramolecular cyclization is completely prevented and only hydrolysis occurs. Taken together, these observations

suggest that the substrate binding pockets of the examined lipopeptide cyclases seem to be highly optimized to accommodate 10-membered peptidolactone rings. Movement of the threonine nucleophile obviously impairs the intrinsic conformation of the peptide substrate or its prefolding through the TE domain. Overall, the spatial proximity of the cyclization nucleophile and electrophile necessary for an intramolecular reaction seems to be not sufficient any longer for the tested substrates.

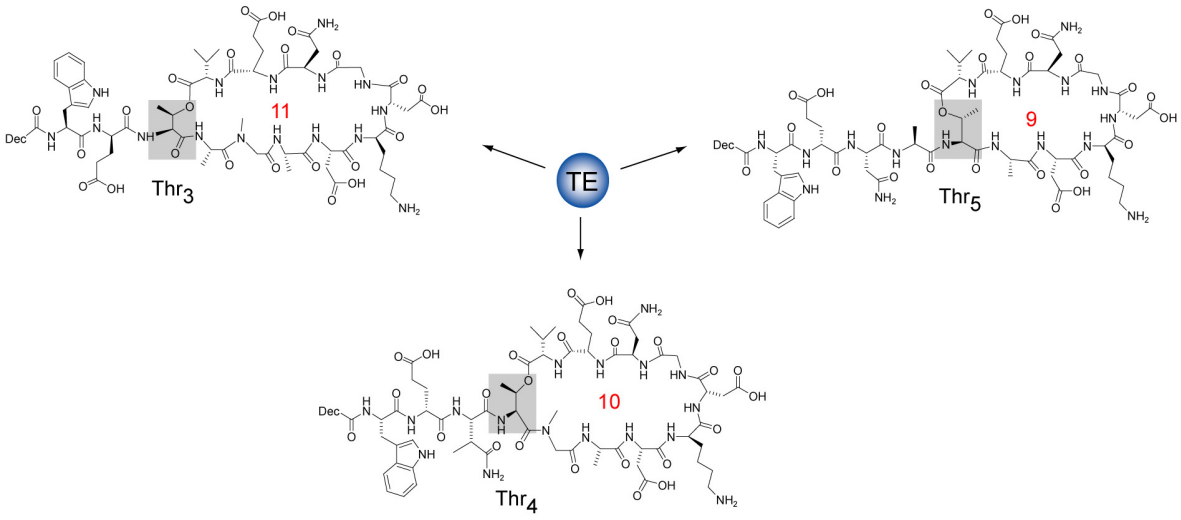

Figure 6.2: The formation of macrolactams with different ring sizes is mediated by A54145 TE domain. The cyclization nucleophile L-threonine is indicated in grey. The ring size of the formed macrolactone is indicated in red.

From the structural point of view, the acidic lipopeptides show several striking similarities. Daptomycin, A54145, and CDA share five common amino acids at identical ring positions, and their nonribosomal assembly is achieved by a highly similar biosynthetic pathway (Figure 2.22) [9, 105]. The final step in biosynthesis, the release of the mature peptide product, is achieved by the TE domains of the associated NRPS systems. In comparison to the overall level of TE identity of ~15%, the level of sequence identity among the acidic lipopeptide cyclases is in the range of 40% (Figure 6.3) [30]. Because of this fact, enzymatic cross reactions of A54145, daptomycin, and CDA cyclases were expected (Table 5.1).

When using the cyclases of A54145 and daptomycin to cyclize the substrate analog **CDA**, only hydrolysis and no product formation was observed. A reasonable explanation for this could be that the undecapeptidyl-substrate, **CDA**, with the shorter hexanoyl fatty acid moiety, is not large enough to fill the substrate pocket of A54145 and the daptomycin cyclase active site, which are optimized for the tridecapeptides that contain a decanoyl fatty acid tail. Therefore, the admission of water molecules and the hydrolytical cleavage

of the acyl-enzyme intermediate could be favored in this situation. In contrast, A54145 cyclase was able to cyclize the peptidyl-thioester analog of **Dap** and *vice versa* Dap PCP-TE cyclized **A54145(Val)**.

Although enzymatic cyclization activity was found to be relaxed for internal amino acid substitutions of the peptidyl-thioester substrates, C- and N-terminal recognition elements are essential for efficient peptide cyclization. CDA and daptomycin contain aromatic amino acids at the C-terminus, and A54145 contains an aliphatic isoleucine or valine residue at this position. Consequently, CDA cyclase was permissive towards daptomycin substrate analogs, but did not catalyze the cyclization of peptidyl-thioester **A54145(Val)**.

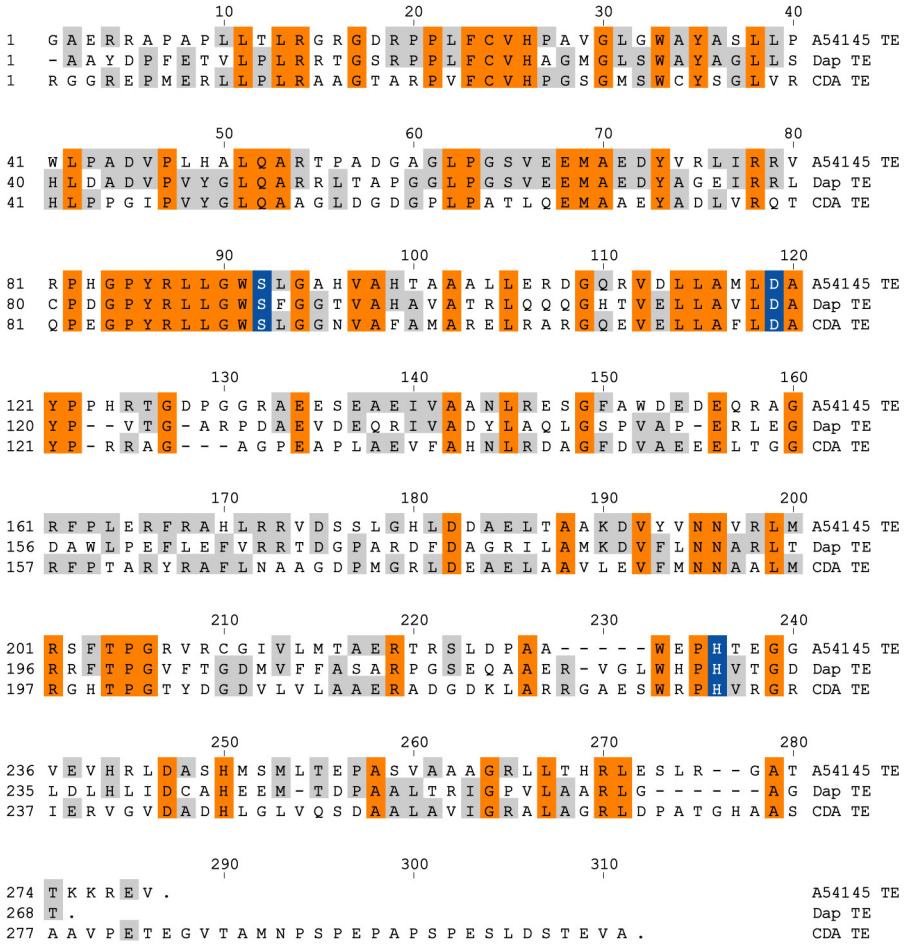

Figure 6.3: Sequence alignment of cyclases of the acidic lipopeptides. Conserved residues are indicated in orange, partially conserved residues are indicated in grey. The canonical catalytic triad is indicated in blue. The C-terminal parts of the enzymes show less homology, while the N-terminal parts show many conserved regions.

Interestingly, within the acidic lipopeptide family intramolecular cyclization is achieved by the formation of either peptidolactones or peptidolactams. For friulimycin, amphomycin, or laspartomycin, the macrocyclic ring is formed via an amide linkage between the

C-terminal proline and diaminopropionic or -butyric acid (Figure 2.22). Daptomycin and CDA cyclases did not exhibit any cyclization activity towards **Dap(DAP)** and **CDA(DAP)**. In contrast, **A54145(DAP)** was efficiently converted to the macrolactam after incubation with A54145 cyclase. Hence, A54145 PCP-TE is the first excised cyclase of a branched lipopeptide NRPS that catalyzes both macrolactonization and macrolactamization (Figure 6.4). The molecular reasons for this outstanding catalytic versatility of A54145 cyclase can not be deduced from sequence alignments as shown in Figure 6.3. Further crystallographic studies might be necessary to obtain a well funded answer to this question.

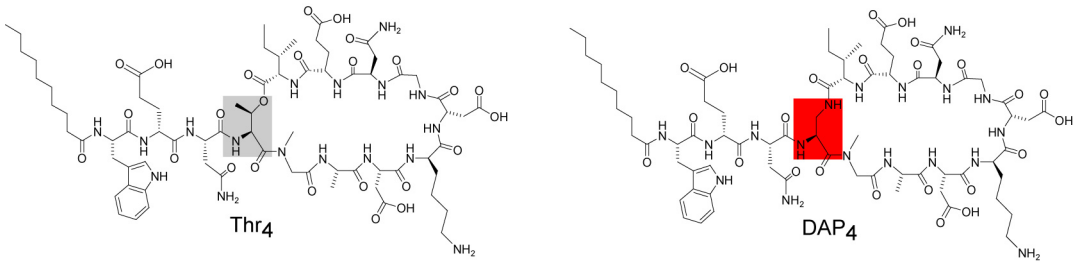

Figure 6.4: A54145 cyclase catalyzes macrolactonization and macrolactamization. To achieve macrolactamization, the cyclization nucleophile Thr_4 was substituted against 2,3-diaminopropionate (DAP).

6.1.2 Structure-activity relationship studies

Encouraged by the versatile catalytic properties of the acidic lipopeptide TE domains, A54145 and daptomycin cyclases were employed for the synthesis of lipopeptide molecules in a semipreparative scale. Subsequent determination of antimicrobial activity by measuring the minimal inhibition concentration (MIC) in the presence of Ca^{2+}-ions allowed further conclusions about the acidic lipopeptide SAR.

Assaying compounds **Dap**, **A54145(Val)**, and **A54145(Ile)**, which are closely related to authentic daptomycin (L-Glu instead of L-3-methylglutamate at position 12) and A54145 (L-Asp instead of L-3-O-methylaspartate at position 3 and L-Asn instead of L-3-hydroxyasparagine at position 9), against *B. subtilis* PY79 underlined the importance of unusual and C-terminal amino acids for bioactivity. Cyclized **Dap** revealed a MIC value that was 6-fold higher than that of authentic daptomycin, reflecting the crucial role of the nonproteinogenic amino acid L-3-methylglutamate (Table 5.2). The two A54145 analogs **A54145(Val)** and **A54145(Ile)** displayed a significant difference in the MIC value that was increased 8-fold for **A54145(Val)** compared to that of **A54145(Ile)**.

Remarkably, the A54145 macrolactam variant **A54145(DAP)** had a MIC value of 25 μg/mL similar to that of **A54145(Ile)**, revealing that the substitution of an ester bond through an amide bond does not affect antimicrobial behavior primarily. Up to now resistance against daptomycin is an isolated event and there are no known resistance mechanisms against lipopeptide antibiotics [133-135]. However, one could speculate with respect to their structure that enzymatic inactivation of these compounds could either occur by the cleavage of the N-terminal fatty acid tail through a fatty acid amide hydrolase or by the action of ring-opening bacterial lyases. The latter case is true for type B streptogramin antibiotics, where the vulnerable intramolecular ester linkage of these hexadepsipeptides is cleaved in a Mg^{2+}-dependent mechanism [136]. Whether macrolactam variants of lipopeptide antibiotics display a lower susceptibility towards potential inactivating enzymes of pathogens remains to be seen. Obviously, additional studies would be necessary to draw a conclusion in terms of the improved *in vivo* stability. However, clinically used antibiotics inevitably select for resistant microbes and there is a continuous need for the discovery of new and the further development of already used antibiotics.

Previous studies have shown that the antibacterial activity of the acidic lipopeptide antibiotics is calcium-dependent and that daptomycin and A54145 reach their maximum antimicrobial activity in the presence of a calcium concentration of ~50 mg/L as found in human serum [137]. To learn more about the significance of acidic amino acid residues of A54145 for the interaction with Ca^{2+}-ions, the peptidolactones **A54145(NXDG)**, **A54145(DXNG)**, and **A54145(NXNG)** were synthesized and tested for biological activity. Notably, the replacement of aspartic acid at positions 7 and/or 9 lead to a total loss of bioactivity for all three compounds and showed that these two amino acids are important structural elements. In addition to the results obtained in this study with chemoenzymatically derived A54145 analogs, experiments with modified CDAs derived from a mutasynthesis approach [104] and daptomycin derivatives that contained aspartate to asparagine substitutions [118] are in good agreement. This also underlines the general importance of the aspartate residues at positions 7 and 9 for acidic lipopeptide antimicrobial potency.

The closer inspection of the peptide sequences from different members of the acidic lipopeptide family reveals that these two aspartate residues are part of a conserved four amino acid motif DXDG within the characteristic 10-membered macrocyclic ring (Figure 2.22). This DXDG motif is also part of the EF-hand motif of ribosomally produced calmodulin, a calcium-dependent regulator protein in eukaryotes (Figure 6.5) [138].

	D	X	D	G		
22	D	K	D	G	27	calmodulin
6	D	A	D	G	11	daptomycin
6	D	Z	D	G	11	A54145
4	D	L	D	G	9	CDA
4	D	G	D	G	9	friulumycin

Figure 6.5: Alignment of the conserved DXDG amino acid motif (highlighted in grey) found in ribosomally produced calmodulin (orange) and nonribosomally synthesized acidic lipopeptide antibiotics [138].

Compared to those of A54145, the three exocyclic amino acids of daptomycin are only subtly different. Both compounds contain tryptophan at position 1, followed by a D-configured amino acid at position 2. Additionally, one acidic residue and asparagine or 3-hydroxymethylasparagine can be found at position 3. These characteristics suggest a similar conformation for this exocyclic part of the tridecapeptide molecules in aqueous solution. In accordance with this, the chemoenzymatically synthesized daptomycin/A54145 hybrid **Dap(A54$_{1-3}$)** did not show a significant change in antimicrobial potency compared to **Dap**. The observation that **Dap(A54$_{1-3}$)** retained bioactivity although aspartate at position 3 was replaced by asparagine, gives rise to further speculations. Either Asp_3 is not essential for the binding of Ca^{2+}-ions, in contrast to the model derived by Jung et al., where Asp_3 is suggested to coordinate Ca^{2+} together with Asp_7 (see also Introduction section) [109]. Otherwise, D-Glu_2 in **Dap(A54$_{1-3}$)** might be able to compensate the function of Asp_3 and coordinates calcium instead.

Further, successive substitution of the daptomycin peptide backbone with amino acids from A54145 as in **Dap(A54$_{1-6}$)** was possible, illustrating the opportunity to construct structural hybrids of these two compounds. As reported in Table 5.2, the MIC of **Dap(A54$_{1-6}$)** was similar to that of **Dap(A54$_{1-3}$)**, indicating the importance of the C-terminal halves of these molecules. Accordingly, the synthesized analogs of the two major found A54145 variants displayed a significant difference in MIC values; that of **A54145(Val)** was increased 8-fold compared to that of **A54145(Ile)**. On the basis of these results, **A54145(Kyn)** was synthesized with the unusual amino acid kynurenine at position 13. The MIC of **A54145(Kyn)** was almost as low as for enzymatically cyclized **Dap**, revealing the crucial role of kynurenine at position 13.

Interestingly, the opposite effect occurred in subsequent studies from Cubist pharmaceuticals, in which modified lipopeptides were successfully generated by reprogramming the daptomycin and A54145 biosynthetic gene clusters through the exchange or replacement of NRPS modules [50, 51]. The daptomycin derivatives produced by the engineered strains contained isoleucine and valine, as found in A54145, at amino

acid position 13 of their peptide backbones. In contrast to the increased bioactivity observed for **A54145(Kyn)** during this study, the substitution of kynurenine through isoleucine or valine caused a reduced antimicrobial potency of the derived daptomycin analogs compared to that of authentic daptomycin [50, 51].

Taken together, it can be assumed that the introduction of the aromatic kynurenine leads to an increased amphipathicity of the A54145 lipopeptide analog **A54145(Kyn)**. The daptomycin NMR structure derived by Ball et al., for example, indicates a hydrophobic cluster with Trp_1, Kyn_{13}, and the decanoic acid moiety at the bottom of the macrocyclic ring structure [108]. Moreover, recent contributions from the Straus laboratory showed that divalent cations, such as Ca^{2+} or Mg^{2+}, have a significant effect on Trp_1 and Kyn_{13} residues, suggesting an important role of these two amino acids in the oligomerization process of daptomycin and the interaction with the bacterial membrane [139].

In conclusion, the identification of structural elements that are important for lipopeptide bioactivity makes them promising sites for the introduction of further chemical modifications. The herein described chemoenzymatic approach towards the synthesis of lipopeptide analogs should allow the lipopeptide SAR to be further extended through the construction of more comprehensive libraries. Having selected promising peptide leads, complementary *in vivo* genetic engineering approaches, as established by Cubist, might be helpful for the large scale production of lead molecules for clinical studies.

6.2 The reductase of the nostocyclopeptide synthetase triggers the formation of a macrocyclic imine

One goal of this study was to investigate different types of peptide macrocyclization including the unusual formation of a macrocyclic imine, as displayed by the nostocyclopeptides (ncps). Imines are rather unusual structural elements to constrain the conformation of a peptide by macrocyclization compared to chemically more stable intramolecular ester and amide bonds, which are frequently found in biologically active peptides. Nevertheless, Moore et al. isolated ncpA1 and ncpA2 from the terrestrial cyanobacterium *nostoc* sp. ATCC53789 and elucidated their biosynthetic origin, which is mediated by a NRPS system [14, 140]. In contrast to most other NRPSs, the termination module contains an uncommon reductase domain instead of the canonical TE domain.

In this study the nostocyclopeptide imine formation was examined biochemically *in vitro*. By the synthesis of linear peptide aldehydes it was possible to show that imine macrocyclization takes place via self-assembly after the reductive release of a reactive

peptide aldehyde by the reductase (R) domain. This distinguishes the ncp R domain from all other known NRPS reductase domains that are engaged in the formation of linear peptide alcohols or amines.

6.2.1 The biochemical characterization of the nostocyclopeptide reductase domain

The sequencing of the ncp biosynthetic gene cluster revealed that the assembly of the linear heptapeptide chain is achieved by a linear NRPS consisting of two subunits NcpA and NcpB [14]. The third module contains an E domain to generate D-Gln, which is found at amino acid position 3 of the ncp peptide backbone. Remarkably, instead of the commonly found TE domain, a relatively rare reductase (R) domain, containing a putative NAD(P)H binding motif, is found at the C-terminal end of NcpB (Figure 6.6).

Recombinant ncp R and ncp PCP-R displayed reductase activity *in vitro* with peptidyl-thioester substrates that were C-terminally activated with CoA or ppan. Thiophenol- and SNAC-activated peptides in contrast were not accepted by the reductase domain, indicating a high enzymatic specificity for substrates that closer mimic the natural situation, where the mature peptide chain is covalently attached to the terminal PCP.

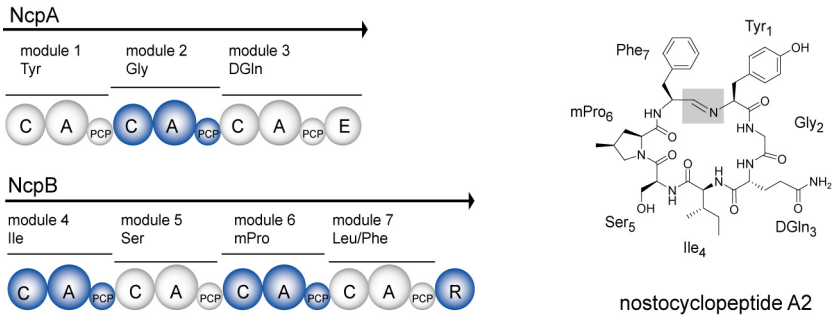

Figure 6.6: The nostocyclopeptide NRPS consists of two subunits, NcpA and NcpB. Seven modules are responsible for the incorporation of seven amino acids. Instead of the commonly found thioesterase domain an R domain occupies the C-terminal position of NcpB.

Interestingly, the reductase activity of ncp PCP-R was significantly higher than for the excised R domain. This observation suggests that the secondary structure of the excised enzyme may be negatively influenced by the absence of the natural protein environment within the NRPSs. The PCP, as a stable autonomous folding unit, may have stabilizing effects, leading to improved catalytic properties of the ncp R domain.

Since assays with ncp R and peptidyl-CoA substrates showed the formation of cyclic imines instead of linear peptide aldehydes, the existence of a second enzyme involved within imine macrocyclization could be excluded. However, the role of the reductase domain in peptide cyclization remained unclear at this state.

To further investigate this issue peptide aldehydes with sequences similar to ncpA1 and ncpA2 were synthesized (for synthetic reasons 4-methylproline was substituted by proline). For both compounds imine macrocyclization occurred without the need of ncp R. With this experiment imine formation was uncoupled from the ncp R-mediated reductive release of the ncp aldehydes and it was shown that the macrocyclization reaction is enzyme-independent. This leads to the conclusion that the offloading of the reactive peptide aldehyde by ncp R triggers the self-assembly of the macrocyclic imine (Figure 6.7). A prerequisite for this process would be that the free linear heptapeptide aldehyde can adopt a "product-like" conformation without the help of ncp PCP-R, so that the distant ends of the peptide aldehyde are in close proximity for intramolecular cyclization.

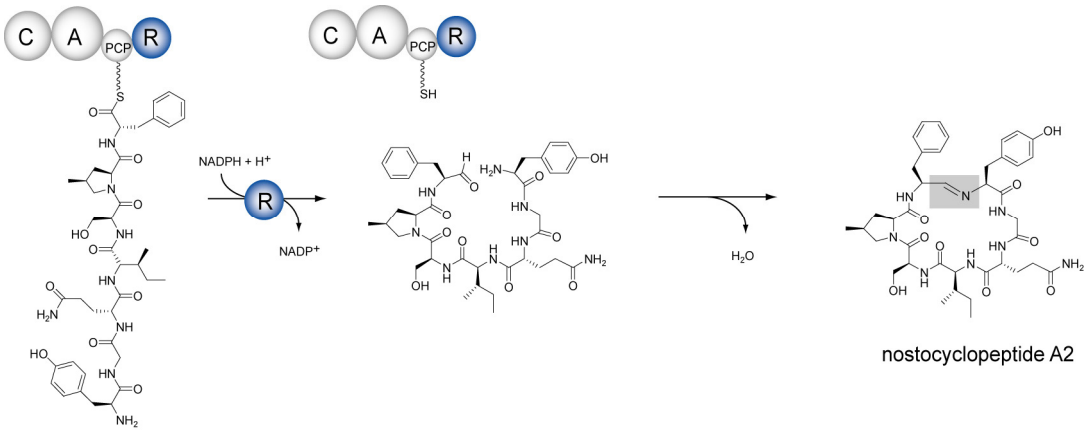

Figure 6.7: Macrocyclization during the biosynthesis of the nostocyclopeptide A2 is triggered by a terminal reductase (R) domain. The release of a peptide aldehyde results in the spontaneous formation of the macrocyclic imine.

6.2.2 Alanine scan experiment

The hypothesis that imine macrocyclization relies on the elaborated prefolding of the linear ncp peptide chain was further supported by an alanine scanning mutagenesis experiment. CoA-derivatives, in which one single amino acid at positions 2-6 of the ncp peptide sequence was substituted by L-alanine, revealed that Pro_6, Ser_5, and Ile_4 side chains were not crucial for imine self-assembly, whereas the replacement of D-Gln_3 and Gly_2 by L-alanine predominantly afforded the linear peptide aldehydes (Figure 6.8).

These experiments strongly suggest that Gly_2 may serve as a flexible hinge that allows the peptide to achieve a precyclic conformation. Interestingly, D-Gln_3 is the amino acid with the highest polarity within the ncp peptide sequence and could be involved in hydrogen bonding with the peptide backbone. Alternatively, as the only D-configured amino acid

within the heptapeptide, D-Gln_3 could be part of a turn motif that critically contributes to the preorganization of the linear molecule.

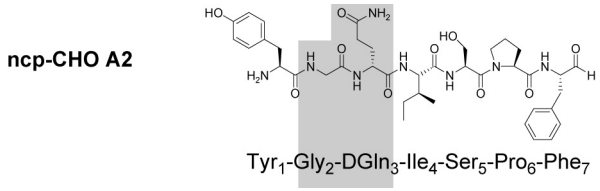

Figure 6.8: Crucial structural elements for imine macrocyclization identified by alanine scanning (indicated in grey).

NMR studies from the Geyer laboratory (Philipps-Universität Marburg) provided a more detailed picture of the intriguing conformation of the linear and cyclic **ncpA2** in aqueous solution. As shown in Figure 6.9, it was confirmed that the linear ncp precursor in fact has a distinct "horseshoe-like" conformation.

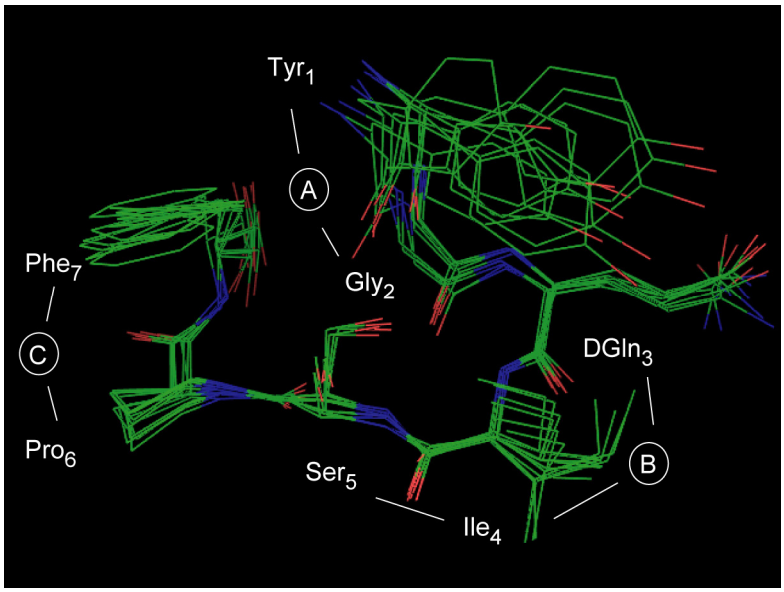

Figure 6.9: Overlay of 10 snap shots (taken in 10 ps steps) of a Molecular Dynamics simulation of the linear ncpA2-CHO. Carbon atoms are shown in green, oxygen atoms in red, and nitrogen atoms in blue. Structural features that contribute to the peptide prefolding are indicated. A: The N-terminal Tyr_1 side chain is highly flexible with Gly_2 acting as a dynamic hinge. B: The D-Gln_3-Ile_4-Ser_5 segment adopts a β-turn motif. C: The C-terminus is rigidified by a stacking interaction between Phe_7 and Pro_6 side chain residues. This figure was kindly provided by S. Enck.

The intermediate segment D-Gln_3-Ile_4-Ser_5 adopts a β-turn and is already preorganized for macrocyclization of the linear peptide chain. The C-terminal amino acids Phe_7 and Pro_6 show an unusually strong stacking interaction, which restricts the dynamics of this molecular part. Further, the high mobility of the N-terminal Tyr_1 adjacent to the

"glycine-hinge" became evident. This molecular flexibility is likely to enable the interaction between the C- and N-terminal part of the molecule, which is necessary for imine formation. In summary, the individual role of each structural element identified by the alanine scanning experiment during peptide prefolding could be specified in more detail by the NMR data, which impressively show that the outstanding conformation of the linear ncp is the basis for imine self-assembly.

6.2.3 Ncp PCP-R substrate specificity

According to previous studies on TE domain-mediated peptide cyclization, we anticipated an important role for the C- and the N-terminal amino acids. However, ncps occur in nature as a mixture of two compounds, ncpA1 and ncpA2, that differ in the C-terminal position, which is occupied by either leucine or phenylalanine. Despite these aromatic and aliphatic amino acids threonine, lysine, or aspartate were incorporated at this position to cover different types of the 20 proteinogenic amino acids. In additional peptidyl-CoA substrates phenylalanine was conserved at the C-terminus, while the N-terminal tyrosine was substituted with leucine, threonine, lysine, or aspartate.

Remarkably, ncp R displayed broad substrate tolerance and reduced all modified peptidyl-CoA substrates, although those carrying aspartate or lysine either at the C- or N-terminus were not capable of imine-cycle formation. One explanation for this could be that electronic effects caused by the charged amino acid substitutes may in general have a high impact on the conformation of the linear heptapeptide. Additionally, the hydrophobic structural motif at the C-terminus may be a necessary structural constraint for the interaction of the N-terminal tyrosine with the C-terminal aldehyde function.

6.2.4 Macrocyclic imines as model systems for peptide cyclization

In general, macrocyclic imines are rather unusual structural elements for the rigidification of a peptide's conformation compared to stable ester and amide bonds. Imino bonds can be easily hydrolyzed in aqueous solution (Figure 6.10) and possibly for this reason imines are only rarely found as structural elements in nature, playing a more important role as metabolic intermediates [141]. Remarkably, the cyclic ncps could be isolated from the cryptophycin producing cyanobacterium *Nostoc* sp. ATCC53789, revealing their comparatively high stability. Although the ncps showed cytotoxicity against human carcinoma cells as reported by Moore and colleagues, the exact biological function of this molecules remained unclear [14].

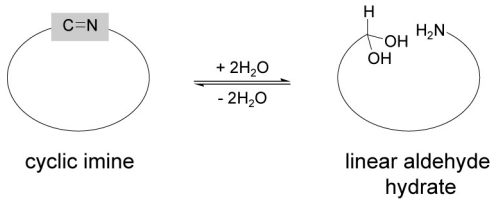

Figure 6.10: Reversibility of the imine macrocycle formation.

Based on the reversibility of imine formation, dependent on the pH value and temperature, Enck et al. were able to quantify the equilibrium constants of the imine cyclization process by NMR. This in turn enabled the calculation of the entropy loss of the linear peptide chain upon macrocyclization (Enck, S., unpublished results). In future, this novel experimental approach may be applicable to determine the cyclization entropy of other macrocyclic peptides of medicinal interest, such as tyrocidine or gramicidin S, if synthetic linear peptide aldehydes corresponding to these compounds also show spontaneous imine formation.

6.2.5 Chain termination by reductase domains during the biosynthesis of other secondary metabolites

Although C-terminal reductase domains are known in a few other NRPS systems, for example those of the myxobacterial natural products myxochelin A and B [43, 143, 144] and linear gramicidin [44], the associated compounds are primary amines and alcohols, obtained by further enzymatic transformation of the released aldehydes. These molecules do not possess a macrocyclic structure.

Our results elucidate a unique and novel type of peptide cyclization via the formation of a macrocyclic imine. In general, the reductive release of reactive peptide aldehyde precursors prior to an intramolecular cyclization reaction may be more commonplace during the biosynthesis of complex NRPs and PKs than originally thought. The antitumor antibiotic safracin B, for example, is likely to undergo a speculated intramolecular Schiff base reaction after the formation of a peptide aldehyde precursor (Figure 6.11) [145, 146]. It will be of interest to see whether this cyclization process is also triggered by a putative reductase domain.

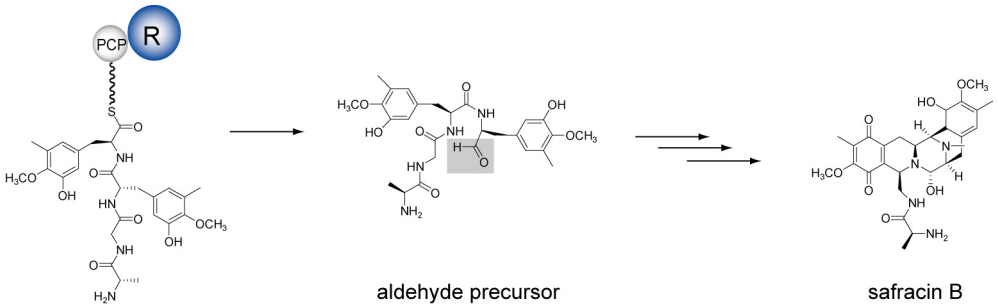

Figure 6.11: Proposed chain termination during safracin biosynthesis. A C-terminal reductase domain (R) is likely to catalyze chain release and concomitant aldehyde formation.

Analogously, a similar reductive thioester cleavage leading to the release of a reactive aldehyde species is likely to be involved in the biosynthesis of pseurotin A, a hybrid PK/NRP produced by the filamentous fungus *Aspergillus fumigatus* [147]. The C-terminal reductase domain has been proposed to release the underneath depicted aldehyde intermediate. After intramolecular cyclization further enzymatic tailoring finally yields pseurotin A (Figure 6.12).

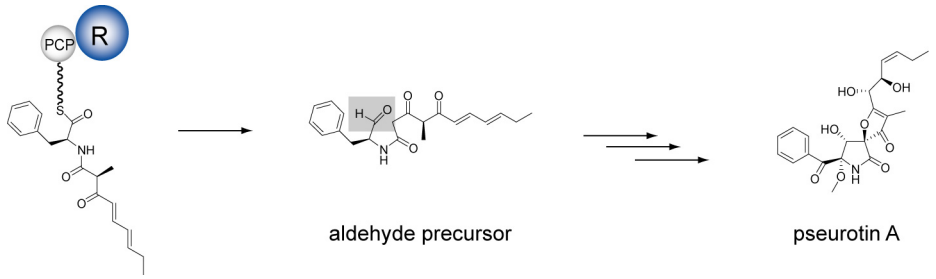

Figure 6.12: Proposed chain termination during pseurotin A biosynthesis. Reductive thioester cleavage presumably leads to the formation of a reactive aldehyde precursor of pseurotin A.

6.3 Fatty acid tailoring during lipopeptide synthesis

Intensive studies on modular biosynthetic assembly line machinery have provided researchers with a profound knowledge of how nonribosomal peptides (NRPs) and polyketides (PKs) are produced in nature. Especially nonribosomal lipopeptides, like CDA and the last-resort antibiotic daptomycin have been in the focus of interest recently. Since the biological properties of these compounds depend to a large extent on the nature of the incorporated fatty acid chain, one goal of this thesis was to investigate the enzymatic tailoring steps underlying the generation of the unique *trans*-2,3-epoxyhexanoic acid building block of CDA.

In the course of these studies it has been shown that fatty acid tailoring enzymes HxcO and HcmO act on ACP-bound substrates. HxcO turned out to be a novel type of enzyme with dual function as an FAD-dependent fatty acid-*S*-ACP oxidase paired with intrinsic epoxidase activity. HcmO was characterized as a second epoxidase, responsible for the production of another 2,3-epoxyhexanoic enantiomer during CDA biosynthesis.

To assign the stereochemistry of the enzymatic reaction products, a new experimental approach based on the chemical activation inherent to thioester-bound intermediates was developed. Utilizing an amide ligation reaction, it was possible to transform the ACP-bound substances into derivatives of smaller size suitable for the rapid and sensitive detection by standard HPLC-MS. Using this powerful approach, the reaction products of the tailoring enzymes HxcO and HcmO from the CDA *trans*-2,3-epoxyhexanoyl biosynthetic pathway could be stereochemically characterized, which was not possible via established methodology. Moreover, the herein presented method holds great potential for the detailed analysis of other biochemical processes involving CP-bound intermediates – a central paradigm in secondary metabolism.

6.3.1 Biochemical characterization of HxcO and HcmO

In order to biochemically characterize the enzymes HxcO and HcmO from the CDA biosynthetic gene cluster *in vitro*, three possible biosynthetic routes of the CDA *trans*-2,3-epoxyhexanoyl side chain were experimentally evaluated. Therefore acyl-CoA substrates, acyl substrates loaded onto an ACP, and chemoenzymatically prepared CDA variants were generated and tested as substrates for HxcO and HcmO. These assays were analyzed by high-resolution FT-MS, the time-dependency was examined as well as the enzymes' substrate specificity for different types of fatty acids.

The obtained results are surprising in two aspects: first, predictions based on sequence similarities favoured HxcO and HcmO to be a fatty acid oxidase and epoxidase, respectively, both acting on acyl-CoA substrates. However, our experiments clearly demonstrate that only fatty acids loaded onto the recombinant ACP (SCO3249) are turned over by the recombinant enzymes. In addition to the physiological substrate hexanoyl-*S*-ACP, HxcO accepted a range of ACP-bound substrate analogs, namely linear fatty acids of 4-10 C-atoms. HcmO epoxidation activity, instead, showed more restricted substrate specificity and was limited to hex-2-enoyl- and shorter crotonyl-*S*-ACP substrates. Second, whereas HcmO showed the expected epoxidase activity, the experiments with the putative dehydrogenase HxcO showed the time-dependent formation of epoxyhexanoyl-*S*-ACP as the main product.

6.3.2 *Proposed mechanism of epoxidation catalyzed by HxcO and HcmO in the context with other flavoproteins*

The fact that HxcO is a new type of FAD-dependent acyl-ACP oxidase with intrinsic epoxidase activity responsible for the desaturation and subsequent epoxidation of the initially formed enoyl-ACP product, gives rise to speculations on the HxcO epoxidation mechanism. In analogy to the related acyl-CoA oxidases, HxcO generates the reduced cofactor $FADH_2$ by the oxidation of the fatty acid-*S*-ACP substrate. Subsequently flavin C4a-hydroperoxide (FADH-OOH) is formed during the reoxidation of $FADH_2$ by molecular oxygen (Figure 6.13). Instead of decomposing to FAD and H_2O_2, FADH-OOH could be deprotonated and directly serve as a nucleophile in the subsequent epoxidation of the electron deficient double bond. Therefore, the enoyl-substrate can undergo conjugated addition with the reactive FAD-OO^- species following a mechanism that has been proposed for the Baeyer-Villiger type oxidation of cyclic ketones by FAD-dependent epoxidases (Figure 6.13) [148].

HcmO was characterized as a second flavin-dependent epoxidase, also responsible for the formation of a 2,3-epoxyhexanoyl residue while acting on the ACP-bound hexenoyl-substrate. In contrast to HxcO, $FADH_2$ is likely to be generated by the oxidation of NAD(P)H through the reductase component of HcmO. The reduced cofactor is then available for the epoxidation reaction that occurs in analogy to HxcO with FAD-OO^- as the nucleophilic species (Figure 6.13).

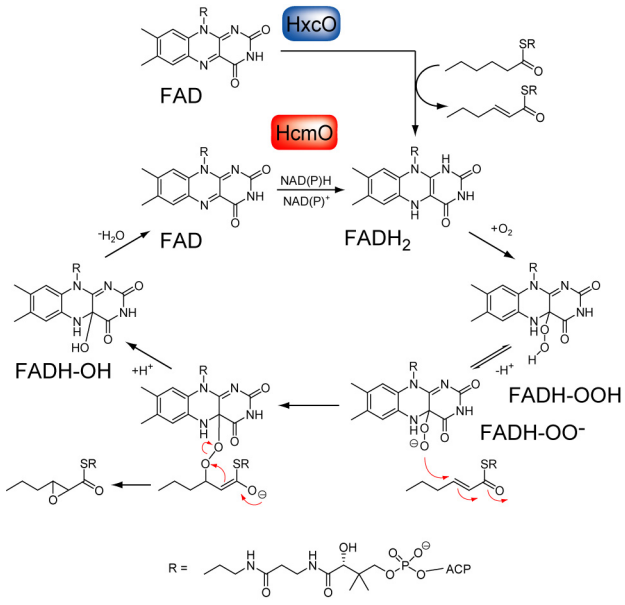

Figure 6.13: Proposed mechanism of epoxidation catalyzed by HxcO and HcmO. During fatty acid oxidation (HxcO) or by the consumption of NAD(P)H (HcmO) the reduced cofactor $FADH_2$ is generated. The reaction with molecular oxygen affords the flavin C4a-hydroperoxide intermediate, which acts as a nucleophile in the attack of the 2,3-hexenoyl-*S*-ACP substrate. Finally, the C4a-hydroxyflavin intermediate dehydrates to regenerate the oxidized FAD.

In the epoxidation mediated by HxcO and HcmO the C4a-hydroperoxide intermediate nucleophilically attacks the electrophilic enoyl substrate in order to install the epoxide function. Depending on the protonation state of the C4a-hydroperoxide intermediate, this versatile peroxide species can also deliver an electrophilic hydroxyl group "OH^+" to nucleophilic substrates [149]. The prototypical reaction for an electrophilic monooxygenation is the *ortho* hydroxylation of 4-hydroxybenzoate, wherein the electron-rich phenol ring allows transfer of an "OH^+" equivalent from the reactive FAD-OOH (Figure 6.14) [150-152].

The diverse properties of flavin cofactors are further illustrated by natural product flavoprotein halogenases. The generation of 7-chlorotryptophan by the flavin-dependent halogenase RebH during biosynthesis of rebeccamycin, for example, employs similar mechanisms for the chlorination of natural product scaffolds [153, 154]. After the formation of C4a-hydroperoxide a chloride ion, Cl^-, can react either with the distal or the proximal oxygen atom of the peroxide species to produce an HOCl equivalent or an FAD-OCl, each of both with presumably comparable reactivity as sources of "Cl^+" (Figure 6.14).

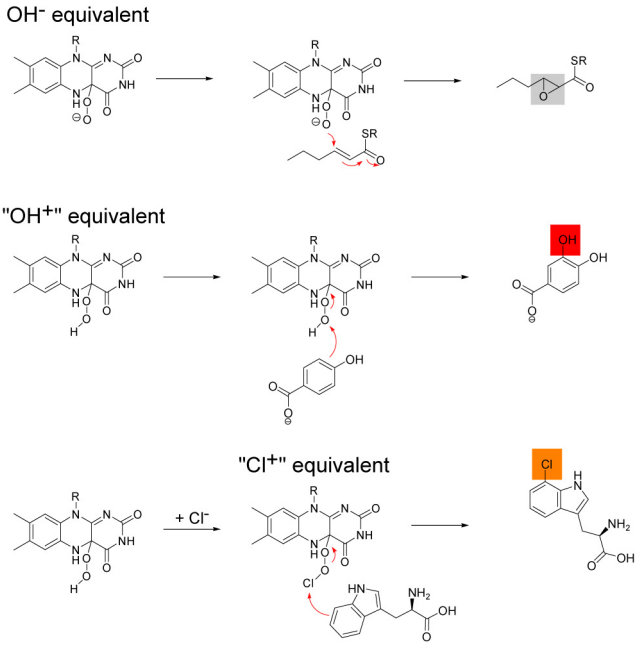

Figure 6.14: Oxygenation and halogenation reactions catalyzed by natural product biosynthetic enzymes. *Trans*-2,3-epoxyhexanoic side chain formation in CDA biosynthesis works via the deprotonated C4a-hydroperoxide species that acts as an OH^- equivalent. In *p*-hydroxybenzoate hydroxylase the reactive C4a-hydroperoxide species delivers an "OH^+" electrophile in the aromatic substitution of position 3 of *p*-hydroxybenzoate. Chlorination by flavin-dependent halogenases, such as RebH from the rebeccamycin biosynthetic system, is also mediated by FAD-OOH, which is likely to oxidize Cl^- to form a "Cl^+" equivalent for subsequent halogenation. The enzymatic product of RebH is 7-chlorotryptophan.

6.3.3 Stereochemical assignment of HxcO and HcmO reaction products by direct amide ligation

The stereochemistry of the two epoxides generated by HxcO and HcmO was assigned via comparison with synthetic standards. Initially, these attempts to characterize the enzymatic products were hampered by the problem that standard methodology for the cleavage and analysis of CP-bound substances could not be applied. Enzymatic cleavage by the hydrolyzing enzyme TEII is only possible for peptidyl carrier protein (PCP)-bound substrates [155] and the use of ACP hydrolases is restricted by their high specificity for native ACPs [80, 156]. Relatively harsh alkaline treatment, on the other hand, would obviously hydrolyze the epoxy function and could further lead to racemization.

To establish alternative conditions that would allow the direct transformation of the ACP-bound enzyme products into derivatives of smaller size appropriate for standard HPLC-MS analysis, the cleavage of the reactive acyl-*S*-ACP thioesters by incubation with amine nucleophiles was envisioned, thereby taking advantage of the chemical activation already inherent to thioester-bound substrates. Initial experiments with hydrophobic amines, e.g. benzylamine, showed indeed the formation of the desired amide ligation products suitable for HPLC analysis and comparison with synthetic standards. However, it was not possible to determine the absolute stereochemistry of the epoxides generated by HxcO and HcmO, respectively, because enantiomeric synthetic standards were not well resolved by HPLC using a chiral column.

Accordingly, the utilization of chiral ligation partners, such as D-α-methylbenzylamine, (*S*)-2-phenyl-1-propylamine or amino acid methyl esters, e.g. D-Phe-OMe was envisioned. The rational for this change was the now diastereomeric relationship of the two possible epoxyhexanoyl amide ligation products, which was anticipated to lead to a better separation by HPLC. Synthesis of 2,3-epoxyhexanoyl amides using racemic 2,3-epoxyhexanoic acid and the amines mentioned above and analysis of the diastereomeric product mixtures by HPLC using a chiral column showed that only in the case of the N-acylated phenylalanine esters **8** and **9** (Figure 5.37) a sufficient peak separation was obtained. Gratifyingly, phenylalanine derivative **2** could also successfully be used as a nucleophile in the amide ligation reaction, where it efficiently cleaved the ACP-bound thioesters. Using this strategy, we could clearly establish that the epoxide generated by HxcO has the *(2R,*3*S)*-configuration (Figure 5.38). Interestingly, the 2,3-epoxyhexanoyl moiety generated by the second putative tailoring enzyme studied here, HcmO, was shown to be of opposite configuration (2*S*,3*R*) based on HPLC analysis of the

ligation product (Figure 5.39). This experimental approach was therefore essential for this study, since it enabled the detailed analysis of the CP-bound HxcO and HcmO enzyme products as well as the unambiguous assignment of product stereochemistry by comparison to synthetic standards.

6.3.4 Proposed model for 2,3-epoxyhexanoyl side chain biosynthesis

Since the absolute configuration of the *trans*-2,3-epoxyhexanoyl moiety in the CDA natural product is unknown, the existence of two epoxidases HxcO and HcmO with different stereoselectivity gives rise to speculations on the overall role of these enzymes in the CDA fatty acid moiety biosynthesis.

A total of five genes comprise the putative *fab* operon that is involved in fatty acid biosynthesis and tailoring of CDA (Figure 2.19). The hexanyol-ACP substrate for HxcO is likely to be produced by the interplay of FabH4 and FabH3, putative β-ketoacyl-ACP synthases encoded within the *fab* operon, together with enzymes from primary metabolism (Figure 6.15). Subsequently, fatty acid tailoring by HxcO occurs on the ACP-bound hexanoyl moiety and results in the (2*R*,3*S*)-2,3-epoxyhexanoyl product and minor amounts of the hex-2-enoyl-ACP, as demonstrated in this study. This "side-product" of HxcO reactivity could then serve as the substrate for subsequent epoxidation by HcmO. Alternatively, the hex-2-enoyl-ACP substrate for HcmO could be directly provided by the same enzymes that are responsible for the generation of the hexanoyl-ACP substrate, but without the final reduction step of the respective ER (Figure 6.15). However, such a scenario would bypass the general need of a fatty acid-*S*-ACP oxidase activity that is a component of HxcO.

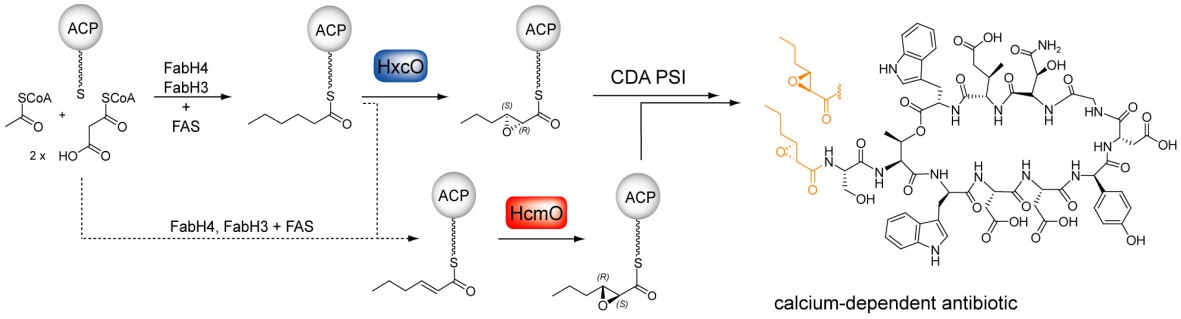

Figure 6.15: Proposed model for the ACP-mediated biosynthesis pathway of the unique 2,3-epoxyhexanoyl moiety found in CDA. The two epoxidases HxcO and HcmO are responsible for the generation of the two shown 2,3-epoxyhexanoyl enantiomers. Either FAS enzymes from primary metabolism together with FabH3 and FabH4, or HxcO are likely to produce the hex-2-enoyl substrate for HcmO. The configuration of the epoxyhexanoyl side chain in the CDA antibiotics is unknown up to now. CDA PSI = CDA Peptide Synthetase I.

Overall, it can not be answered at the moment, whether the two enantiomers produced by HxcO and HcmO are then transferred from the ACP to the first module of the CDA peptide synthetase, because of the unknown stereochemistry of the epoxyhexanoic side chain found in the natural product. NMR studies allied with a total synthesis approach are currently underway to investigate the absolute configuration of the *trans*-2,3-epoxyhexanoyl moiety in naturally produced CDA.

Recently, our results were accomplished by *in vivo* data concerning the biosynthetic origin of the CDA 2,3-epoxyhexanoyl fatty acid side chain [157]. The Micklefield and Smith laboratories could show that the deletion of *hxcO* gene results in CDA products with saturated hexanoyl side chains. First, this indicates that the unmodified hexanoyl-*S*-ACP is able to initiate lipopeptide biosynthesis and that fatty acid transfer to the substrate serine on the CDA peptide synthetase is not specific for the epoxidized hexanoyl-moiety. Consequently, it becomes more likely that both epoxyhexanoyl enantiomers formed by HxcO and HcmO are incorporated into the CDA scaffold during biosynthesis. Second, since no epoxidized products were detected for the Δ*hxcO* mutant, one can speculate that the 2,3-hexenoyl-*S*-ACP originating from HxcO is the favored substrate for HcmO. Otherwise, products containing the 2,3-epoxyhexanoyl side chain should have been observed, due to the action of HcmO on 2,3-hexenoyl-*S*-ACP formed during fatty acid synthesis.

A second *S. coelicolor* mutant with a *hcmO* gene deletion was screened for CDA production but did not reveal the formation of any CDA-like compounds. While this result supports the view that HcmO is essential for CDA biosynthesis, it does not explain why the (2*R*,3*S*)-2,3-epoxyhexanoyl and 2,3-hexenoyl products of HxcO should not be recognized by the NRPS.

6.3.5 Implications for the biosynthesis of modified fatty acid building blocks found in other nonribosomal lipopeptides

The biochemical data from this study demonstrate that fatty acid epoxidation during CDA assembly occurs on ACP-bound substrates. However, are similar biosynthetic concepts also applied during the biosynthesis of other nonribosomal lipopeptides? The cloning and sequencing of the gene clusters of enduracidin [158], ramoplanin [159], and friulimycin [160, 161] revealed fatty acid tailoring enzymes encoding segments in close proximity to the genes encoding for the NRPS. Additionally, each of these biosynthetic systems also included a putative ACP.

In the friulimycin NRPS system gene knock-outs confirmed the role of an acyl-CoA-dehydrogenase to be involved in the formation of the *cis* double bond of the N-terminal lipid moiety, but the enzymatic activity could not be reconstituted *in vitro* with fatty acid-CoA substrates [160, 161]. In light of the results obtained in this study, it is most likely that the cognate substrates of the recombinant acyl-CoA dehydrogenase are fatty acid-*S*-ACPs rather than fatty acid-CoAs in analogy to the ACP-mediated oxidation/epoxidation of HxcO (Figure 6.16 A). Another intriguing feature of the friulimycin NRPS is the absence of a C domain that usually represents the first domain within the initiation modules of NRPSs responsible for the biosynthesis of lipopeptides. Persumably, the stand-alone acyltransferase LipE compensates the C domain function during friulimycin lipoinitiation. Taken together, these considerations lead to a biosynthetic model for fatty acid tailoring as depicted in Figure 6.16.

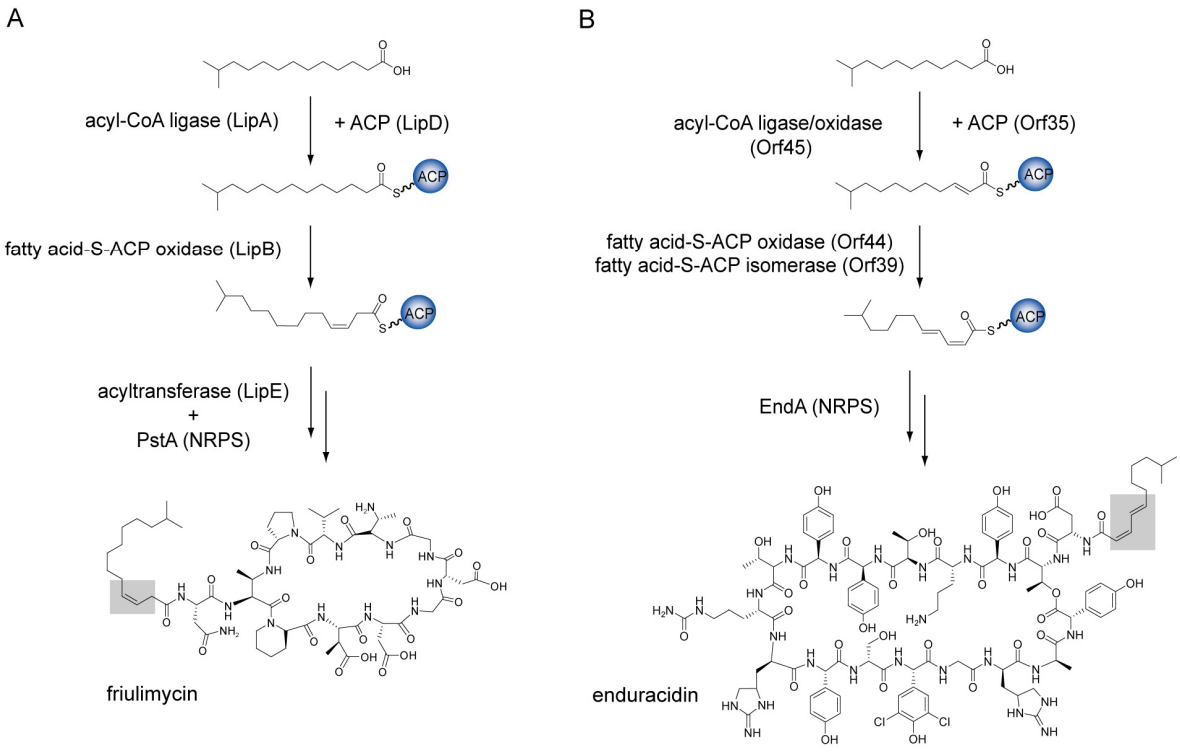

Figure 6.16: Proposed model for fatty acid tailoring during the biosynthesis of friulimycin (A) and enduracidin (B).

Further, the enduracidin cluster also contains an open reading frame encoding for an ACP-like protein. Fatty acid tailoring leading to the 2*Z*,4*E*-unsaturated lipid tail by a putative acyl ligase/oxidase fusion protein (Orf45), an additional oxidase (Orf44), and a double bond isomerase (Orf39) is also likely to occur on ACP-bound substrates (Figure 6.16 B). Counterparts of these proteins are found in the ramoplanin pathway,

which incorporates a shorter, but otherwise structurally identical unsaturated lipid tail as enduracidin [159]. It will be of interest to see, whether the hypothesis that fatty acid tailoring generally occurs on ACP-bound substrates can be confirmed by follow-up studies.

7 References

1. Fischbach, M.A., and Walsh, C.T. (2006). Assembly-line enzymology for polyketide and nonribosomal Peptide antibiotics: logic, machinery, and mechanisms. Chem. Rev. *106*, 3468-3496.
2. Grunewald, J., and Marahiel, M.A. (2006). Chemoenzymatic and template-directed synthesis of bioactive macrocyclic peptides. Microbiol. Mol. Biol. Rev. *70*, 121-146.
3. Weissman, K.J., and Leadlay, P.F. (2005). Combinatorial biosynthesis of reduced polyketides. Nat. Rev. Microbiol. *3*, 925-936.
4. Rizo, J., and Gierasch, L.M. (1992). Constrained peptides: models of bioactive peptides and protein substructures. Annu. Rev. Biochem. *61*, 387-418.
5. Craik, D.J. (2006). Chemistry. Seamless proteins tie up their loose ends. Science *311*, 1563-1564.
6. Roskoski, R., Jr., Kleinkauf, H., Gevers, W., and Lipmann, F. (1970). Isolation of enzyme-bound peptide intermediates in tyrocidine biosynthesis. Biochemistry *9*, 4846-4851.
7. Trauger, J.W., Kohli, R.M., Mootz, H.D., Marahiel, M.A., and Walsh, C.T. (2000). Peptide cyclization catalysed by the thioesterase domain of tyrocidine synthetase. Nature *407*, 215-218.
8. Konz, D., Klens, A., Schorgendorfer, K., and Marahiel, M.A. (1997). The bacitracin biosynthesis operon of Bacillus licheniformis ATCC 10716: molecular characterization of three multi-modular peptide synthetases. Chem. Biol. *4*, 927-937.
9. Miao, V., Coeffet-Legal, M.F., Brian, P., Brost, R., Penn, J., Whiting, A., Martin, S., Ford, R., Parr, I., Bouchard, M., Silva, C.J., Wrigley, S.K., and Baltz, R.H. (2005). Daptomycin biosynthesis in Streptomyces roseosporus: cloning and analysis of the gene cluster and revision of peptide stereochemistry. Microbiology *151*, 1507-1523.
10. Micklefield, J. (2004). Daptomycin structure and mechanism of action revealed. Chem. Biol. *11*, 887-888.
11. Gehring, A.M., Mori, I., and Walsh, C.T. (1998). Reconstitution and characterization of the Escherichia coli enterobactin synthetase from EntB, EntE, and EntF. Biochemistry *37*, 2648-2659.
12. Hori, K., Yamamoto, Y., Minetoki, T., Kurotsu, T., Kanda, M., Miura, S., Okamura, K., Furuyama, J., and Saito, Y. (1989). Molecular cloning and nucleotide sequence of the gramicidin S synthetase 1 gene. J. Biochem. (Tokyo) *106*, 639-645.
13. Lombo, F., Velasco, A., Castro, A., de la Calle, F., Brana, A.F., Sanchez-Puelles, J.M., Mendez, C., and Salas, J.A. (2006). Deciphering the biosynthesis pathway of the antitumor thiocoraline from a marine actinomycete and its expression in two streptomyces species. Chembiochem *7*, 366-376.
14. Becker, J.E., Moore, R.E., and Moore, B.S. (2004). Cloning, sequencing, and biochemical characterization of the nostocyclopeptide biosynthetic gene cluster: molecular basis for imine macrocyclization. Gene *325*, 35-42.
15. Shin-ya, K., Wierzba, K., Matsuo, K., Ohtani, T., Yamada, Y., Furihata, K., Hayakawa, Y., and Seto, H. (2001). Telomestatin, a novel telomerase inhibitor from Streptomyces anulatus. J. Am. Chem. Soc. *123*, 1262-1263.
16. Lambalot, R.H., and Cane, D.E. (1992). Isolation and characterization of 10-deoxymethynolide produced by Streptomyces venezuelae. J. Antibiot. (Tokyo) *45*, 1981-1982.

17. Cortés, J., Haydock, S.F., Roberts, G.A., Bevitt, D.J., and Leadlay, P.F. (1990). An unusually large multifunctional polypeptide in the erythromycin-producing polyketide synthase of Saccharopolyspora erythraea. Nature *348*, 176-178.
18. Leadlay, P.F., Staunton, J., Aparicio, J.F., Bevitt, D.J., Caffrey, P., Cortés, J., Marsden, A., and Roberts, G.A. (1993). The erythromycin-producing polyketide synthase. Biochem. Soc.Trans. *21*, 218-222.
19. Donadio, S., Staver, M.J., McAlpine, J.B., Swanson, S.J., and Katz, L. (1991). Modular organization of genes required for complex polyketide biosynthesis. Science *252*, 675-679.
20. August, P.R., Tang, L., Yoon, Y.J., Ning, S., Müller, R., Yu, T.W., Taylor, M., Hoffmann, D., Kim, C.G., Zhang, X., Hutchinson, C.R., and Floss, H.G. (1998). Biosynthesis of the ansamycin antibiotic rifamycin: deductions from the molecular analysis of the rif biosynthetic gene cluster of Amycolatopsis mediterranei S699. Chem. Biol. *5*, 69-79.
21. Rascher, A., Hu, Z., Viswanathan, N., Schirmer, A., Reid, R., Nierman, W.C., Lewis, M., and Hutchinson, C.R. (2003). Cloning and characterization of a gene cluster for geldanamycin production in Streptomyces hygroscopicus NRRL 3602. FEMS Microbiol. Lett. *218*, 223-230.
22. Du, L., and Shen, B. (2001). Biosynthesis of hybrid peptide-polyketide natural products. Curr. Opin. Drug Discov. Devel. *4*, 215-228.
23. Motamedi, H., and Shafiee, A. (1998). The biosynthetic gene cluster for the macrolactone ring of the immunosuppressant FK506. Eur. J. Biochem. *256*, 528-534.
24. Wu, K., Chung, L., Revill, W.P., Katz, L., and Reeves, C.D. (2000). The FK520 gene cluster of Streptomyces hygroscopicus var. ascomyceticus (ATCC 14891) contains genes for biosynthesis of unusual polyketide extender units. Gene *251*, 81-90.
25. Tang, L., Shah, S., Chung, L., Carney, J., Katz, L., Khosla, C., and Julien, B. (2000). Cloning and heterologous expression of the epothilone gene cluster. Science *287*, 640-642.
26. Chatterjee, C., Paul, M., Xie, L., and van der Donk, W.A. (2005). Biosynthesis and mode of action of lantibiotics. Chem. Rev. *105*, 633-684.
27. Patton, G.C., and van der Donk, W.A. (2005). New developments in lantibiotic biosynthesis and mode of action. Curr. Opin. Microbiol. *8*, 543-551.
28. Christianson, D.W. (2006). Biochemistry. Five golden rings. Science *311*, 1382-1383.
29. Schwarzer, D., Finking, R., and Marahiel, M.A. (2003). Nonribosomal peptides: from genes to products. Nat. Prod. Rep. *20*, 275-287.
30. Finking, R., and Marahiel, M.A. (2004). Biosynthesis of nonribosomal peptides. Annu. Rev. Microbiol. *58*, 453-488.
31. Walsh, C.T. (2004). Polyketide and nonribosomal peptide antibiotics: modularity and versatility. Science *303*, 1805-1810.
32. Mootz, H.D., Schwarzer, D., and Marahiel, M.A. (2002). Ways of assembling complex natural products on modular nonribosomal peptide synthetases. Chembiochem *3*, 490-504.
33. Dieckmann, R., Lee, Y.O., van Liempt, H., von Dohren, H., and Kleinkauf, H. (1995). Expression of an active adenylate-forming domain of peptide synthetases corresponding to acyl-CoA-synthetases. FEBS Lett. *357*, 212-216.
34. Stachelhaus, T., Huser, A., and Marahiel, M.A. (1996). Biochemical characterization of peptidyl carrier protein (PCP), the thiolation domain of multifunctional peptide synthetases. Chem. Biol. *3*, 913-921.

35. Bergendahl, V., Linne, U., and Marahiel, M.A. (2002). Mutational analysis of the C-domain in nonribosomal peptide synthesis. Eur. J. Biochem. *269*, 620-629.
36. Stachelhaus, T., Mootz, H.D., Bergendahl, V., and Marahiel, M.A. (1998). Peptide bond formation in nonribosomal peptide biosynthesis. Catalytic role of the condensation domain. J. Biol. Chem. *273*, 22773-22781.
37. Kohli, R.M., and Walsh, C.T. (2003). Enzymology of acyl chain macrocyclization in natural product biosynthesis. Chem. Commun. (Camb.), 297-307.
38. Kopp, F., and Marahiel, M.A. (2007). Macrocyclization strategies in polyketide and nonribosomal peptide biosynthesis. Nat. Prod. Rep. *24*, 735-749.
39. Bruner, S.D., Weber, T., Kohli, R.M., Schwarzer, D., Marahiel, M.A., Walsh, C.T., and Stubbs, M.T. (2002). Structural basis for the cyclization of the lipopeptide antibiotic surfactin by the thioesterase domain SrfTE. Structure (Camb.) *10*, 301-310.
40. Samel, S.A., Wagner, B., Marahiel, M.A., and Essen, L.O. (2006). The thioesterase domain of the fengycin biosynthesis cluster: a structural base for the macrocyclization of a non-ribosomal lipopeptide. J. Mol. Biol. *359*, 876-889.
41. Tseng, C.C., Bruner, S.D., Kohli, R.M., Marahiel, M.A., Walsh, C.T., and Sieber, S.A. (2002). Characterization of the surfactin synthetase C-terminal thioesterase domain as a cyclic depsipeptide synthase. Biochemistry *41*, 13350-13359.
42. Keating, T.A., Ehmann, D.E., Kohli, R.M., Marshall, C.G., Trauger, J.W., and Walsh, C.T. (2001). Chain termination steps in nonribosomal peptide synthetase assembly lines: directed acyl-S-enzyme breakdown in antibiotic and siderophore biosynthesis. Chembiochem *2*, 99-107.
43. Gaitatzis, N., Kunze, B., and Muller, R. (2001). In vitro reconstitution of the myxochelin biosynthetic machinery of Stigmatella aurantiaca Sg a15: Biochemical characterization of a reductive release mechanism from nonribosomal peptide synthetases. Proc. Natl. Acad. Sci. U S A *98*, 11136-11141.
44. Schracke, N., Linne, U., Mahlert, C., and Marahiel, M.A. (2005). Synthesis of linear gramicidin requires the cooperation of two independent reductases. Biochemistry *44*, 8507-8513.
45. Kopp, F., Mahlert, C., Grunewald, J., and Marahiel, M.A. (2006). Peptide macrocyclization: the reductase of the nostocyclopeptide synthetase triggers the self-assembly of a macrocyclic imine. J. Am. Chem. Soc. *128*, 16478-16479.
46. Weber, G., Schorgendorfer, K., Schneider-Scherzer, E., and Leitner, E. (1994). The peptide synthetase catalyzing cyclosporine production in Tolypocladium niveum is encoded by a giant 45.8-kilobase open reading frame. Curr. Genet. *26*, 120-125.
47. Walsh, C.T. (2002). Combinatorial biosynthesis of antibiotics: challenges and opportunities. Chembiochem *3*, 125-134.
48. Kittendorf, J.D., and Sherman, D.H. (2006). Developing tools for engineering hybrid polyketide synthetic pathways. Curr. Opin. Biotechnol. *17*, 597-605.
49. Stachelhaus, T., Schneider, A., and Marahiel, M.A. (1995). Rational design of peptide antibiotics by targeted replacement of bacterial and fungal domains. Science *269*, 69-72.
50. Nguyen, K.T., Ritz, D., Gu, J.Q., Alexander, D., Chu, M., Miao, V., Brian, P., and Baltz, R.H. (2006). Combinatorial biosynthesis of novel antibiotics related to daptomycin. Proc. Natl. Acad. Sci. U S A *103*, 17462-17467.
51. Miao, V., Coeffet-Le Gal, M.F., Nguyen, K., Brian, P., Penn, J., Whiting, A., Steele, J., Kau, D., Martin, S., Ford, R., Gibson, T., Bouchard, M., Wrigley, S.K., and Baltz, R.H. (2006). Genetic engineering in Streptomyces roseosporus to produce hybrid lipopeptide antibiotics. Chem. Biol. *13*, 269-276.

52. Parenty, A., Moreau, X., and Campagne, J.M. (2006). Macrolactonizations in the total synthesis of natural products. Chem. Rev. *106*, 911-939.
53. Kopp, F., and Marahiel, M.A. (2007). Where chemistry meets biology: the chemoenzymatic synthesis of nonribosomal peptides and polyketides. Curr. Opin. Biotechnol. *18*, 513-520.
54. Bordusa, F. (2001). Enzymes for peptide cyclization. Chembiochem *2*, 405-409.
55. Sieber, S.A., Tao, J., Walsh, C.T., and Marahiel, M.A. (2004). Peptidyl thiophenols as substrates for nonribosomal peptide cyclases. Angew. Chem. Int. Ed. Engl. *43*, 493-498.
56. Grünewald, J., Sieber, S.A., and Marahiel, M.A. (2004). Chemo- and regioselective peptide cyclization triggered by the N-terminal fatty acid chain length: the recombinant cyclase of the calcium-dependent antibiotic from Streptomyces coelicolor. Biochemistry *43*, 2915-2925.
57. Kohli, R.M., Walsh, C.T., and Burkart, M.D. (2002). Biomimetic synthesis and optimization of cyclic peptide antibiotics. Nature *418*, 658-661.
58. Trauger, J.W., Kohli, R.M., and Walsh, C.T. (2001). Cyclization of backbone-substituted peptides catalyzed by the thioesterase domain from the tyrocidine nonribosomal peptide synthetase. Biochemistry *40*, 7092-7098.
59. Lin, H., Thayer, D.A., Wong, C.H., and Walsh, C.T. (2004). Macrolactamization of glycosylated peptide thioesters by the thioesterase domain of tyrocidine synthetase. Chem. Biol. *11*, 1635-1642.
60. Lin, H., and Walsh, C.T. (2004). A chemoenzymatic approach to glycopeptide antibiotics. J. Am. Chem. Soc. *126*, 13998-14003.
61. Mukhtar, T.A., Koteva, K.P., and Wright, G.D. (2005). Chimeric streptogramin-tyrocidine antibiotics that overcome streptogramin resistance. Chem. Biol. *12*, 229-235.
62. Mahlert, C., Sieber, S.A., Grünewald, J., and Marahiel, M.A. (2005). Chemoenzymatic approach to enantiopure streptogramin B variants: characterization of stereoselective pristinamycin I cyclase from Streptomyces pristinaespiralis. J. Am. Chem. Soc. *127*, 9571-9580.
63. Beck, Z.Q., Aldrich, C.C., Magarvey, N.A., Georg, G.I., and Sherman, D.H. (2005). Chemoenzymatic synthesis of cryptophycin/arenastatin natural products. Biochemistry *44*, 13457-13466.
64. Magarvey, N.A., Beck, Z.Q., Golakoti, T., Ding, Y., Huber, U., Hemscheidt, T.K., Abelson, D., Moore, R.E., and Sherman, D.H. (2006). Biosynthetic characterization and chemoenzymatic assembly of the cryptophycins. Potent anticancer agents from cyanobionts. ACS Chem. Biol. *1*, 766-779.
65. Walsh, C.T., Gehring, A.M., Weinreb, P.H., Quadri, L.E., and Flugel, R.S. (1997). Post-translational modification of polyketide and nonribosomal peptide synthases. Curr. Opin. Chem. Biol. *1*, 309-315.
66. Mahlert, C., Kopp, F., Thirlway, J., Micklefield, J., and Marahiel, M.A. (2007). Stereospecific enzymatic transformation of alpha-ketoglutarate to (2S,3R)-3-methyl glutamate during acidic lipopeptide biosynthesis. J. Am. Chem. Soc. *129*, 12011-12018.
67. Milne, C., Powell, A., Jim, J., Al Nakeeb, M., Smith, C.P., and Micklefield, J. (2006). Biosynthesis of the (2S,3R)-3-methyl glutamate residue of nonribosomal lipopeptides. J. Am. Chem. Soc. *128*, 11250-11259.
68. Strieker, M., Kopp, F., Mahlert, C., Essen, L.O., and Marahiel, M.A. (2007). Mechanistic and structural basis of stereospecific Cbeta-hydroxylation in calcium-dependent antibiotic, a daptomycin-type lipopeptide. ACS Chem. Biol. *2*, 187-196.

69. Neary, J.M., Powell, A., Gordon, L., Milne, C., Flett, F., Wilkinson, B., Smith, C.P., and Micklefield, J. (2007). An asparagine oxygenase (AsnO) and a 3-hydroxyasparaginyl phosphotransferase (HasP) are involved in the biosynthesis of calcium-dependent lipopeptide antibiotics. Microbiology *153*, 768-776.
70. Christenson, S.D., Liu, W., Toney, M.D., and Shen, B. (2003). A novel 4-methylideneimidazole-5-one-containing tyrosine aminomutase in enediyne antitumor antibiotic C-1027 biosynthesis. J. Am. Chem. Soc. *125*, 6062-6063.
71. Stachelhaus, T., and Walsh, C.T. (2000). Mutational analysis of the epimerization domain in the initiation module PheATE of gramicidin S synthetase. Biochemistry *39*, 5775-5787.
72. Miller, D.A., and Walsh, C.T. (2001). Yersiniabactin synthetase: probing the recognition of carrier protein domains by the catalytic heterocyclization domains, Cy1 and Cy2, in the chain-initiating HWMP2 subunit. Biochemistry *40*, 5313-5321.
73. Zerbe, K., Woithe, K., Li, D.B., Vitali, F., Bigler, L., and Robinson, J.A. (2004). An oxidative phenol coupling reaction catalyzed by oxyB, a cytochrome P450 from the vancomycin-producing microorganism. Angew. Chem. Int. Ed. Engl. *43*, 6709-6713.
74. Woithe, K., Geib, N., Zerbe, K., Li, D.B., Heck, M., Fournier-Rousset, S., Meyer, O., Vitali, F., Matoba, N., Abou-Hadeed, K., and Robinson, J.A. (2007). Oxidative phenol coupling reactions catalyzed by OxyB: a cytochrome P450 from the vancomycin producing organism. implications for vancomycin biosynthesis. J. Am. Chem. Soc. *129*, 6887-6895.
75. Kelly, W.L., Boyne, M.T., 2nd, Yeh, E., Vosburg, D.A., Galonic, D.P., Kelleher, N.L., and Walsh, C.T. (2007). Characterization of the aminocarboxycyclopropane-forming enzyme CmaC. Biochemistry *46*, 359-368.
76. Vaillancourt, F.H., Yeh, E., Vosburg, D.A., O'Connor, S.E., and Walsh, C.T. (2005). Cryptic chlorination by a non-haem iron enzyme during cyclopropyl amino acid biosynthesis. Nature *436*, 1191-1194.
77. Losey, H.C., Jiang, J., Biggins, J.B., Oberthur, M., Ye, X.Y., Dong, S.D., Kahne, D., Thorson, J.S., and Walsh, C.T. (2002). Incorporation of glucose analogs by GtfE and GtfD from the vancomycin biosynthetic pathway to generate variant glycopeptides. Chem. Biol. *9*, 1305-1314.
78. Losey, H.C., Peczuh, M.W., Chen, Z., Eggert, U.S., Dong, S.D., Pelczer, I., Kahne, D., and Walsh, C.T. (2001). Tandem action of glycosyltransferases in the maturation of vancomycin and teicoplanin aglycones: novel glycopeptides. Biochemistry *40*, 4745-4755.
79. Zhang, C., Griffith, B.R., Fu, Q., Albermann, C., Fu, X., Lee, I.K., Li, L., and Thorson, J.S. (2006). Exploiting the reversibility of natural product glycosyltransferase-catalyzed reactions. Science *313*, 1291-1294.
80. Mercer, A.C., and Burkart, M.D. (2007). The ubiquitous carrier protein--a window to metabolite biosynthesis. Nat. Prod. Rep. *24*, 750-773.
81. White, S.W., Zheng, J., Zhang, Y.M., and Rock, C.O. (2005). Annu. Rev. Biochem. *74*, 791-831.
82. Lu, Y.J., Zhang, Y.M., and Rock, C.O. (2004). Biochem. Cell. Biol. *82*, 145-155.
83. Guchhait, R.B., Polakis, S.E., Dimroth, P., Stoll, E., Moss, J., and Lane, M.D. (1974). Acetyl coenzyme A carboxylase system of Escherichia coli. Purification and properties of the biotin carboxylase, carboxyltransferase, and carboxyl carrier protein components. J. Biol. Chem. *249*, 6633-6645.
84. Marini, P., Li, S.J., Gardiol, D., Cronan, J.E., Jr., and de Mendoza, D. (1995). The genes encoding the biotin carboxyl carrier protein and biotin carboxylase subunits

of Bacillus subtilis acetyl coenzyme A carboxylase, the first enzyme of fatty acid synthesis. J. Bacteriol. *177*, 7003-7006.

85. Harder, M.E., Ladenson, R.C., Schimmel, S.D., and Silbert, D.F. (1974). Mutants of Escherichia coli with temperature-sensitive malonyl coenzyme A-acyl carrier protein transacylase. J. Biol. Chem. *249*, 7468-7475.
86. D'Agnolo, G., Rosenfeld, I.S., Awaya, J., Omura, S., and Vagelos, P.R. (1973). Inhibition of fatty acid synthesis by the antibiotic cerulenin. Specific inactivation of beta-ketoacyl-acyl carrier protein synthetase. Biochim. Biophys. Acta *326*, 155-156.
87. D'Agnolo, G., Rosenfeld, I.S., and Vagelos, P.R. (1975). Multiple forms of beta-ketoacyl-acyl carrier protein synthetase in Escherichia coli. J. Biol. Chem. *250*, 5289-5294.
88. Garwin, J.L., Klages, A.L., and Cronan, J.E., Jr. (1980). Structural, enzymatic, and genetic studies of beta-ketoacyl-acyl carrier protein synthases I and II of Escherichia coli. J. Biol. Chem. *255*, 11949-11956.
89. Fichtlscherer, F., Wellein, C., Mittag, M., and Schweizer, E. (2000). A novel function of yeast fatty acid synthase. Subunit alpha is capable of self-pantetheinylation. Eur. J. Biochem. *267*, 2666-2671.
90. Joshi, A.K., Rangan, V.S., Witkowski, A., and Smith, S. (2003). Engineering of an active animal fatty acid synthase dimer with only one competent subunit. Chem. Biol. *10*, 169-173.
91. Rangan, V.S., Joshi, A.K., and Smith, S. (2001). Mapping the functional topology of the animal fatty acid synthase by mutant complementation in vitro. Biochemistry *40*, 10792-10799.
92. Rock, C.O., and Cronan, J.E. (1996). Escherichia coli as a model for the regulation of dissociable (type II) fatty acid biosynthesis. Biochim. Biophys. Acta *1302*, 1-16.
93. Marrakchi, H., Zhang, Y.M., and Rock, C.O. (2002). Mechanistic diversity and regulation of Type II fatty acid synthesis. Biochem. Soc.Trans. *30*, 1050-1055.
94. Kirkpatrick, P., Raja, A., LaBonte, J., and Lebbos, J. (2003). Daptomycin. Nat. Rev. Drug Discov. *2*, 943-944.
95. Baltz, R.H., Miao, V., and Wrigley, S.K. (2005). Natural products to drugs: daptomycin and related lipopeptide antibiotics. Nat. Prod. Rep. *22*, 717-741.
96. Fox, J.L. (2003). Concerns raised over declining antiinfectives R&D. Nat. Biotechnol. *21*, 1255-1256.
97. Harvey, A. (2000). Strategies for discovering drugs from previously unexplored natural products. Drug Discov. Today *5*, 294-300.
98. Debono, M., Abbott, B.J., Molloy, R.M., Fukuda, D.S., Hunt, A.H., Daupert, V.M., Counter, F.T., Ott, J.L., Carrell, C.B., Howard, L.C., Boeck, L.D., and Hamill, R.L. (1988). Enzymatic and chemical modifications of lipopeptide antibiotic A21978C: the synthesis and evaluation of daptomycin (LY146032). J. Antibiot. (Tokyo) *41*, 1093-1105.
99. Aron, Z.D., Dorrestein, P.C., Blackhall, J.R., Kelleher, N.L., and Walsh, C.T. (2005). Characterization of a new tailoring domain in polyketide biogenesis: the amine transferase domain of MycA in the mycosubtilin gene cluster. J. Am. Chem. Soc. *127*, 14986-14987.
100. Hansen, D.B., Bumpus, S.B., Aron, Z.D., Kelleher, N.L., and Walsh, C.T. (2007). The loading module of mycosubtilin: an adenylation domain with fatty acid selectivity. J. Am. Chem. Soc. *129*, 6366-6367.
101. Aron, Z.D., Fortin, P.D., Calderone, C.T., and Walsh, C.T. (2007). FenF: servicing the Mycosubtilin synthetase assembly line in trans. Chembiochem *8*, 613-616.

102. Duitman, E.H., Hamoen, L.W., Rembold, M., Venema, G., Seitz, H., Saenger, W., Bernhard, F., Reinhardt, R., Schmidt, M., Ullrich, C., Stein, T., Leenders, F., and Vater, J. (1999). The mycosubtilin synthetase of Bacillus subtilis ATCC6633: a multifunctional hybrid between a peptide synthetase, an amino transferase, and a fatty acid synthase. Proc. Natl. Acad. Sci. U S A *96*, 13294-13299.
103. Trivedi, O.A., Arora, P., Sridharan, V., Tickoo, R., Mohanty, D., and Gokhale, R.S. (2004). Enzymic activation and transfer of fatty acids as acyl-adenylates in mycobacteria. Nature *428*, 441-445.
104. Hojati, Z., Milne, C., Harvey, B., Gordon, L., Borg, M., Flett, F., Wilkinson, B., Sidebottom, P.J., Rudd, B.A., Hayes, M.A., Smith, C.P., and Micklefield, J. (2002). Structure, biosynthetic origin, and engineered biosynthesis of calcium-dependent antibiotics from Streptomyces coelicolor. Chem. Biol. *9*, 1175-1187.
105. Miao, V., Brost, R., Chapple, J., She, K., Gal, M.F., and Baltz, R.H. (2005). The lipopeptide antibiotic A54145 biosynthetic gene cluster from Streptomyces fradiae. J. Ind. Microbiol. Biotechnol., 1-12.
106. Straus, S.K., and Hancock, R.E. (2006). Mode of action of the new antibiotic for Gram-positive pathogens daptomycin: comparison with cationic antimicrobial peptides and lipopeptides. Biochim. Biophys. Acta *1758*, 1215-1223.
107. Silverman, J.A., Perlmutter, N.G., and Shapiro, H.M. (2003). Correlation of daptomycin bactericidal activity and membrane depolarization in Staphylococcus aureus. Antimicrob. Agents Chemother. *47*, 2538-2544.
108. Ball, L.J., Goult, C.M., Donarski, J.A., Micklefield, J., and Ramesh, V. (2004). NMR structure determination and calcium binding effects of lipopeptide antibiotic daptomycin. Org. Biomol. Chem. *2*, 1872-1878.
109. Jung, D., Rozek, A., Okon, M., and Hancock, R.E. (2004). Structural transitions as determinants of the action of the calcium-dependent antibiotic daptomycin. Chem. Biol. *11*, 949-957.
110. Rotondi, K.S., and Gierasch, L.M. (2005). A well-defined amphipathic conformation for the calcium-free cyclic lipopeptide antibiotic, daptomycin, in aqueous solution. Biopolymers *80*, 374-385.
111. Kieser, T., Mervyn, J.B., Buttner, M.J., Chater, K.F., and Hopwood, D.A. (2000). Practical Streptomyces Genetics. The John Innes Foundation, Norwich, England.
112. Linne, U., and Marahiel, M.A. (2004). Reactions catalyzed by mature and recombinant nonribosomal peptide synthetases. Methods Enzymol. *388*, 293-315.
113. Sambrook, J., Fritsch, E.F., and Maniatis, T. (1989). Molecular cloning: a laboratory manual. Cold Spring Laboratory press, Cold spring Harbor, NY.
114. Bradford, M.M. (1976). A rapid and sensitive method for the quantitation of microgram quantities of protein utilizing the principle of protein-dye binding. Anal. Biochem. *72*, 248-254.
115. La Clair, J.J., Foley, T.L., Schegg, T.R., Regan, C.M., and Burkart, M.D. (2004). Manipulation of carrier proteins in antibiotic biosynthesis. Chem. Biol. *11*, 195-201.
116. Vertesy, L., Ehlers, E., Kogler, H., Kurz, M., Meiwes, J., Seibert, G., Vogel, M., and Hammann, P. (2000). Friulimicins: novel lipopeptide antibiotics with peptidoglycan synthesis inhibiting activity from Actinoplanes friuliensis sp. nov. II. Isolation and structural characterization. J. Antibiot. (Tokyo) *53*, 816-827.
117. Banerjee, D.K., Scher, M.G., and Waechter, C.J. (1981). Amphomycin: effect of the lipopeptide antibiotic on the glycosylation and extraction of dolichyl monophosphate in calf brain membranes. Biochemistry *20*, 1561-1568.

118. Grünewald, J., Sieber, S.A., Mahlert, C., Linne, U., and Marahiel, M.A. (2004). Synthesis and derivatization of daptomycin: a chemoenzymatic route to acidic lipopeptide antibiotics. J. Am. Chem. Soc. *126*, 17025-17031.
119. Thorpe, C., and Kim, J.J. (1995). Structure and mechanism of action of the acyl-CoA dehydrogenases. Faseb J. *9*, 718-725.
120. Lea, W., Abbas, A.S., Sprecher, H., Vockley, J., and Schulz, H. (2000). Long-chain acyl-CoA dehydrogenase is a key enzyme in the mitochondrial beta-oxidation of unsaturated fatty acids. Biochim. Biophys. Acta *1485*, 121-128.
121. Kieweg, V., Krautle, F.G., Nandy, A., Engst, S., Vock, P., Abdel-Ghany, A.G., Bross, P., Gregersen, N., Rasched, I., Strauss, A., and Ghisla, S. (1997). Biochemical characterization of purified, human recombinant Lys304-->Glu medium-chain acyl-CoA dehydrogenase containing the common disease-causing mutation and comparison with the normal enzyme. Eur. J. Biochem. *246*, 548-556.
122. Sieber, S.A., Walsh, C.T., and Marahiel, M.A. (2003). Loading peptidyl-coenzyme A onto peptidyl carrier proteins: a novel approach in characterizing macrocyclization by thioesterase domains. J. Am. Chem. Soc. *125*, 10862-10866.
123. Dorrestein, P.C., Bumpus, S.B., Calderone, C.T., Garneau-Tsodikova, S., Aron, Z.D., Straight, P.D., Kolter, R., Walsh, C.T., and Kelleher, N.L. (2006). Facile detection of acyl and peptidyl intermediates on thiotemplate carrier domains via phosphopantetheinyl elimination reactions during tandem mass spectrometry. Biochemistry *45*, 12756-12766.
124. Ortiz-Maldonado, M., Ballou, D.P., and Massey, V. (1999). Use of free energy relationships to probe the individual steps of hydroxylation of p-hydroxybenzoate hydroxylase: studies with a series of 8-substituted flavins. Biochemistry *38*, 8124-8137.
125. Buch, K., Stransky, H., and Hager, A. (1995). FAD is a further essential cofactor of the NAD(P)H and O2-dependent zeaxanthin-epoxidase. FEBS Lett. *376*, 45-48.
126. Vorkonov, M.V., Gontcharov, A.V., Wang, Z., Richardson, P.F., and Kolb, H.C. (2004). Tetrahedron *60*, 9043-9048.
127. Gao, Y., Hanson, R.M., Klunder, J.M., Ko, S.Y., Masamune, H., and Sharpless, K.B. (1987). J. Am. Chem. Soc. *109*, 5765-5780.
128. Wohlleben, W., and Pelzer, S. (2002). New compounds by combining "modern" genomics and "old-fashioned" mutasynthesis. Chem. Biol. *9*, 1163-1164.
129. Siedlecki, J., Hill, J., Parr, I., Yu, X., Morytko, M., Zhang, Y., Silverman, J., Controneo, N., Laganas, V., Li, T., Li, J., Keith, D., Shimer, G., and Finn, J. (2003). Array synthesis of novel lipodepsipeptide. Bioorg. Med. Chem. Lett. *13*, 4245-4249.
130. Hill, J., Siedlecki, J., Parr, I., Morytko, M., Yu, X., Zhang, Y., Silverman, J., Controneo, N., Laganas, V., Li, T., Lai, J.J., Keith, D., Shimer, G., and Finn, J. (2003). Synthesis and biological activity of N-Acylated ornithine analogues of daptomycin. Bioorg. Med. Chem. Lett. *13*, 4187-4191.
131. Yeh, E., Lin, H., Clugston, S.L., Kohli, R.M., and Walsh, C.T. (2004). Enhanced macrocyclizing activity of the thioesterase from tyrocidine synthetase in presence of nonionic detergent. Chem. Biol. *11*, 1573-1582.
132. Wagner, B., Sieber, S.A., Baumann, M., and Marahiel, M.A. (2006). Solvent engineering substantially enhances the chemoenzymatic production of surfactin. Chembiochem *7*, 595-597.
133. Lamp, K.C., Rybak, M.J., Bailey, E.M., and Kaatz, G.W. (1992). In vitro pharmacodynamic effects of concentration, pH, and growth phase on serum bactericidal activities of daptomycin and vancomycin. Antimicrob. Agents Chemother. *36*, 2709-2714.

134. Lewis, J.S., 2nd, Owens, A., Cadena, J., Sabol, K., Patterson, J.E., and Jorgensen, J.H. (2005). Emergence of daptomycin resistance in Enterococcus faecium during daptomycin therapy. Antimicrob. Agents Chemother. *49*, 1664-1665.
135. Mangili, A., Bica, I., Snydman, D.R., and Hamer, D.H. (2005). Daptomycin-resistant, methicillin-resistant Staphylococcus aureus bacteremia. Clin. Infect. Dis. *40*, 1058-1060.
136. Korczynska, M., Mukhtar, T.A., Wright, G.D., and Berghuis, A.M. (2007). Structural basis for streptogramin B resistance in Staphylococcus aureus by virginiamycin B lyase. Proc. Natl. Acad. Sci. U S A *104*, 10388-10393.
137. Eliopoulos, G.M., Thauvin, C., Gerson, B., and Moellering, R.C., Jr. (1985). In vitro activity and mechanism of action of A21978C1, a novel cyclic lipopeptide antibiotic. Antimicrob. Agents Chemother. *27*, 357-362.
138. Yazawa, M., and Yagi, K. (1980). The amino acid sequence of the calmodulin obtained from sea anemone (metridium senile) muscle. Biochem. Biophys. Res. Commun. *96*, 377-381.
139. Ho, S.W., Jung, D., Calhoun, J.R., Lear, J.D., Okon, M., Scott, W.R., Hancock, R.E., and Straus, S.K. (2007). Effect of divalent cations on the structure of the antibiotic daptomycin. Eur. Biophys. J.
140. Golakoti, T., Yoshida, W.Y., Chaganty, S., and Moore, R.E. (2001). Isolation and structure determination of nostocyclopeptides A1 and A2 from the terrestrial cyanobacterium Nostoc sp. ATCC53789. J. Nat. Prod. *64*, 54-59.
141. Stryer, L. (1996). Biochemie. Spektrum Akademischer Verlag Heidelberg Berlin Oxford, 4. Auflage.
142. Ehmann, D.E., Gehring, A.M., and Walsh, C.T. (1999). Lysine biosynthesis in Saccharomyces cerevisiae: mechanism of alpha-aminoadipate reductase (Lys2) involves posttranslational phosphopantetheinylation by Lys5. Biochemistry *38*, 6171-6177.
143. Silakowski, B., Kunze, B., Nordsiek, G., Blocker, H., Hofle, G., and Müller, R. (2000). The myxochelin iron transport regulon of the myxobacterium Stigmatella aurantiaca Sg a15. Eur. J. Biochem. *267*, 6476-6485.
144. Silakowski, B., Nordsiek, G., Kunze, B., Blocker, H., and Müller, R. (2001). Novel features in a combined polyketide synthase/non-ribosomal peptide synthetase: the myxalamid biosynthetic gene cluster of the myxobacterium Stigmatella aurantiaca Sga15. Chem. Biol. *8*, 59-69.
145. Pospiech, A., Cluzel, B., Bietenhader, J., and Schupp, T. (1995). A new Myxococcus xanthus gene cluster for the biosynthesis of the antibiotic saframycin Mx1 encoding a peptide synthetase. Microbiology *141 (Pt 8)*, 1793-1803.
146. Pospiech, A., Bietenhader, J., and Schupp, T. (1996). Two multifunctional peptide synthetases and an O-methyltransferase are involved in the biosynthesis of the DNA-binding antibiotic and antitumour agent saframycin Mx1 from Myxococcus xanthus. Microbiology *142 (Pt 4)*, 741-746.
147. Maiya, S., Grundmann, A., Li, X., Li, S.M., and Turner, G. (2007). Identification of a hybrid PKS/NRPS required for pseurotin A biosynthesis in the human pathogen Aspergillus fumigatus. Chembiochem *8*, 1736-1743.
148. Sheng, D., Ballou, D.P., and Massey, V. (2001). Mechanistic studies of cyclohexanone monooxygenase: chemical properties of intermediates involved in catalysis. Biochemistry *40*, 11156-11167.
149. van Berkel, W.J., Kamerbeek, N.M., and Fraaije, M.W. (2006). Flavoprotein monooxygenases, a diverse class of oxidative biocatalysts. J. Biotechnol. *124*, 670-689.

150. Massey, V. (1994). Activation of molecular oxygen by flavins and flavoproteins. J. Biol. Chem. *269*, 22459-22462.
151. Entsch, B., Ballou, D.P., and Massey, V. (1976). Flavin-oxygen derivatives involved in hydroxylation by p-hydroxybenzoate hydroxylase. J. Biol. Chem. *251*, 2550-2563.
152. Entsch, B., Husain, M., Ballou, D.P., Massey, V., and Walsh, C. (1980). Oxygen reactivity of p-hydroxybenzoate hydroxylase containing 1-deaza-FAD. J. Biol. Chem. *255*, 1420-1429.
153. Vaillancourt, F.H., Yeh, E., Vosburg, D.A., Garneau-Tsodikova, S., and Walsh, C.T. (2006). Nature's inventory of halogenation catalysts: oxidative strategies predominate. Chem. Rev. *106*, 3364-3378.
154. Yeh, E., Garneau, S., and Walsh, C.T. (2005). Robust in vitro activity of RebF and RebH, a two-component reductase/halogenase, generating 7-chlorotryptophan during rebeccamycin biosynthesis. Proc. Natl. Acad. Sci. U S A *102*, 3960-3965.
155. Schwarzer, D., Mootz, H.D., Linne, U., and Marahiel, M.A. (2002). Regeneration of misprimed nonribosomal peptide synthetases by type II thioesterases. Proc. Natl. Acad. Sci. U S A *99*, 14083-14088.
156. Thomas, J., and Cronan, J.E. (2005). The enigmatic acyl carrier protein phosphodiesterase of Escherichia coli: genetic and enzymological characterization. J. Biol. Chem. *280*, 34675-34683.
157. Powell, A., Borg, M., Amir-Heidari, B., Neary, J.M., Thirlway, J., Wilkinson, B., Smith, C.P., and Micklefield, J. (2007). Engineered biosynthesis of nonribosomal lipopeptides with modified fatty acid side chains. J. Am. Chem. Soc. *129*, 15182-15191.
158. Yin, X., and Zabriskie, T.M. (2006). The enduracidin biosynthetic gene cluster from Streptomyces fungicidicus. Microbiology *152*, 2969-2983.
159. McCafferty, D.G., Cudic, P., Frankel, B.A., Barkallah, S., Kruger, R.G., and Li, W. (2002). Chemistry and biology of the ramoplanin family of peptide antibiotics. Biopolymers *66*, 261-284.
160. Heinzelmann, E., Berger, S., Muller, C., Hartner, T., Poralla, K., Wohlleben, W., and Schwartz, D. (2005). An acyl-CoA dehydrogenase is involved in the formation of the Delta cis3 double bond in the acyl residue of the lipopeptide antibiotic friulimicin in Actinoplanes friuliensis. Microbiology *151*, 1963-1974.
161. Muller, C., Nolden, S., Gebhardt, P., Heinzelmann, E., Lange, C., Puk, O., Welzel, K., Wohlleben, W., and Schwartz, D. (2007). Sequencing and analysis of the biosynthetic gene cluster of the lipopeptide antibiotic Friulimicin in Actinoplanes friuliensis. Antimicrob. Agents Chemother. *51*, 1028-1037.

Acknowledgement

First of all, I would like to thank Prof. Dr. M. A. Marahiel for his excellent scientific guidance and the generous support of my PhD thesis. I gratefully acknowledge his scientific advice and continuous willingness for helpful discussions. He always supported new ideas and helped to develop them further, which was for the great benefit of my work. I would also like to acknowledge his enthusiasm for science, which was always inspiring to me and made work in his laboratory very exciting.
Further, I am indebted for the opportunity to participate in numerous conferences and workshops. Especially the NRPS/PKS meeting in Santa Cruz as well as the 56th meeting of Nobel Prize Winners in Lindau have been an outstanding experience.

I would like to thank Prof. Dr. A. Geyer for interesting scientific discussions in the context of the nostocyclopeptide project and the reviewing of this thesis. I would like to thank Prof. Dr. W. Buckel and Prof. Dr. L.-O. Essen for being in my thesis committee.

I gratefully acknowledge Prof. Dr. A. Geyer, Sebastian Enck as well as Dr. M. Oberthür for the fruitful scientific collaboration.

I would like to acknowledge the whole Marahiel laboratory for the nice working atmosphere and the great time in the lab. In particular, I would like to thank my colleagues of "4707", Dr. Christoph Mahlert, Dr. Jan Grünewald, Matthias Strieker, and Verena Pohlmann, for many helpful discussions and the superb cooperation. I really enjoyed our time in and outside the lab.

I would like to thank Dr. Uwe Linne for his expert opinion in bioanalytic questions and many helpful discussions.

I would like to thank Antje Schäfer and her trainees, Carola Kisselbach and Sebastian Friedrich, as well as Katja Kräling for technical assistance. For practical support I would also like to thank my lab students Joachim Zettler, Johannes Ahrens, Katrin Eicher, Jessica Fischer and Gunther Zimmermann.

I gratefully acknowledge Christoph Mahlert, Sebastian Enck as well as Verena Pohlmann for proof reading of this thesis.

I would like to thank the "Fonds der Chemischen Industrie" for financial support during my studies by a "Jubiläumstipendium" and a "Doktorandenstipendium".

Special thanks to my family, in particular my mother.

The biggest support came from my wife Katharina – thanks for everything. I wish to dedicate this thesis to her.

Erklärung

Ich versichere, dass ich meine Dissertation *„Macrocyclization and Fatty Acid Modification during the Synthesis of Nonribosomal Peptides“* selbstständig, ohne unerlaubte Hilfe angefertigt und mich dabei keiner anderen als der von mir ausdrücklich angegebenen Quellen und Hilfen bedient habe.
Die Dissertation wurde in der jetzigen oder einer ähnlichen Form noch bei keiner anderen Hochschule eingereicht und hat noch keinen sonstigen Prüfungszwecken gedient.

_____ _____

(Ort, Datum) (Unterschrift mit Vor- und Zuname)